Master's Thesis

CHARACTERISATION OF THE MORPHOLOGY OF INCLINED SCC CRACKS IN AUSTRALIAN GAS PIPELINES

BY

LUKE ZADOW

B.E., Mechanical Engineering

School of Mechanical Engineering

The University of Adelaide

October 2013

i. Declaration

This work contains no material that has been accepted for the award of any other Degree or Diploma in any university or other tertiary institution and, to the best of my knowledge and belief, contains no material previously published or written by another person, except where due reference has been made in the text. I give consent for this copy of my thesis, when present in the University of Adelaide Library, being available for loan and photocopying.

L. Zadow

08/10/2013

ii. Acknowledgements

Special acknowledgements for their contribution to the progress and success of this project as well as their advice and contribution to achieving the results:

- Geoff Callar
- Craig Clarke
- Vijay Vijayaraghavan.

This work was funded by the Energy Pipelines Cooperative Research Centre, supported through the Australian Government's Cooperative Research Centres Program.

The cash and in-kind support from the Australian Pipeline Industry Association Research and Standards Committee (APIA RSC) is gratefully acknowledged.

The author would like to thank Adelaide Microscopy for their generous help and assistance in advising the best approach for achieving optimal results for this project. Their support is highly valued.

The assistance provided by the Mechanical Engineering workshop in the manufacture and preparation of samples for tomography is greatly appreciated. In particular, the assistance of, and advice from, Richard Pateman is acknowledged.

A special thanks to Valerie Linton and Erwin Gamboa for their advice on the direction of this project, which ensured its success.

The author would like to thank Michael Giuliani for his contribution to the project with his knowledge in the area of tomography.

The author would also like to thank his mother and family for their support and help with editing this thesis and other reports.

iii. Publications from Thesis

Zadow, L & Gamboa, E 2012, 'Tomography of Inclined SCC Cracks in Australian Gas Pipelines', *Proceedings of the 9th International Pipeline Conference*, IPC2012 - 90363

Zadow, L Gamboa, E & Lavigne, O 2013, 'Morphology of Australian Inclined SCC', *Corrosion Science*, (in progress).

Zadow, L Gamboa, E & Lavigne, O 2013, 'Comparison of Inclined SCC between Canada and Australia', *Corrosion Science*, (in progress).

iv. Abstract

Stress Corrosion Cracking (SCC) in pipeline steel occurs when an aggressive environment and tensile stresses act on a susceptible microstructure. Typically, SCC in gas pipelines tends to travel perpendicular to the hoop stresses in the through-wall direction. Studies conducted on the TransCanada pipeline, where a rupture had occurred, revealed the incidence of SCC cracks, whose crack path deviated at an angle from the normal. These unusual inclined cracks have also been found in an Australian pipeline, resulting in a need for a more comprehensive understanding of inclined SCC.

As a result, this study has been undertaken to investigate SCC in Australia, in particular the morphology of inclined SCC and together with the many inclined crack features and crack interactions and anomalies (inclusions) in the pipe steel. This study revealed that 81% of SCC cracks investigated were inclined. The majority of cracks analysed were over 4 mm in length, which corresponded to the calculated critical crack length according to industry guidelines. Inclined cracks morphologically presented with a straight section before they inclined away from the perpendicular direction. The straight section tended to be between 200-900 µm and the inclination angle varied between 30-60^{o}. This inclination angle increased as the crack grew deeper into the pipe wall, resulting in long cracks travelling a considerable distance in the hoop direction (3.8 mm travel for a 51 mm longitudinal surface SCC crack). In two cases (out of 120 cracks), subsurface longitudinal crack travel was observed to be approximately 1.5 mm. In most other cases, no subsurface longitudinal travel was observed.

Observed crack interactions did not breach current industry guidelines used for SCC threat assessment. Hence, procedures currently employed for critical crack assessment are still deemed valid and conservative enough for Australian operations.

Keywords: Stress Corrosion Cracking, Tomography, Pipeline Steel

v. Table of Contents

vii. List of Figures

viii. List of Tables

ix. Nomenclature

Term	Description
CC	Confirmation colony
CP	Cathodic protection
CT	Computed tomography
DC	Direct current
FC	Fatigue colony
FOV	Field of view
ID	Inner diameter
IG	Intergranular
LC	Leaking colony
M–S	Moomba to Sydney
MPI	Magnetic particle inspection
NN	Near neutral (pH)
OD	Outer diameter
SCC	Stress corrosion cracking
SIF	Stress intensity factor
SS	Straight section
SMYS	Specified minimum yield strength
TC	Teething colony
TG	Transgranular
UoA	University of Adelaide

1. Introduction

Stress Corrosion Cracking (SCC) is destructive cracking in pipeline steel that occurs when there is an aggressive environment and a tensile stress acting on a susceptible microstructure (Parkins 1987, Jayaraman & Prevey 2005). Without all three of these conditions present, SCC will not initiate or propagate. Figure 1-1 shows the envelope in which SCC occurs. As the majority of steel energy pipelines are buried, there is always the potential for a corrosive environment to form due to soil chemistry and humidity. Various forms of cathodic protection (CP) and coatings (Roberge 1999, Fotheringham 1983, Gan et. al. 1994) are installed on in-service pipelines to protect the steel pipeline from many forms of corrosion. However, small faults or defects in the coating can result in regions of unprotected steel, which are vulnerable to SCC.

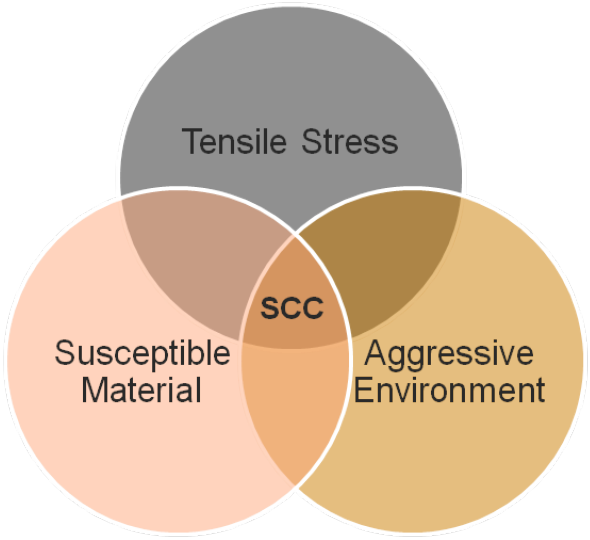

Figure 1-1: Requirements for the initiation or propagation of SCC.

Ultrasonic pigging is used on the buried sections of in-service pipelines to identify any significant flaws in the steel. Pigs are devices that travel through a pipeline that can be used for cleaning or maintenance purposes (utility pigs) as well as for gathering information about the condition, features and integrity of a pipeline. If any significant flaws are found, the pipe is exposed by excavation at great cost to the operator and the coating is removed to enable closer examination of the pipe surface. Magnetic particle inspection (MPI)

technique is used on the outer surface of the pipeline to reveal the presence of cracks that could be SCC. The first step in the method of MPI typically involves grit blasting the outer pipe surface in the region where pigging has indicated the possible presence of SCC. The surface is then painted white (to provide contrast) prior to the application of a black magnetic film to the white surface. A strong magnetic field is applied to the pipe and the magnetic particles in the film segregate to any discontinuities, which in this case are SCC cracks, and produce the black outlines of the cracks as shown in Figure 1-2.

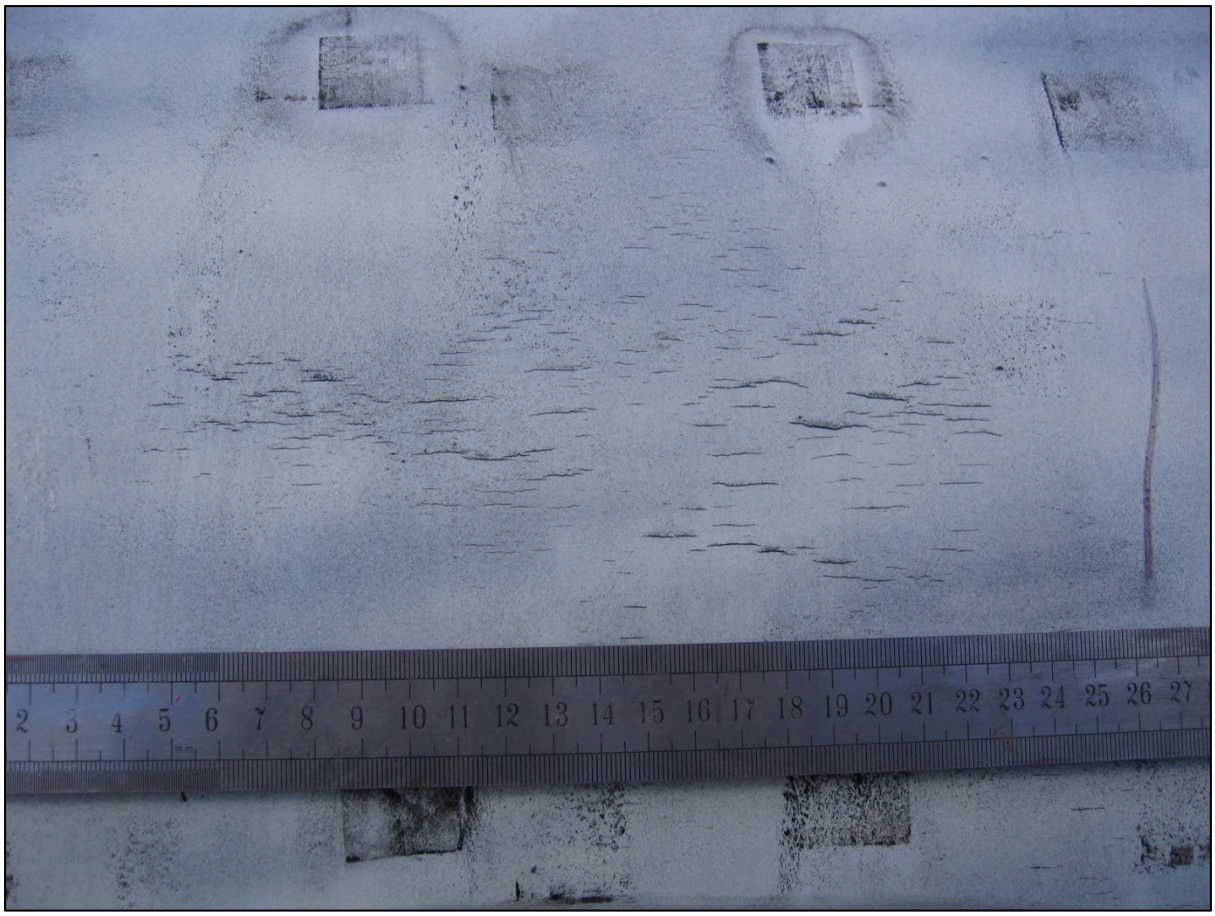

Figure 1-2: Presence of SCC on a pipeline surface as detected by MPI.

On the surface, SCC travels in the pipe axial direction, which is perpendicular to the hoop stresses that occur during operation (Parkins & Fessler 1978). In addition, SCC is found in groups of cracks (termed “colonies”), as shown in Figure 1-3. Typically, the crack propagates in a direction perpendicular to the tangent of the outer pipe surface at the initiation point (Parkins & Fessler 1978, Sutherby & Chen 2004; Xie et al. 2009).

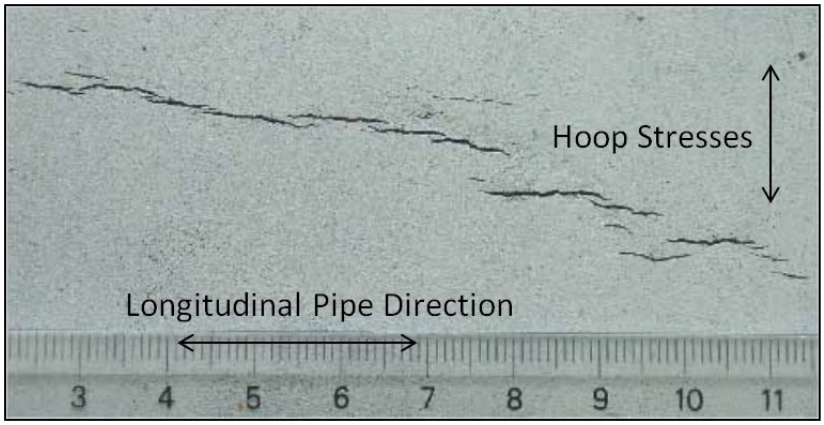

Figure 1-3: SCC colony as seen on an MPI treated pipe surface.

As discovered in Canada (Xie et al 2009, Sutherby et al 2004) and now in Australia (Zadow & Gamboa 2011), SCC does not always propagate in a perpendicular direction. Inclined SCC is a phenomenon where the crack tip significantly deviates from the perpendicular at the initiation point. The mechanism of inclined SCC is not well understood and the instances present in Australia have not been characterised. Thus, there is a significant gap in the knowledge in this specific area and one that this project begins to address. Figure 1-4 illustrates the phenomenon of inclined SCC by showing a polished transverse section of the pipe wall, clearly showing an inclined SCC crack. The outer surface of the pipe is towards the top of the Figure.

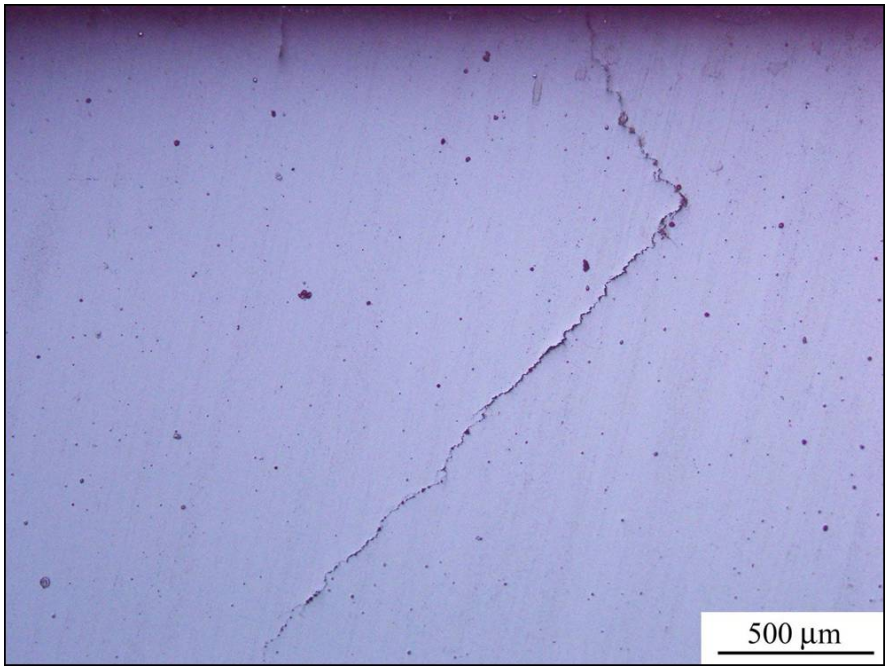

Figure 1-4: Typical inclined SCC

The primary objective of this project is to quantify the morphological aspects of Australian inclined SCC. The impact of inclined SCC on procedures used to evaluate the critical nature of existing SCC is uncertain. In addition, the possibility of these inclined cracks unexpectedly growing together and interacting under the pipe free surface is a major cause for concern. Consequently, this study is highly relevant and important for the safety of personnel and security of pipeline assets.

This investigation is a precursor for future work on the analysis of the driving factors behind inclined SCC.

1.1. Background

Since the recognition of the existence of SCC in steel energy pipelines around the world, much work has been done to gain a meaningful understanding of the driving mechanisms behind SCC (Parkins & Fessler 1978, Parkins 1980, Perez, Rodrigo & Gontard 2011). In addition, it has been vitally important to design effective management systems to mitigate and reduce the potentially dangerous impacts of SCC. This increased awareness, and the subsequent investigations of destructive cracking in steel pipes, has resulted in SCC being observed in a number of countries and regions including Canada, the United States of America (USA), Russia, the Middle East and Australia (Leis & Eiber 1997).

SCC was first observed in a gas pipeline in Australia in 1982 (Fotheringham 1983), and it has been the cause of many significant pipeline ruptures around the world. The rupture of an Australian pipeline in 1982 caused a 12-metre segment of pipe to be blown 170 metres upstream from the failure location (Fotheringham 1983). The subsequent investigation revealed SCC as the likely primary cause for the rupture. In the area surrounding the rupture point, SCC was found on the surface of the pipe, and a number of cracks had interacted with one another.

A significant portion of the SCC threat assessment performed by industry on in-service pipelines uses the *Stress corrosion cracking: recommended practices,* as released by the Canadian Energy Pipeline Association (CEPA 2007). This publication was the product of much work done on various pipelines, particularly those located in Canada. The guideline is based on perpendicular cracks and is intended to provide a conservative method for evaluating the severity of cracks located on the pipe wall, as well as interactions between cracks. However, inclined cracks could potentially add complexities to crack interactions that are not addressed in the guidelines. Australian industry requires that all methods used on pipelines located in Australia be sufficiently conservative for safe operations. Therefore, SCC present in Australian pipelines requires thorough investigation, characterisation and evaluation particularly with respect to crack interactions, to determine whether inclined SCC cracks can still be safely assessed by CEPA guidelines.

Work undertaken on this project analysed cracks from the SCC affected areas of a segment of the Moomba to Sydney (M–S) pipeline. This section of pipe had been removed from the pipeline due to the severity of the SCC found in it.

1.2. Scope and Objectives

The objective of this study is to examine or survey a number of SCC cracks with the purpose of quantifying the crack morphology, with a particular interest in the occurrence of inclined cracks and any observable crack interactions. The more specific primary objectives of this project, for a single section of pipe are as follows:

- determine the percentage of inclined cracks
- determine the percentage of co-linear/non-co-linear cracks
- develop a relationship between hoop travel and crack length

- determine the level of subsurface travel present
- determine the level of interaction between cracks
- develop guidelines for crack interaction (in this pipe section with the aim of extrapolating the results to the remainder of this pipeline).

It is the belief[1] that current industry techniques for analysing specific cracks and their interactions are conservative for operations within Australia. It is important that it be confirmed that these guidelines are proven sufficiently conservative even when inclined SCC are present. This is the motivation for the project and the completion of the stated objectives.

The principle methods chosen for analysis of SCC in the present study were metallography and X-ray tomography. Metallography was used to satisfactorily describe the morphology of each crack subjected to investigation. A method for the application of X-ray tomography was developed because tomography has great potential for viewing potential crack interactions within the steel.

1.2.1. Statistical Significance

Work analysing the SCC cracks in the ex-service samples was preceded by ensuring that the results would be relevant to both industry and the objectives of this project. In addition, it was essential to ensure that the results obtained were from a sufficiently large sample size to be statistically significant. Before analysis commenced, the aim was to study a minimum of 96 cracks. This number was determined using the 90% confidence formula:

$$n = \left(\frac{1.96}{2e}\right)^2$$

The estimated error 'e' was chosen to be 0.1. This showed that a minimum of 96 SCC cracks were required for analysis to satisfy the statistical 90% confidence level. With this known, the tentative aim was to analyse an optimistic number of 200 cracks improving the significance.

[1] Sourced from private communication with an industry representative (November 2011)

As the analysis progressed, it became apparent that due to time constraints, it was not feasible to analyse 200 samples. The maximum number that could be analysed in the time available was determined to be 120. The results are still statistically significant and conclusions and observations over the data set could be made with a 91% confidence level determined using a set sample size in the above formula.

1.2.2. Limits and Exclusions

Practical specimen preparation limitations determined that the minimum distance between polished cross-sections was 1 mm. For cracks longer than 25 mm, the spacing between cross sections was at times increased to 3 mm to reduce specimen preparation time. The number of samples analysed was limited due to the time taken to complete a single metallographic slice as previously stated.

The examination of the samples was time intense. Each slice was removed from the pipe section using a wet abrasive saw and subsequently required mounting, manual grinding, polishing, metallographic examination, data recording and a comprehensive image collation. This further limited the number of samples that could be examined in the time available. With a more automated procedure of the grinding and polishing for each sample, samples could have been analysed more quickly and efficiently.

The vast majority of the 120 cracks analysed were taken from three colonies of cracks that were all from the same 12-metre section of pipe. The three primary colonies were spread axially along a 4.1-metre length of the pipe, which is not a large sample when compared to the many thousands of kilometres of pipeline spread across Australia. However, they are separated enough to rule out highly localised conditions that may have existed.

1.3. Report Structure

This report will use Chapter 2 – Literature Review to introduce and detail SCC in terms of classification, typical features or trends, and the reported observations of inclined SCC. The purpose of this review is to enable the gaps in the knowledge regarding inclined SCC to be outlined in Chapter 3 – Gap, as it is the objective of the current work to address these gaps.

Chapter 4 – Experimental Method outlines the methodologies used for specimen preparation and to enable the gathering of the data as detailed in Chapter 5 – Crack Analysis

Methodology. Chapter 6 – Results presents the results, which are compared with those from Canadian studies in Chapter 7 – Comparison. A discussion of the results in relation to current theories and models is provided in Chapter 8 – Review of Existing Theories. The Importantly, the Implications for Australian Industry are provided in Chapter 9 and this is followed by the Conclusions – Chapter 10.

2. Literature Review

2.1. Introduction

The purpose of this literature review is to provide a background and understanding of the fundamentals of SCC. The primary focus is on the manifestation and morphology of SCC cracks in pipelines, in particular, inclined SCC cracks observed in Canada and Australia.

2.2. SCC Classification

SCC in underground pipelines is divided into two fundamental classifications: high pH SCC and near neutral (NN) pH SCC. Both these classifications of SCC contain colonies of many small cracks that link up in a longitudinal direction. The differences between these two classifications of SCC lie in the SCC growth mechanisms through the pipe wall. NN-pH SCC has been observed primarily in the United States and Canada. High pH SCC has been observed in the United States and Australia as well as various countries in the Middle East (Leis & Eiber 1997).

SCC has been found mainly in low resistivity soils (Baker, Rochfort & Parkins 1987a), but it is questionable as to whether this is a principal environmental factor for SCC. High pH SCC generally occurs above a stress level in the pipe known as the 'threshold stress'. Failures for this type of SCC and NN pH SCC have occurred when the hoop stresses in the pipe are between 46–76% of the specified minimum yield strength (SMYS) for the line pipe (Song 2008). The actual threshold stress can vary greatly and is dependent on whether the applied stress is cyclical and on environmental factors. It has been found that the local environment immediately adjacent to the pipe, which may be quite different to the bulk (soil) environment, dictates which of the two types of SCC is more likely to occur (Gan 1994).

2.2.1. High pH SCC

A feature of high pH SCC is the intergranular (IG) nature of the cracking. Surface corrosion such as pitting or general surface corrosion is not usually obvious on the surface of the steel associated with the crack. General conditions surrounding high pH SCC include a pH window between pH 9 and pH 13 and temperatures greater than 40^{o}C (Elboujdaini & Shehata 2004; Parkins 1987).

2.2.2. Near-Neutral pH SCC

NN pH SCC is a type of transgranular (TG) cracking. It occurs in environments where the groundwater adjacent to the pipe contains dissolved CO_2, possibly from decaying organic matter. Disbonding of the coating allows the presence of dilute solutions of NN pH, which can also develop due to the presence of CO_2 in ground water adjacent to the pipe (Elboujdaini & Shehata 2004). The initiation of this type of SCC is still not fully understood, but a local environment between the coating and the pipe surface with a pH of between five and seven in the free corrosion condition has been associated with TG SCC (Eslami et al. 2010; Kim, Zheng & Oguchi 2004; Parkins, Blanchard & Delanty 1994).

2.2.3. Comparison Between Types of SCC

In a paper by Xie et al. (2009), a table was developed comparing the characteristics of NN pH SCC to that of high pH SCC. Table 2-1, taken from that report, shows that there are many similarities, principally in the orientation of the cracks on the pipe wall and the existence of the cracks in groupings called “colonies”. Table 2-1 also suggests the key differences are the differing fracture modes and the corrosion of the crack walls.

Table 2-1: Comparison of NN pH SCC with high pH SCC (Xie et al. 2009 adapted from Beavers et al. 2001 & Parkins, Blanchard & Delanty 1994)

Table 4 Comparison of inclined SCC with high pH SCC and NN pH SCC characteristics	**NN pH SCC**	**High pH SCC**
Electrolyte pH	6.5–7.5	9–10
Fracture mode	TG	IG
Cracking orientation	Longitudinal	Longitudinal
Numerous cracks	Yes	Yes
Linking of crack	Yes	Yes
Colonies of cracks	Yes	Yes
Corrosion of crack walls	Yes	No
Corrosion of pipes	Sometimes	Usually not
Fe3O4 and FeCO3 films	Yes	Yes

The different fracture modes referred to above are depicted in Figure 2-1 where the cracks (illustrated in red) are progressing through the microstructure. The IG cracking is growing along the crack boundaries and the TG cracking is going through the grains.

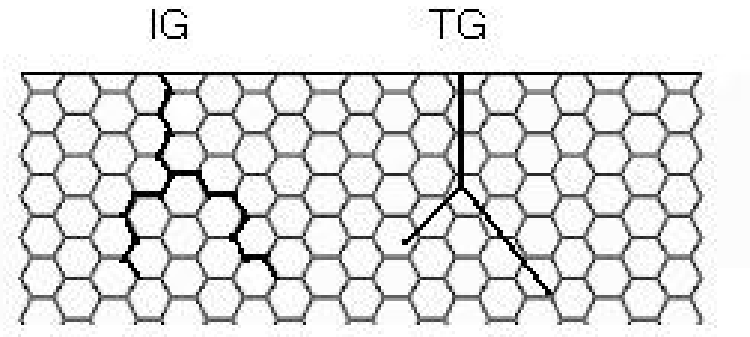

Figure 2-1: IG and TG SCC fracture modes.

2.3. SCC Initiation

SSC can be initiated in multiple ways in a steel pipeline, most commonly through pitting corrosion. Pits, in the presence of hoop stresses in a pipe, act stress concentrators resulting in increased likelihood of SCC initiation at the periphery of the pit. Crevice corrosion can also promote the initiation of SCC, as it provides encouraging conditions for cracking in the region and direction of the crevice (Gan 1994). Once initiated, the crack will propagate along the pipe as SCC.

Pipelines are protected against corrosion by protective coatings in combination with passive and active cathodic protection (CP) systems. Passive CP systems comprise galvanic coupling of the pipeline to a metal anode such as magnesium, which corrodes preferentially to the steel These are termed sacrificial anodes and require periodic replacement. The impressed current CP systems provide an external direct current (DC) and are capable of providing a continuous, constant protecting current on the pipe. The pipeline is kept at a negative potential relative to its surroundings and the current is dependent on the local environment surrounding the pipe, eg the acidity of the soil and the temperature. The CP systems are used on energy pipelines as a second layer of protection against corrosion and move the free potential (voltage) of the structure away from conditions likely to cause corrosion.

It is believed that SCC only occurs in regions where the protective coating has become disbonded (Baker, Rochfort & Parkins 1987a). The disbonded coating shields the pipe wall from the full protection of the CP system allowing the electrochemical potential at the pipe surface to fall into the region for SCC.

For the pipeline being assessed in the current study, a passive system consisting of lengths of 9m magnesium ribbon was put in place initially. After 18 months (Fotheringham 1983), a permanent active CP system was put in place at locations along its length which were designated MW29, MW83, MW130. Surveys undertaken between April 1979 and June 1982 showed that the pipe-to-ground potentials at certain locations were within the intended design limits of between -0.85V to -1.20V potential versus a Cu/Cu SO_4 reference electrode (Fotheringham 1983).

As discussed previously, if the pipe coating is flawed or is not bonded properly to the pipe, it can shield the pipe from the full protecting current of the CP system, with the result that the pipe will be at a potential favourable for SCC initiation and growth. (Gan et al. 1994). Unfortunately, some sections of the coating were applied to the M–S pipeline under non-ideal conditions. These conditions are described below.

During construction, the pipeline was subject to two construction delays due to rain. These delays resulted in pipe sections being scrapped due to excessive corrosion or pitting (Fotheringham 1983). In addition, scheduling pressures (compounded by rain delays), resulted in sections of the pipeline coating being poorly applied. Inspections reported that the coating was not bonded to the pipe itself. This resulted in exposed regions of the pipe where the CP system may not have been fully effective making them susceptible to SCC (Fotheringham 1983).

Figure 2-2 illustrates a crack that has initiated from pitting on the steel surface.

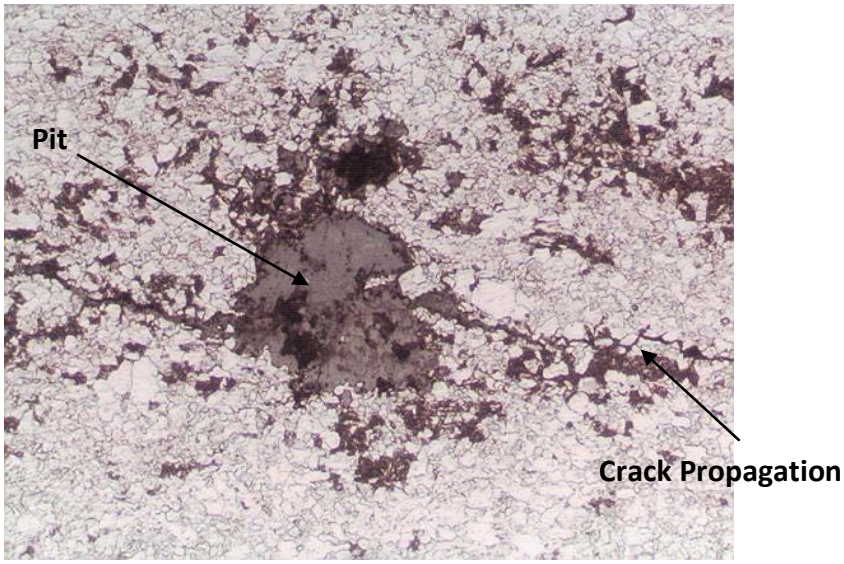

Figure 2-2: Initiation of SCC from pitting (looking at pipe free surface) (Xie et al. 2009).

Under suitable environmental and stress conditions, SCC can also initiate intergranularly on the surface of the pipe without any visible imperfection or initiation location. Figure 2-3 shows SCC initiating at the IG grain boundaries of the steel. There are no obvious signs of pitting corrosion or general corrosion on the surface of the pipe.

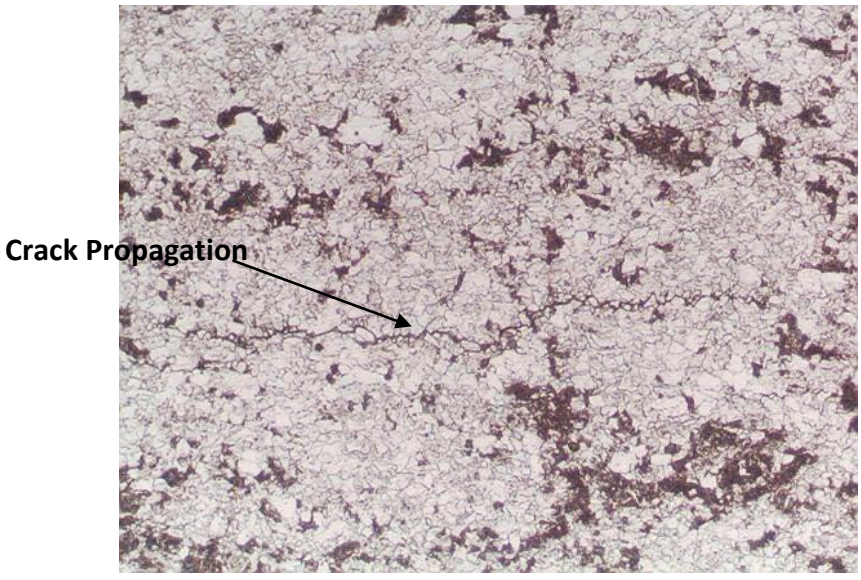

Figure 2-3: Initiation of SCC at the IG boundaries (looking at pipe free surface) (Xie et al. 2009).

Whether it establishes from a pit or from IG corrosion, the stress concentrations in the areas of the corrosion initiate the SCC into the wall thickness (Xie et al. 2009).

2.4. SCC Colonies

Both high pH SCC and NN pH SCC, despite their differences, grow in colonies (Elboujdaini & Shehata 2004). There are two main types of SCC crack colonies: dense and sparse. These classifications relate to the circumferential spacing between the cracks in the colony. A point to note is that this project does not aim to address possible drivers for determining colonies as sparse or dense. It does aim to characterise existing SCC cracks from all available colonies in the ex-service pipe that are available. Sparse colonies are of particular interest, as they have been associated with field failures in the past (Leis & Colwell 1997). Leis and Colwell (1997) explored these two types of observed crack colonies and concluded that sparse colonies (colonies with larger circumferential spacing) contained or had the potential to contain deep cracks, whilst dense colonies (colonies with smaller circumferential spacing) contained shallower cracks. This leads to the conclusion that sparse colonies of cracks are more likely to be the locations for failure in a pipeline.

The results of Leis and Colwell 1997 are presented in Figure 2-4. These results suggest that the cracks in the sparse colony (Figure 2-4a) had a higher propensity to continue to grow in depth. Colonies with dense spacing showed very little evidence of growth in depth (Figure 2-4b). The normalized average crack depth (vertical axis in Figure 2-4) is the average crack depth of each colony analysed, not individual crack depths.

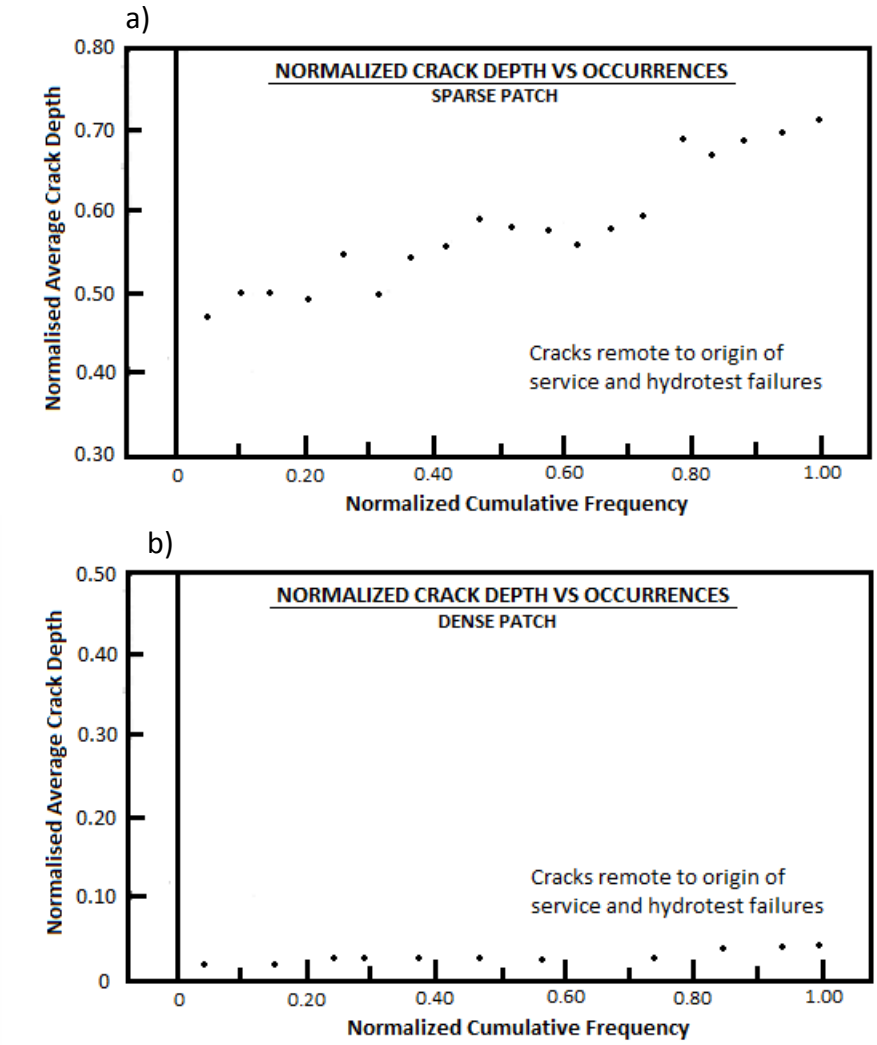

Figure 2-4: Depth of cracks in a) sparse colonies and b) dense colonies that are remote to failures a) 160 cracks from 17 hydrotest failures. b) cracking found in digs remote to failures (replicated from Leis & Colwell 1997).

Subsequently the Canadian Energy Pipeline association has prepared guidelines for classifying dense and sparse colonies relative to the wall thickness of the pipe (CEPA 2007). Colonies of cracks that have a typical circumferential spacing greater than 20% of the wall thickness are classified as sparse colonies and those with a spacing of less than 20% of the wall thickness are classified as dense colonies as shown in Table 2-2.

Table 2-2: Definition of SCC density classification (CEPA 2007)

SCC density	Approximate circumferential spacing
Dense	< 0.2 wall thickness
Sparse	> 0.2 wall thickness

The *SCC condition assessment report* (CEPA 2007) is in agreement with the work of Leis and Colwell 1997 and indicates that sparse SCC colonies are typically found at or near a pipeline failure location and dense colonies are found at a remote distance from the failure location. Gamboa (Gamboa 2011) confirmed this result for a pipeline failure in Australia. Consequently, it is considered more important to analyse cracks within sparse colonies.

2.5. Length to Depth Ratio

The effective crack depth can be plotted as a function of the crack length. The term 'effective' refers to the perpendicular displacement from the surface of the pipe where the crack is located. This is best illustrated in Figure 2-5, where the total effective depth is shown for a theoretical inclined crack.

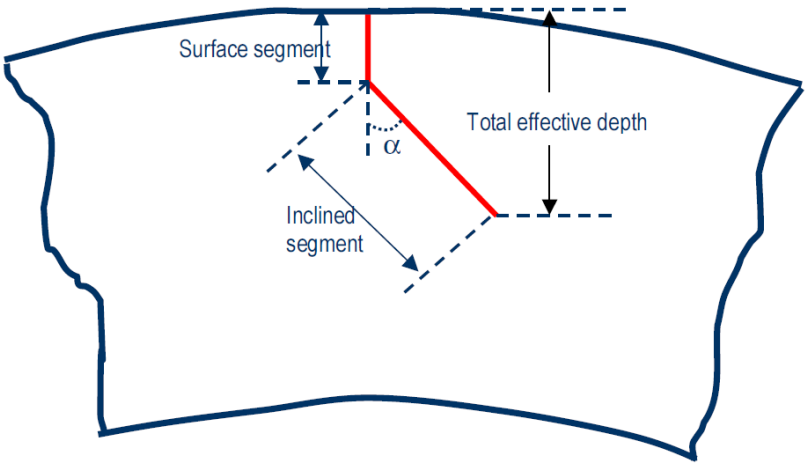

Figure 2-5: Illustration showing measured crack dimensions (Sutherby & Chen 2004).

Since the discovery of SCC in gas pipelines, several studies have been undertaken to characterise the typical aspect ratio for cracks of different lengths (Baker, Rochfort &

Parkins. 1987b; Leis & Colwell 1997). Sutherby & Chen (2004) characterised a number of cracks and plotted the crack lengths at the surface versus crack depths for each crack as shown in Figure 2-6. The results show a linear relationship between surface crack length and crack depth.

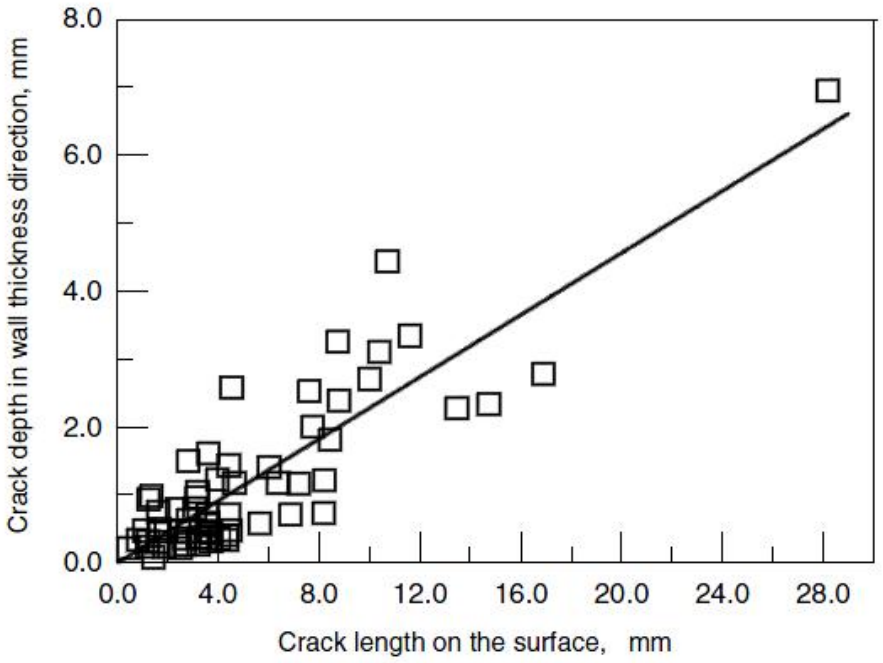

Figure 2-6: Relation between crack length and depth in the perpendicular direction (Sutherby & Chen 2004).

As shown in Figure 2-7, the aspect ratio, which is the ratio of the depth over the surface length, can then be plotted against the crack length:

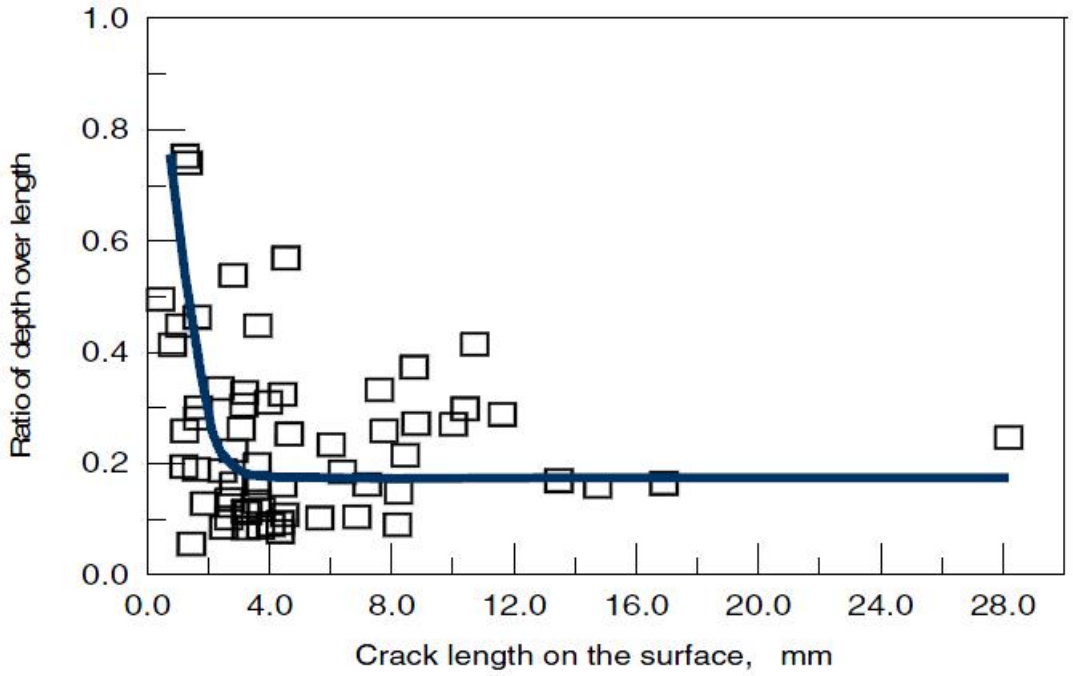

Figure 2-7: Relation between the crack length and the aspect ratio (Sutherby & Chen 2004).

The relationship observed suggested that for cracks with a surface length greater than 3.0 mm the aspect ratio of the cracks remained constant at approximately 1.8. The majority of the data shown in Figure 2-7 is for cracks less than 18 mm in length with only one crack analysed at a crack length of 28 mm.

In 1987b, Baker, Rochfort and Parkins completed a study showing the relationship between the depth and the surface length of cracks. The effective depth of each crack was measured normal to the surface of the steel pipe. This study included both individual and merged (or coalesced) cracks. A plot of their data is shown in Figure 2-8.

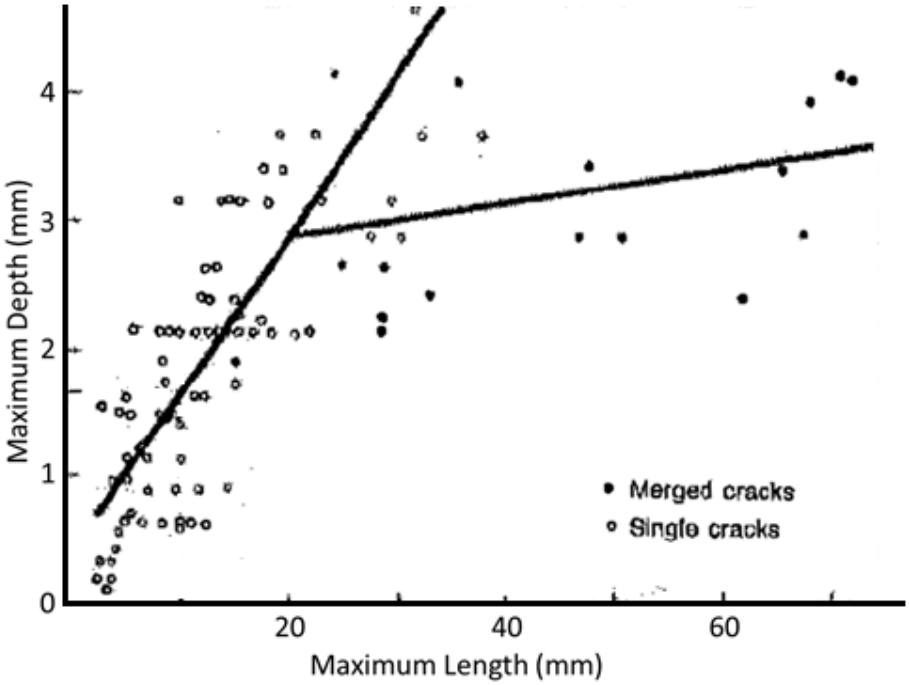

Figure 2-8: Maximum length (x-axis) plotted against maximum depth (y-axis) (Baker, Rochfort & Parkins 1987b).

From Figure 2-8, for individual cracks, the aspect ratio of crack depth to crack length changes at a rate of approximately 0.127. However for merged cracks the rate of change of the aspect ratio for cracks longer than 20 mm is reduced to 0.013. That is the depth of the crack increased at a rate approximately one tenth of that for an individual crack for a similar increase in length. The values shown in Figure 2-8 for individual cracks are in agreement with the previously presented study (Sutherby & Chen 2004).

Numerous studies have been conducted on single cracks concerning the length to depth ratio (Baker, Rochfort & Parkins 1987b; Leis & Colwell 1997; Sutherby & Chen 2004). These studies—most notably that of Baker, Rochfort and Parkins 1987b—imply that the aspect ratio will be smaller for merged cracks. However, the full effect on the length to depth ratio when two or more cracks combine is not fully known, especially with the more recent observation of inclined SCC cracks. Inclined cracks interactions have not been characterised and therefore are not a fully understood phenomena. As a result, one of this project's objectives is to record the appearance of interaction of all cracks analysed. A point to note is that the primary method used in SCC crack analysis, metallography, is not the most ideal

method for analysing crack interactions due to the smallest feasible distance between transverse views existing at 1 mm. However, from the results available, crack interaction guidelines can be assessed to determine the conservative nature of them as well as determining the validity of some reported SCC models.

The CEPA guidelines (CEPA 2007) observe both a qualitative and quantitative SCC depth determination. This indicates the allowable limits of the depth to length aspect ratio for a particular pipe with respect to the wall thickness. A crack is deemed significant if it correlates to a crack with a depth greater than 10% of the wall thickness (Leis & Colwell 1997). Hence the remainder of this report is reporting results primarily of 'significant' crack (depth greater than 10% of wall thickness).

2.6. Inclined SCC

A typical SCC crack would propagate in a direction normal to the surface of the pipe (normal to the hoop stresses). As has been found with initial studies into an SCC affected pipeline in Australia (Zadow & Gamboa 2011), and more comprehensively in a pipeline in Canada (Sutherby & Chen 2004; Xie et al. 2009), the cracks do not always travel perpendicular to the hoop stresses. The crack path of some SCC cracks has been observed to travel at an angle to the perpendicular and these cracks are referred to as inclined SCC cracks. This phenomenon has been observed, or at least recognised, in only two countries in the world (Gamboa 2011), with a very small number of publications to date. Inclined SCC therefore has only recently been recognised and research in this area is required to assess its impact on previously accepted maintenance and inspection procedures.

A recent study has shown that SCC cracks can be classified into three categories based on their visual appearance (Xie et al. 2009). This method of classification is more of a description of the geometry of the crack and the way it propagates through the pipe wall. The geometrical classifications are:

- straight (where the crack propagates in an approximately straight path normal to the principal stresses)
- zig-zag (where the crack propagates initially in a straight fashion and then changes direction towards the circumferential direction at an angle and then changes to the opposite direction)

- inclined (where the crack initially propagates normal to the surface and then changes direction to an angle regarding the radial direction and continues to grow in that direction—Figure 2-3 illustrates what an inclined SCC crack looks like).

A snapshot of the differences in appearance of straight and inclined cracks can be seen in Figure 2-9:

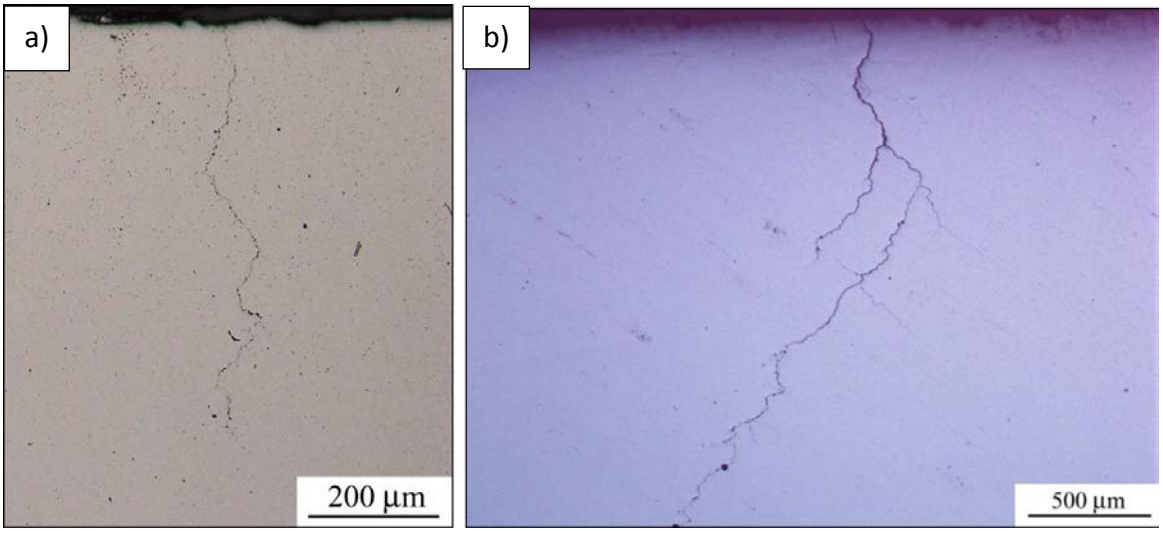

Figure 2-9: a) straight crack propagation, b) inclined crack propagation.

All of the inclined SCC cracks analysed in the Canadian pipeline study were found to be IG and therefore high pH SCC (Xie et al. 2009). This may not be representative of all cases around the world, but could indicate that high pH SCC crack paths are more likely to be inclined than NN pH SCC cracks.

SCC cracks are approximately straight and normal to the principal stresses. The lack of understanding of inclined SCC (cause, growth) may be a contributing factor to previous failures of energy pipelines. Therefore, understanding the nature and morphology of inclined SCC may provide improved SCC detection mechanisms and maintenance strategies.

Inclined cracks penetrate deeper than straight cracks that travel in a direction normal to the hoop stresses. This has been observed in Canadian surveys, which compared the length of inclined cracks to that of straight cracks (Sutherby & Chen 2004; Xie et al. 2009).

Research conducted on the TransCanada pipelines (Xie et al. 2009) revealed that the shape of inclined SCC cracks followed a pattern. The cracks travel perpendicular to the hoop stresses to a depth of between 200 and 600 µm and then the crack would change direction (or deflect) at an angle of approximately 30-60^{o} to the circumferential direction. Consequently, the length and depth results from previous studies where possibly only the perpendicular component of a crack was considered may be incorrect if inclined SCC cracks were present. In addition there are no results available in the literature to indicate the typical distance an inclined crack travels in the direction of the hoop stresses within a pipe under a particular applied stress.

2.7. Inclined SCC Case Studies (Canada)

As previously noted, the information gathered from the SCC affected pipeline in Canada has proven vital in discovering more about the nature and characteristics of inclined SCC, including appearance and frequency. All SCC cracks investigated on that pipeline displayed as longitudinal cracks on the outer diameter (OD) surface of the pipeline, a typical SCC characteristic. The primary report used in this case study examined three SCC colonies. With detailed experimentation and analysis carried out on two of the crack colonies. The majority of the cracks investigated were short with depths less than 40 µm (Xie et al. 2009). Inclined cracks were noted to have a deeper initial perpendicular depth and this was used as a determining factor for the selection of cracks for further study.

The report on the Canadian pipeline provided a table of results reporting all the cracks that were more than 40 µm in depth. Table 2-3 shows the summary of cracks analysed, broken down in terms of the recorded crack depths.

Table 2-3: Statistical analysis of all SCC cracks investigated (Xie et al. 2009)

Colony	**Total cracks**	**<200 µm**	**200–600 µm**		**>600 µm**
			Crack #	Inclined	
#1	18	5 (5%)*	12 (67%)*	8 (67%)**	1 (5%)*
#2	56	32 (57%)*	23 (41%)*	12 (52%)**	1 (2%)*

*ratio of the cracks in a depth range to the total cracks deeper than 40 µm
**ratio of inclined cracks to the total cracks in the range of 200-600 µm

As can be seen in Table 2-3, the ratio of inclined cracks to the total number of cracks in the depth range of 200-600 µm for both colonies investigated was approximately 50%. A slightly larger percentage of cracks in this category were recorded as inclined for Colony #1. However, due to the close proximity of the colonies analysed and the much larger sample size of cracks taken from Colony #2, the tentative conclusion is that if a crack is greater than 200 µm in depth there is a 50% chance it would be inclined. More confidence could be attained through this kind of analysis if a larger sample size of cracks was analysed from colonies further apart. The location of the colonies analysed in this study on the pipeline in Canada with respect to each other is shown in Figure 2-10. Note that the Canadian study initially cut out three sections (all within a metre or so of each other), but only reported crack characteristics for two of these sections (shown above).

Figure 2-10: Locations of the crack colonies on the pipe panel for the TransCanada study (Xie et al. 2009).

As noted previously, the literature on the SCC affected pipeline located in Canada, does not provide any indication of the typical distance the crack travels in the direction of the hoop stresses. In this current study the distance travelled by the crack in the direction of the hoop stresses is referred to as the 'hoop travel' of the crack.

As a result, one of the goals of this research is to survey crack colonies at a significant distance from one another (in the order of several metres) to avoid localised anomalies in the pipe or environment. This will provide a better understanding of whether the cracks follow a trend, inclining in a certain direction, or whether the location of the colonies in the pipe (with respect to the seam of the pipe) has an effect. The data obtained through this literature can then be used to serve a point of comparison.

2.8. Surface Crack Interaction and Coalescence

Visible surface deviations in the path of a crack tip as it grows can be caused by interactions with another nearby crack. The interaction or coalescence of two or more cracks to form one larger crack is strongly dependent on their location relative to each other in the circumferential and axial directions and the cracks' aspect ratios (i.e. the length/depth ratio), (Lam & Phua 1991). Cracks that are a small distance from one another tend to

interact (Lam & Phua 1991), and the crack path is affected. The way this union occurs is dependent on the angle of the cracks to the pipe's surface and to each other.

Crack interaction—assuming that crack growth is perpendicular to the pipe surface—means that when crack coalescence occurs, the crack will merge all the way down to the crack tip (Wang et al. 1996). Attraction between cracks is expected when they are within a specified distance and location from each other. When merging, the depth of the crack will usually increase.

The minimum specified distance between cracks in both the circumferential direction and the axial direction to avoid coalescence is outlined in the CEPA guidelines (CEPA 2007). These can be represented by the following formulae (CEPA 2007):

$$Y \leq \frac{0.14(l_1 + l_2)}{2}$$

where Y is the maximum circumferential distance of interaction, and l_1 and l_2 are the longitudinal lengths of the interacting cracks and

$$X \leq \frac{0.25(l_1 + l_2)}{2}$$

where X is the maximum axial separation of the crack tips of the two potentially interacting cracks. These relationships provide a guideline to indicate whether a crack is likely to interact with another nearby crack. It is important to note that these circumferential and axial relationships were adapted from a previous work (Parkins 1989) that explains the devising of the produced formulae. However, the process by which Parkins work was inputted into the guidelines is not known.

A crack tip in SCC grows in an axial direction along the pipe wall. Deviations can occur in the growth direction of a crack tip due to a number of factors. A major contributing factor to the growth direction of a crack tip is the presence of nearby cracks. The stress intensity factors of the crack tips increase as the cracks approach each other. The stress intensity factor (SIF) is a unit-less term (denoted as K) used to predict the stress state and is explained in more detail in Chapter 7. As they pass one another, K_{II} (the Mode II stress intensity factor) changes sign from positive to a negative and the direction of movement of the crack tip is

altered. This also means that the cracks will converge after the crack tips have passed one another at a certain distance (Wang et al. 1996). This can be seen in Figure 2-11 where the tips of Crack A and Crack B have passed one another and then grow towards each other. This also has the effect of leaving an 'island' of steel in the middle.

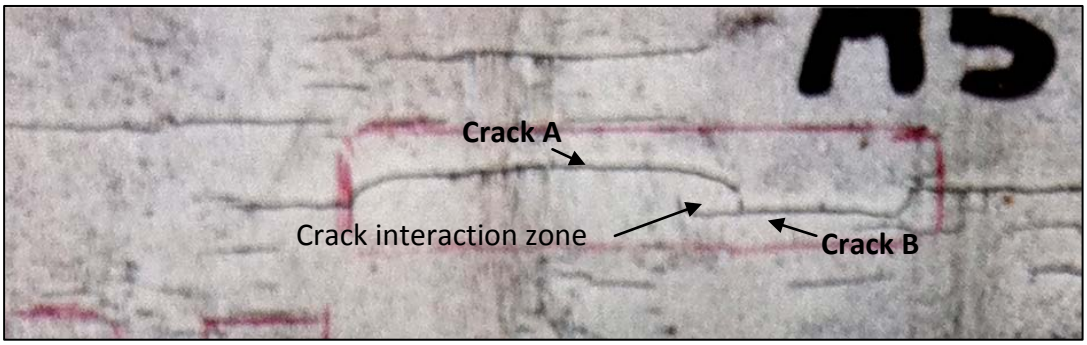

Figure 2-11: Visible crack interaction on the OD surface of the ex-service Australian pipe sample.

An experiment was conducted to study crack interaction and how this might affect the structure of a material (Xie et al. 2009). Crack interaction was found to occur in multiple ways. This interaction is not limited to two cracks combining but also includes the effect on immediate cracks surrounding the interaction.

Factors such as stress shielding will prevent a crack from interacting destructively with another nearby crack. Depending on the relative locations of the cracks, the interaction between the cracks will either enhance the crack growth or "shield" the other crack from the applied stress, resulting in a retardation of crack growth (Lam & Phua 1991). Similarly microcracks can hinder the growth of a crack and in some cases prevent further growth (Lam & Wen 1993).

During the present study, no literature on the study of crack interactions with inclined cracks has been found and some factors that hinder crack interaction are unknown.

Conditions where two adjacent cracks may coalesce is very important in assessing the integrity of a pipeline structure. It is also necessary to understand coalescence in crack colonies containing many cracks (Wang et al. 1996). In 1990, Parkins and Singh (Parkins & Singh 1990) determined that where SCC is present, crack coalescence will also be involved.

Therefore, the need for more research into crack coalescence and the development of effective predictive models (Parkins 1980; Venegas et al. 2009) for the interaction of cracks in a colony is vital.

2.9. Tomography

As stated in Chapter 1.2., this project will examine the feasibility of using high resolution tomography to precisely image cracks. High resolution tomography is a quick and non-destructive method of producing X-ray images that correspond accurately to an object's cross section. By taking sequential images at different depths through the sample of the pipe wall and compiling these images a three dimensional representation of the object can be created. This three dimensional computer generated image can then be digitally manipulated to enable a large number of measurements and observations to be made. (Ketcham & Carlson 2001). Tomography can reveal the morphology of crack paths through a metal. The computer generated images are geometrically precise and therefore can be used to determine linear distances, angles, areas, volumes and symmetry (Conroy & Vannier 1984) of the cracks.

Tomography has been used for viewing the three dimensional nature of SCC in stainless steel where the cracks have been induced in specimens (Marrow et al. 2006). The visualisation of crack morphology is based on variations in absorption coefficients of the material along the path of the transmitted X-ray beam through the specimen. The absorption coefficient has a correlation with density. A change in density within a material will result in a change in grey scale in the image readily enabling the visualisation of defects in metals (Connolly et al. 2006).

There are three components for X-ray tomography. The beam from the X-ray source, which is collimated towards the specimen and a detector which collects the X-rays once they have passed through the specimen. Figure 2-12 is a demonstration of a sample held in a stationary position while the source and detector rotate around it.

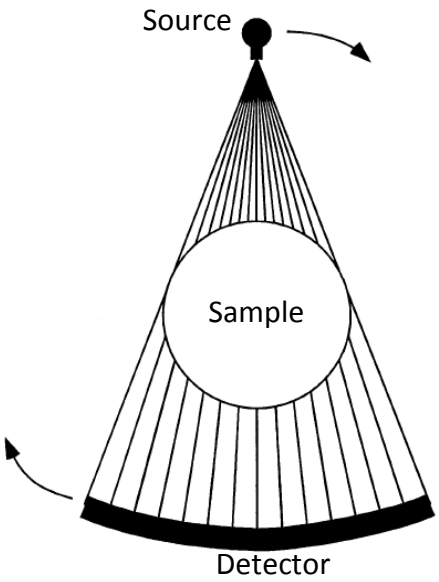

Figure 2-12: Example of X-ray tomography. In this diagram, the X-ray source and the detector rotate around the stationary sample in the centre. The axis of rotation is the centre of the sample (Ketcham & Carlson 2001).

The number and intensity of X-rays striking each region of the detector are translated into an image of the specimen cross section showing defects, cracks or breaks in the material. The following results from an aluminium parent specimen used in a different study illustrate this process. Figure 2-13 from Connolly et al. 2006 demonstrates the results that can be obtained using X-ray tomography. Cross sectional images were obtained from an aluminium sample along its length at the locations indicated.

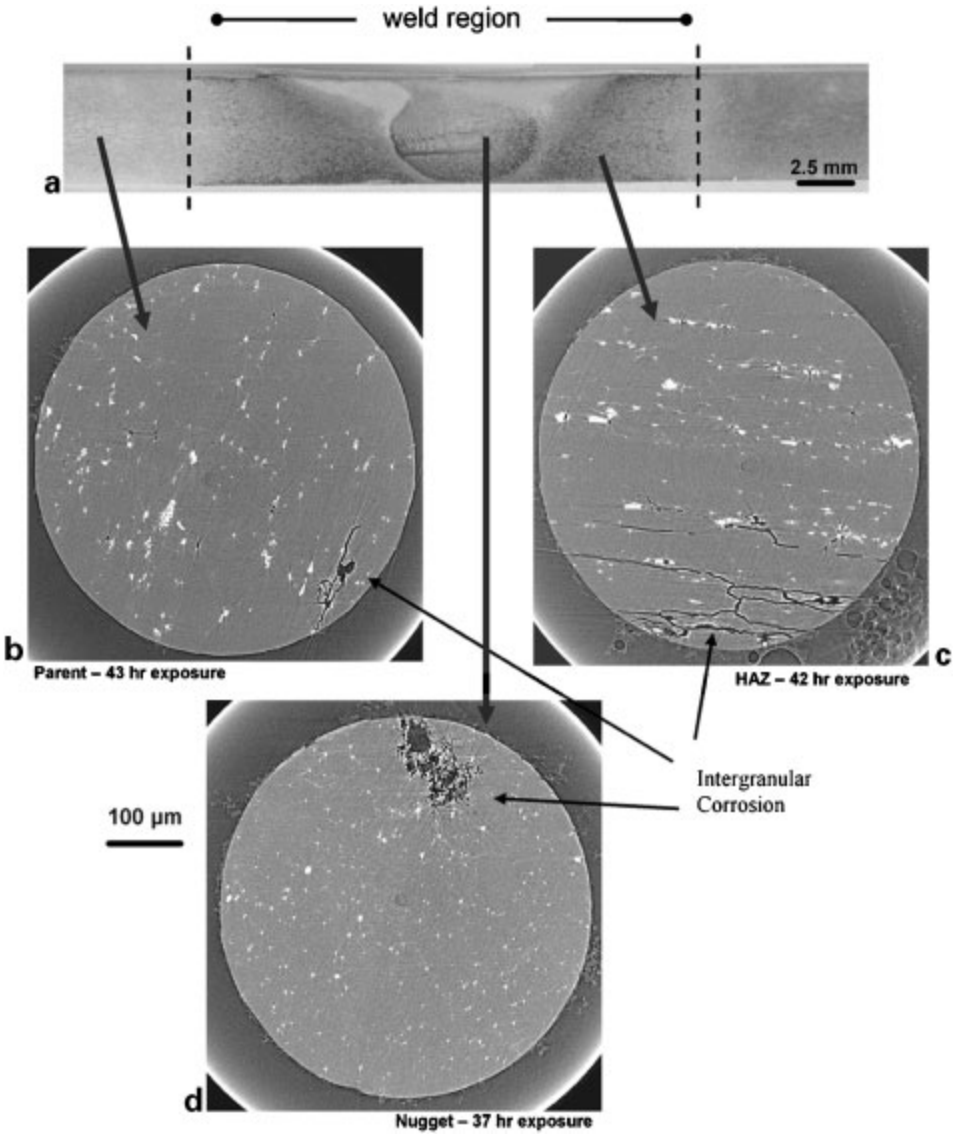

Figure 2-13: Cross sections from three different regions of the sample shown in a) using tomography. SCC had been induced in the aluminium samples and IG corrosion had taken place b), c), d) (Connolly et al. 2006).

The X-ray images of the cross sections (similar to those shown in Figure 2-13) can then be compiled in sequence to create a three dimensional representation of the features being observed. This three dimensional representation can be manipulated on a computer to show different aspects or orientations of the sample. This method of compiling and colourising sequential images is termed rendering. Many cross sections were taken above and below image (c) from Figure 2-13 and rendered to create Figure 2-14, illustrating the induced SCC cracks (green) in the specimen.

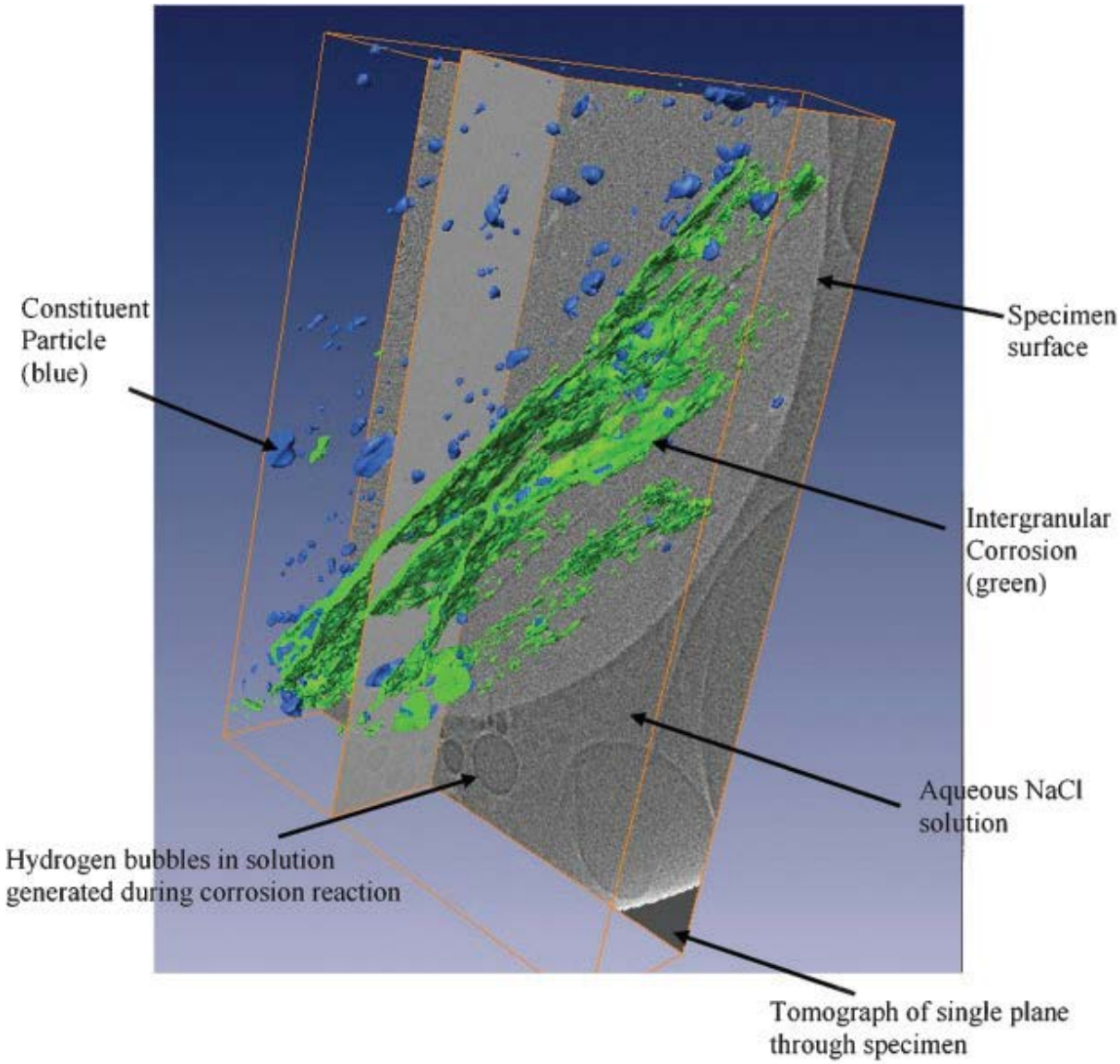

Figure 2-14: A 3-D rendering of Image (c) from Figure 2-13. Only the IG SCC has been visualised along with the constituent particles. This is a compilation of 200 cross sectional slices created a 3-D image (Connolly et al. 2006).

Figure 2-14 is an example of tomography used to create a three dimensional representation of the crack morphology in a cylindrical sample of aluminium. Rendering of this nature is considered useful for visualising crack interactions

Previous studies have shown that tomography is useful for the examination of cracks in steels. Marrow et al. (2006) used tomography during an investigation of IG SCC in type 302 stainless steel. Gamboa and Sneddon (2011) completed a feasibility study using the equipment available at the University of Adelaide (UoA), using pipeline steel samples. The

results of this study demonstrated that the equipment at the UoA could be used successfully to visualise cracks and the associated interactions. The same equipment and procedures will be used in the present study.

The resolution of X-ray tomography available is approximately six micrometres, meaning that features at, or above, six micrometres in size can be resolved using this tool in a time effective manner. Therefore, crack morphology results are expected to be within six microns and tomography can be used to accurately map SCC cracks to determine whether they are inclined and if so, how they interact with one another when in close proximity. For the machine available, this was the maximum resolution achievable.

Ideally the aim of this report is to show development of this method of crack analysis with particular interest in crack interactions. The main work through this project was focused primarily on metallography as previously stated.

2.10. Pipeline Details and Specifications

The pipeline steel samples selected were taken from segments of the Sydney to Moomba pipeline. Cracks have been observed in this pipeline, which is made from submerged arc welded API 5L grade X65 steel, and has a pipe diameter of 864 mm OD and an approximate overall thickness of 8.4 mm.

The tested physical properties of this steel are listed in Table 2-4:

Table 2-4: Material properties for pipe analysed[2]

Test no	Sample id	U.T.S MPa	0.2% Proof stress MPa	Elongation %
T9792	T1	579	435	25
T9791	T2	574	444	25
T9789	B1	579	484	26
T9790	B2	578	464	26

Three of the four colonies analysed (CC, FC and LC) were taken from the same pipe section. Appendix A shows the location of the colonies relative to the pipe segments. As these

[2] Material properties obtained through testing API 5LX65 steel using the test specification ASTM A370

segments of pipe were likely from the same batch in the manufacturing process, the chemical composition of the steel would not be expected to vary much. The chemical composition measured for both relevant sections, shown in Table 2-5, illustrates this.

Table 2-5: Chemical composition of the X65 pipe steel (industry tested).

	C	P	Mn	Si	S	Ni	Cr	Cu	Al	Nb	Ti	V	N
Section B	0.070	0.013	1.49	0.30	0.0035	0.024	0.32	0.16	0.025	0.046	0.003	0.003	0.0065
Section D	0.075	0.022	1.57	0.33	0.0040	0.024	0.32	0.21	0.037	0.054	0.003	0.004	0.0063

As already mentioned, the pipeline used in this study is from the Sydney-Moomba pipeline, already known to suffer from instances of SCC that negatively affect the original asset's lifetime predictions and require expensive maintenance. Further details of this pipeline and examination of the SCC in this pipeline have been presented in previous APIA research project reports (Gamboa & Linton 2010; Linton, Gamboa & Law 2007).

'Pigging' results in the pipeline revealed a long section of pipe that had dispersed colonies of SCC. Pigging refers to the commonly used practice of sending pipeline inspection gauges or 'pigs' through a pipeline while it is still in service. In this case, the pigging locates SCC in pipe sections. The severely SCC affected section of pipeline was cut out for further investigation and studies have been carried out on colonies in the pipeline (Linton, Gamboa & Law 2007). That Linton report primarily analysed four colonies in this section of pipe and these sections have been identified in terms of location and crack density in a subsequent study (Zadow & Gamboa 2011).

The colony codes and distances from one another are noted in Table 2-6.

Table 2-6: Colony locations and longitudinal distances (Zadow & Gamboa 2011)

Pipe number	**Colony Name**	**Pipe Section**	**Colony Code**	**Angle (deg)**	**Distance along pipe (m)**	**Longitudinal diff(m)**
0092–11038	Leaking Colony	B	LC	12	137742.34	
0092–08286	Confirmation Colony	B	CC	358	137745.21	2.87
0092–08297	Fatigue Colony	B	FC	22	137746.41	1.2
0092–08632	Teething Colony	D	TC	215	137801.21	55.1
					Total	**58.87**

The angle shown in Table 2-6 is the distance each colony was around the pipeline from the weld seam in the pipe section. Of interest is that this also provides information concerning the circumferential separation of the colonies.

The results from the pigging data, which was obtained for the section of pipe analysed, gave information on the relative location of all SCC colonies within the pipe section. The locations of these colonies can be seen in Appendix A.[3]

2.11. Summary and Conclusions

SCC currently poses a significant problem for the pipeline industry. Investigations in Canada, combined with early indications in Australian pipelines, show the presence of SCC cracks that do not grow perpendicular to the free surface. These cracks grow at angles away from the perpendicular; they are termed inclined SCC.

SCC generally initiates from pitting in areas on the pipeline where the coating applied to protect the pipeline has become disbonded. Additionally, it has been reported that SCC is not necessarily preceded by general corrosion on the surface of the pipe.

Most SCC cracks in the field have been observed to be aligned along the main longitudinal axis of the pipeline, growing perpendicular to the axis of main hoop tensile stresses. SCC in general is classified as either high pH SCC or NN SCC. The main difference in these types of SCC is that high pH SCC is IG and NN SCC is TG in nature.

SCC cracks tend to be found in groupings termed ‘colonies’. These colonies are classified as either dense or sparse, depending on the approximate circumferential spacing between cracks. Sparse colonies generally contain the deeper cracks. This situation contrasts with dense colonies, which although normally containing more cracks, actually contain relatively shallow cracks in comparison. Thus, cracks in sparse colonies threaten pipeline integrity more severely, and cracks in sparse colonies have previously been observed near the location of pipeline failures.

The length to depth ratio is an important factor for understanding the cracks that are considered critical or warrant further investigation. Different aspect ratios are expected

[3] Appendix A has been constructed from pigging data supplied by APA

between sparse and dense crack colonies. The aspect ratio of cracks attained from literature will be used to decide what cracks in the pipeline under investigation have the potential for significant depth.

SCC crack interaction guidelines have been produced in the past (CEPA 2007) to assess the cracks that will interact, based on the spacing between them. These interactions occur when two cracks are within a certain circumferential and axial distance from one another and tend towards each other after the crack tips pass. This study is aimed at confirming that current SCC detection procedures are indeed conservative and safe for industry in Australia. The intention is to ensure public safety in the future through potentially improved SCC maintenance parameters.

Crack coalescence is the union of two or more cracks after they interact and grow towards each other. Although it is known that factors such as stress shielding affect the way cracks interact there is little in the literature on crack interaction and coalescence in three dimensions or the distance inclined SCC travels in the direction of the hoop stresses.

Inclined SCC has been observed and investigated in a section of pipe in Canada. However, preliminary work carried out in Australia indicates that the morphology of the Australian inclined SCC cracks may be different to that observed in the Canadian case.

Data can be generated (primarily concerning crack interactions) with the use of X-ray tomography. Tomography utilises X-rays to create cross sectional images that can be rendered as three-dimensional representations of cracks or defects in the sample. Tomography is an effective and precise way to observe the morphology of cracks and to aid in better understanding how cracks interact with one another.

3. Gap

The gap in knowledge, as evident from the literature study, is concerned primarily with the lack of available data pertaining to inclined SCC morphology. Completed work has been chiefly limited to investigation on the length to depth ratio only.

The current research focuses on investigating the morphology of SCC for a large number of cracks present in an ex-service Australian gas pipeline. This crack morphology characterisation will focus on the following:

- percentage of cracks inclined
- typical straight section depth (and observed trends)
- typical hoop travel (in hoop direction)
- inclination factor (ratio of hoop travel to crack depth)
- typical angle of inclination
- subsurface extension of cracks in the axial pipe direction
- observed crack interactions.

The guidelines, developed from work on the pipeline that ruptured in Canada regarding crack interactions, are used in Australian industry as a conservative method for operations (CEPA 2007). To date, this method has proved sufficient, but the margin of safety has not been adequately determined.

Inclined cracks interacting unexpectedly beneath the free surface have damaging potential. This could explain the behaviour of certain cracks that have not interacted for any visible reason on the free surface, or cracks that interact but fail to join up and become dormant. This study will observe trends on crack interaction and will aid in developing techniques to identify the probable direction of crack inclination.

The effect of interaction and coalescence of cracks on the depth direction of the cracks remains to be fully understood. This current study will not only seek to ascertain the proportion at which cracks are inclined, but also to determine qualitatively how such cracks interact with each other, and if there is a potentially serious concern for the pipeline industry. With this study, it is hoped that pipe operators would be able to estimate the likelihood that a crack is inclined, requiring extra considerations, while assessing failure

propensity. In addition, this will provide a duty of care to the public by confirming that current industry practices are conservative regarding safety.

It is desirable that in the future, the results of the current work can be used as guidelines for the assessment of Australian pipelines containing SCC

4. Experimental Methods

Two methods were used to produce the results for this project: optical metallography and X-ray tomography. Prior to analysing the SCC cracks in the failed Australian pipeline, the pipe surface required preparation to enable the accurate determination of the locations and lengths of the SCC.

The preparation process in cleaning the surface of pipeline consists of removing coating on the steel and grit blasting leaving it with the pure steel pipeline finish. Once cleaned, magnetic particle inspection (MPI) was used to reveal the surface crack path, any crack interactions and for measuring both the crack length and the distance between cracks. The use of MPI involved applying a thin coating of white paint on the surface of the pipeline. Once dried, a solution containing small magnetic particles is sprayed onto the appropriate surface regions. A strong magnetic field is then applied across the regions of interest and the magnetic particles accumulate at discontinuities, e.g. cracks.

Details of the surface crack paths, any observable crack interactions, crack lengths, crack directions and the distance between cracks were recorded and then using the following criteria particular cracks were selected for further analysis.

4.1. Crack Selection

This project aimed to select a large number of cracks considered as significant from an industry perspective. Previous work (Xie et al. 2009) has recorded that small cracks (less than 4 mm in length) are typically less than 600 µm in depth. As this is within the typical recorded range for the straight section length of a crack, cracks greater than this length were desirable.

For a more concrete guideline, the CEPA *Recommended Practices* defines what a critical crack is. It suggests that a critical crack is predicted to have a depth of over 10%wt (wall thickness). With the typical aspect ratio for a crack with a given length reported previously (Sutherby & Chen 2004, Baker, Rochfort & Parkins 1987b), a critical crack length can be determined. The wall thickness of the pipeline analysed was 8.48 mm.

A crack of length 4 mm or greater was considered to be critical and adequate for selection based on the literature review estimation of crack depth.

4.2. Metallography

Metallography is the science of the constitution and structure of metals and alloys as revealed by the unaided eye or using optical, electron optical and X-ray techniques. Before a sample can be examined metallographically it must be appropriately prepared. In this study, for accurate observation of the SCC using an optical microscope, the main preparation steps were sectioning, grinding, polishing and etching.

4.2.1. Sectioning

Once a crack or group of cracks had been isolated for analysis, the cracks were sectioned at 1 mm intervals and analysed. To achieve this, a course grit sand paper was used to grind 1 mm of material away before polishing. This procedure was repeated for all sections analysed.

On occasions for the larger cracks, a spacing of 3 mm was used between cross sectional slices due to time constraints. Instead of grinding the 3 mm away, a metallographic saw was used to cut the material away. The finish remaining was quite smooth and little to no grinding was required before the polishing commenced.

4.2.2. Metallographic Mounting

The majority of samples analysed were mounted in a Bakelite resin to aid in the process of grinding and polishing as this was a manual process. The mounting process included positioning the sample in a compression mould and then pouring the appropriate amount of Bakelite powder on top of the sample. The mould cap was screwed onto the top of the mould. The sample and Bakelite were then heated to the melting point of the Bakelite whilst maintaining a constant pressure applied using a manual hydraulic pump of 25MPa for approximately 10 minutes. After this time, the heater was turned off and when cool, the sample, now embedded in the solid Bakelite, was removed from the mould. The setup used for the mounting of the samples is shown in Figure 4-1.

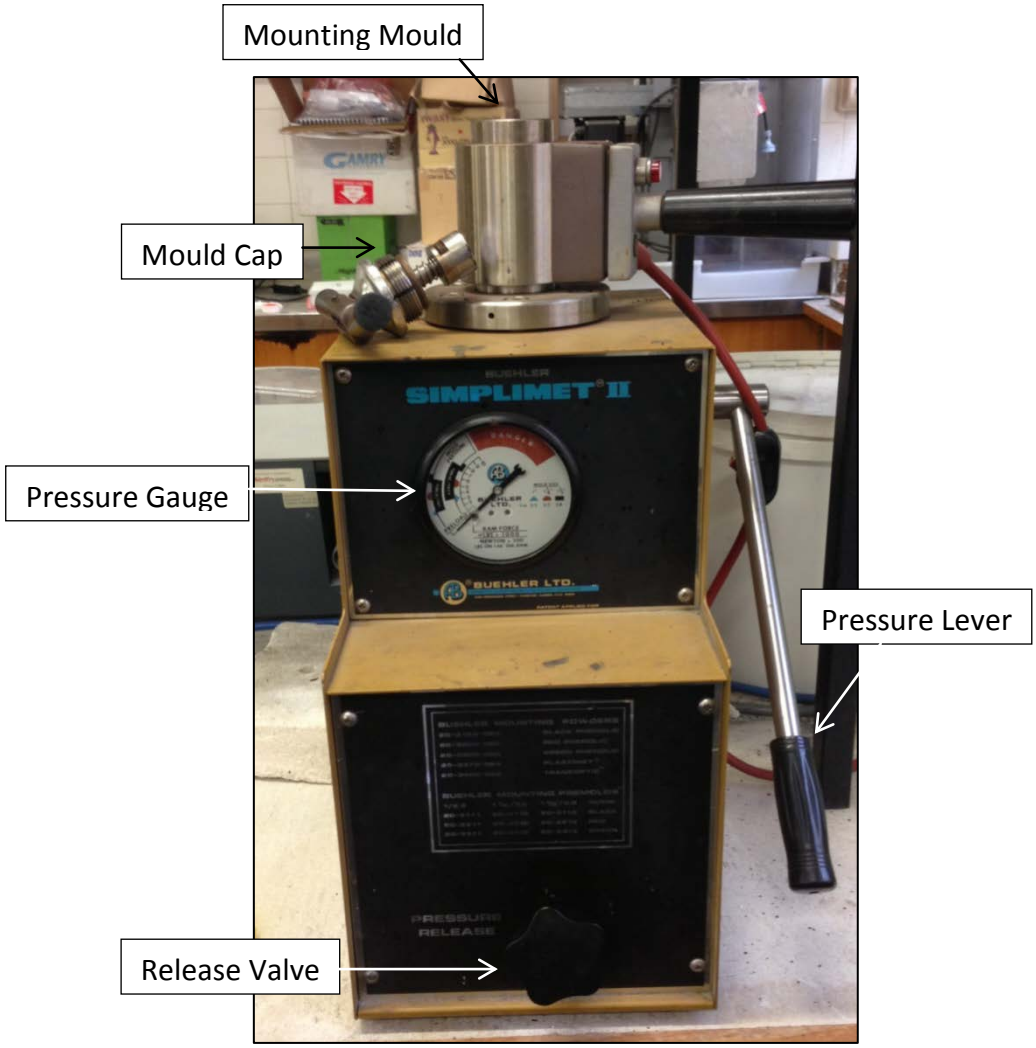

Figure 4-1: Manual sample mounting press.

This process of mounting the sample in the Bakelite mould made the future processes of grinding, polishing and subsequent analysis significantly more efficient and accurate.

4.2.3. Grinding

A series of silicon carbide (SiC) grinding papers were used, to remove the 1 mm of material between each cross sectional slice and to provide a flat surface for subsequent polishing. The coarsest paper which removed most of the material, had a grit size of 80. Once a sufficient amount of material was removed, progressively smaller grit size papers were used to prepare the surface for polishing. The finest paper used had a grit size of 1200. It is important to note that the grinding procedure was carried out with water flowing on to the SiC carbides. The water removes the debris from the paper and acts as a coolant to ensure that the pipeline steel is kept cool to prevent any microstructural changes. The experimental

setup for manual grinding with the papers positioned on two grinding disks is shown in Figure 4-2.

Figure 4-2: Rotating disks used for grinding.

Immediately after grinding the samples were washed with ethanol to prevent the rapid onset of general corrosion on the exposed surface.

4.2.4. Polishing

After the sample had been ground on the 1200 grit sandpaper, it was ready for polishing. The polishing surface was a rotating felt base with 1 µm diamond paste infused across the surface. A methanol-based lubricant was used throughout the polishing procedure. The samples were polished until they had a 'mirror' finish with no observable surface blemishes. Care was taken to ensure that the edges of the samples were not rounded in the polishing process, as this would affect the optical examination and measuring under the microscope. This problem was minimised for samples mounted in Bakelite.

4.2.5. Mounting for Analysis

An optical microscope was used to analyse the polished transverse section of the SCC sample. The sample was placed on plasticine on a metal slide and gently pressed down (shown in Figure 4-3) to ensure the surface of the sample was normal to the microscope

stage to enable the clearest possible image. The ramification of an inclined polished surface to the microscope was an unclear image, particularly at higher magnifications.

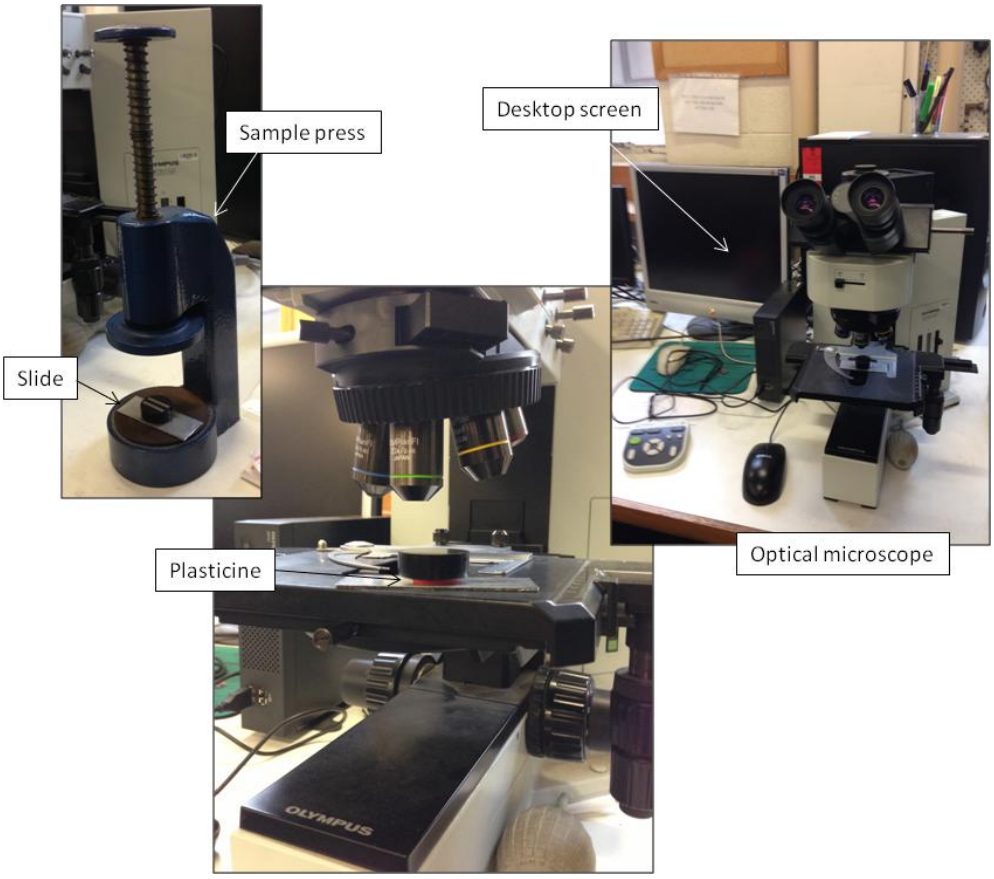

Figure 4-3: Optical microscope and the crack analysis system.

After the sample was mounted and focused correctly, the microscope image was projected onto the desktop screen using an Olympus camera attached to the microscope. With the software available on the microscope camera, measurements of the cracks could be made and recorded and photographs could be taken of each crack analysed.

4.2.6. Etching

After the polishing process was completed, the transverse view of the cracks in the samples could be analysed. However, to observe the microstructure of the sample, the sample required etching. An etchant reveals the microstructural phases as well as the grain size. In order to effectively etch the pipeline steel for analysis, a 2% Nital etchant was used. The etchant was poured onto the surface of the polished sample for a short period and then washed off in running water before being rinsed in alcohol and dried with a heater. Leaving the etchant on for too long can result in an over-etched sample, with indistinguishable

features. Etching was used primarily to determine whether the SCC cracks in the samples were intergranular or transgranular.

4.2.7. Summary

The metallographic process was time consuming. However, the results produced—particularly regarding the crack morphology—are very accurate. However, metallography is not entirely suitable or accurate for analysing crack interactions. Considering these factors, the technique of X-ray tomography was explored. Due to the time required to develop this technique, metallography continued to be the primary method for data acquisition, and it yielded reliable results.

4.3. Tomography

The computed tomography (CT) procedure using the equipment available through Adelaide Microscopy comprised two fundamental steps; sample scanning and image reconstruction.

4.3.1. Scanning

Prior to the scanning process, the sample preparation involved identifying the critical crack for analysis and then carefully machining the sample into a 4 mm diameter sample around the crack. The 4 mm diameter sample was then mounted in the machine in the specimen holder. The following steps were then followed to ensure the best image of the sample:

- Set voltage and current to maximum (100kV, 100µA) = 10W power.
- Select the 1 mm thick aluminium filter (this was the best choice for the machine due to its power limitations).
- Locate the sample in the centre of the field of view (FOV) by translating the stage using the stage motors (a new projection was to be taken each time the stage was moved to observe the changes in positioning made due to no live position feed).
- Use the maximum practical zoom while ensuring that sample stays within the FOV (a new projection was needed for each movement made as there was not a live feed of the position of the sample on the screen).
- Rotate the sample from -90 to +90 degrees using 30 degree steps to ensure that during the scanning process the sample will not go out of the FOV at any time. The sample must be vertical in the FOV. If it is at an angle, the sample needs to be

manually adjusted in the mount. (again, a new projection for each change in sample angle to view changes due to no live positioning feed).

- Set the number of projections to 800 (maximum for the equipment available), corresponding to a 180 degree / 0.225 step size.
- Set exposure time to 10 seconds per step (maximum available).
- Ensure that bright spot reduction is turned on (removes faulty pixels).

Following these steps, the scanning process was ready to begin.

4.3.2. Reconstruction

Once the scan was completed, there were a large number of raw images corresponding to the cross sections through the sample. The reconstruction process followed for the samples analysed was:

- open the projections/scan (files) with the NRecon software
- select a beam hardening correction factor, ring reduction factor and a centre pixel shift.

The three main components are fundamental in removing artefacts that exist in the raw data and improving image clarity. Once a satisfactory setting was found for all these parameters, reconstruction was set in progress.

4.4. Technical Requirements

This study utilised several techniques for crack detection and analysis. The initial crack detection was performed using an MPI kit. The equipment required for metallography included the preparation of a sample and through metallography, grinding papers ranging from a grit size of 80 (coarse) to 1200 (fine) were required before the polishing process. For the polishing process, felt pads mounted on aluminium rotating disks were infused with 1 µm diamond paste and there needed to be enough in supply. An optical microscope was required for analysing the polished samples to obtain accurate morphological data.

Tomography required outsourcing to Adelaide Microscopy. The CT equipment available was required for further investigation.

Analysis was required on all cracks longer than 25 mm, or a group of cracks that had coalesced to a total length of 25 mm or more. In this study, six cracks fitted into this category. No further cracks were available, as industry does not allow SCC cracks to progress to this state without intervention or repair.

5. Crack Analysis Methodology

A major objective of this study was to produce a 'survey' for use as a tool to characterise SCC in a colony with cracks of a given length. Of particular importance is the maximum crack depth and hoop extension of the crack tip from the initiation point on the pipe wall surface.

5.1. Introduction

An effective and proven method for viewing SCC in steel is through metallographic analysis. In the present study the key outcome from this analysis was to determine the morphology of the SCC in the Australian pipeline. Etching was used for each crack to determine whether the cracks were as anticipated IG in nature. A brief micro hardness analysis was completed to determine if there was any observable relationship between the hardness of the pipeline steel in the through-thickness direction and the SCC crack inclination.

Tomography was included in the experimental plan because it has been shown that it has the potential to provide accurate morphological data as well as a three dimensional representation of SCC.

5.2. Data Collection Method

With the metallographic method known, the next step in obtaining results was to ascertain the morphological features that would form the raw data for the SCC present in the samples analysed. For each crack analysed the crack length was recorded.

For the data collection, the data was entered under four main sections that describe the cracks' morphology:

- straight section
- total crack geometry
- inclined segment
- branching.

Under these headings all of the morphological data best describing the crack could be recorded. To record the inclination direction of the inclined crack segments, all cracks were analysed looking in the downstream direction of the pipe when it had been in service. All inclined segments inclining to the left were defined as inclined towards the 8 o'clock

position or clockwise (CW) and segments inclined to the right were defined as inclined towards the 4 o'clock position or counter clockwise (CCW). To obtain the most effective crack visualisation, measurements were taken at 1 mm intervals along the crack path for many of the cracks.

5.2.1. Straight Section

Previous studies have shown (Sutherby & Chen 2004; Xie et al. 2009) that cracks typically have a small segment at the initiation point for a short distance where the crack is perpendicular to the pipe surface. The most important aspect for data collation was to obtain the straight section depth for all the inclined cracks analysed. The straight section can be described in the following terms:

- depth
- number of small turns
- hoop range left (looking downstream)
- hoop range right. (looking downstream)

The straight section was generally not perfectly straight but went through small deviations in direction ($<5^{o}$). The number of directional changes that existed were recorded. In addition, the maximum hoop travel to the left and right of the initiation point was recorded. The left and right directions were determined while looking at the cracks in the downstream direction of the pipe when it had been in service.

5.2.2. Total Crack Geometry

The total crack geometry contains the data that describes the morphological characteristics of the crack 'extremes'. In this section of data collation the following list of measurements were made:

- total depth
- maximum hoop travel (from initiation point)
- maximum hoop travel right (looking downstream)
- maximum hoop travel left (looking downstream)
- number of inclined segments.

The total depth, as well as the maximum hoop extension either side of the initiation point, were measured. In addition, the number of inclined segments of crack after the straight section was recorded. For each of the inclined segments further observations were made.

5.2.3. Inclined Segment

Each inclined segment had a point where it initiated and terminated. The objective of this part of the data collation was to describe the significant inclined segment/s that existed within each crack. The inclined segments were described by:

- inclined depth initiation
- incline direction (looking downstream; o'clock)
- inclination angle
- inclined depth termination
- maximum hoop travel.

The inclination initiation and termination depths were measured vertically from the crack initiation point. The inclination direction was recorded, along with the inclination angle, which was measured from the perpendicular straight crack path. The direction was recorded as either 4 o'clock or 8 o'clock and therefore clearly denoting the inclination direction looking downstream at each sample. The maximum hoop travel measured was the total distance in the hoop direction from the initiation point of the inclination to the termination at the crack tip.

5.2.4. Branching

When crack branching was observed, a recording method was used to best describe the branch. This was done in a very similar manner to that of the inclination angle, where the point at which the branch commenced and terminated were measured. In addition, the hoop travel was recorded as well as the inclination angle of the branching crack, if applicable.

5.2.5. Application of Tomography

The method of analysing the transverse sections using X-ray tomography enabled a more accurate description of each crack analysed to be obtained, albeit at the expense of more post-processing. To determine features such as the maximum depth and hoop travel of each

crack, a three dimensional representation of the crack was required. The point at which these features were found could be determined and the corresponding dimensions could be measured.

5.2.6. Collation of Results and Summary

Using metallography, the transverse section of each SCC crack was analysed with the objective of best describing the crack profile by using the data obtained. The maximum values for the depth, hoop travel and straight section depth could subsequently be determined by collating the data. This method of analysis may not have been absolutely accurate for each crack because the maximum depth may have been located at a position between the transverse sections examined for each crack (typically 1 mm spacing). However, the discrepancy was deemed insignificant, as good crack depth profiles were obtained.

Tomography has the potential to provide very accurate data, as well as a better description of any SCC crack. However a three dimensional representation of each crack was required before the data describing the morphological features of the crack could be recorded.

5.3. Crack Measuring Procedure

For each SCC crack analysed, a specific procedure was followed for measuring the parameters of each crack. This was to ensure that each set of measurements were complete and consistent.

To illustrate this procedure, Figure 5-1 shows the cross section of a single crack (CMI-1 cut 7) with measurements shown. The initial setup procedure was to ensure the sample was positioned in the transverse direction of the microscope stage (pipe sample OD surface was as straight as possible at the top of the image for effective measurements) so that all measurements were parallel to, or perpendicular to, the stage travel. This enabled easier and more accurate measurements to be made using the micrometres used for shifting the stage. The depth measurements were made first and these were done in line with the crack initiation point. The reasoning for this was the following measurements in the hoop direction were all measured from the line representing the location of the initiation point. Therefore, the hoop measurements were made either side of the initiation point.

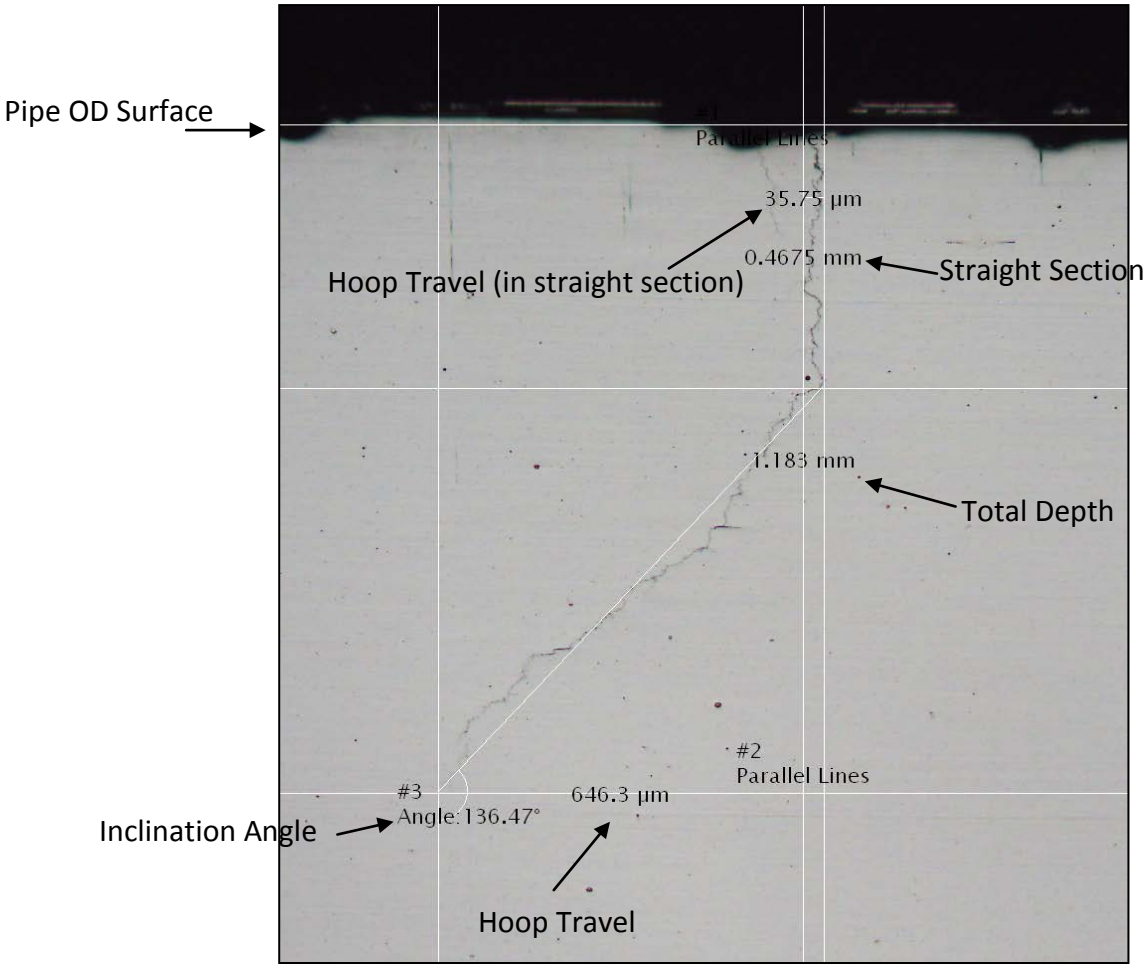

Figure 5-1: Illustration of sample measuring procedure for each cross section.

The crack inclination angle measurement (shown in Figure 5-1) was taken from the crack tip to the point where the crack inclination initiated. This was the typical procedure for most cracks. However, for larger cracks, where the inclination angle changed over the length of the inclined region, the inclination angle was measured in segments.

The sample measurement shown above (Figure 5-1) contains much of the data for entry into the spreadsheet designed for the raw crack data. As explained previously, the recording of data was broken down into four main sections.

Table 5-1 shows the data input into the straight section of this sample measurement.

Table 5-1: Straight section raw data input for CMI-1

Straight section				
CMI-1	Depth (µm)	No. of small turns	Radial range (µm)	
			Left	Right
Cut 7 mm	468	3	0	36

The same recording procedure was adopted for the raw data input for the total crack geometry and this is illustrated in Table 5-2.

Table 5-2: Total crack geometry raw data input for CMI-1 (cut 7 mm)

Total crack geometry				
Total depth (mm)	Max radial travel (µm)	Max radial range (µm)		Number of inclined segments
		Left	Right	
1.183	646	646	36	1

It is important to note that for the section shown in Figure 5-1, there is only one observable inclined crack segment and therefore the input value for number of inclined segments is one. This means that data for only one inclined segment field is required. The raw data entered for the inclined segment in this sample is presented in Table 5-3.

Table 5-3: Inclined segment raw data input for CMI-1 (Cut 7 mm)

Incline segment 1				
Incline depth initiation (µm)	Incline direction (looking downstream) (o'clock)	Incline angle (°)	Incline depth termination (µm)	Max radial travel (µm)
468	8	44	1183	682

The measuring and recording procedure illustrated was completed for each cross section of

each crack analysed. This resulted in a series of raw data for each crack analysed at the defined cut locations.

The data was summarised in a separate worksheet and further under the following headings:

- summary of all cracks (aspect ratio and hoop travel ratio)
- summary of inclination angles
- crack interactions
- straight section
- inclination direction.

The appropriate data were filed into each work sheet, providing the data in a suitable format for further analysis. A sample of this bulk sorted data can be found in Appendix B.

6. Results

6.1. Metallography

Using the data obtained from the SCC cracks in the ex-service Australian pipeline, observations could be made with confidence as to the morphology of the SCC present. Before analysing the cracks, it was confirmed that all existing SCC cracks were travelling axially along the external pipeline wall surface.

The results of this study were divided into key fields. In the past (Sutherby & Chen 2004, Xie et al 2009), these fields have been used to characterise cracks and their behaviour. These fields are:

- SCC crack type
- colonies (dense/sparse)
- percentage inclined
- inclination direction
- length to depth ratio
- straight section
- inclination angle
- hoop travel to length ratio
- branching
- inclusion interactions
- longitudinal subsurface extension
- crack interactions.

These characteristics best describe the SCC crack samples investigated. Cracks interacting and coalescing with one another were also observed. During this investigation of 120 cracks approximately 400 slices were taken using this method of metallography.

6.1.1. SCC Crack Type

From previous work done on the same Australian pipeline (Baker et al. 1987), the SCC has been observed to be IG, indicating high pH SCC. Therefore, it was expected that the SCC analysed in this study would be IG in nature. As stated, for each crack, a 2% Nital etch was

used to reveal the microstructure and in turn, the path the crack travelled through the pipe wall. As expected, all cracks studied were primarily IG in nature.

Figure 6-1 shows one example of an SCC crack examined at the highest magnification available after the polished surface was etched. In the micrograph, the microstructural grain boundaries are evident. The crack path shown is clearly IG as it follows the grain boundaries. The IG crack path (seen in Figure 6-1) is rough and messy as it follows the grain boundaries.

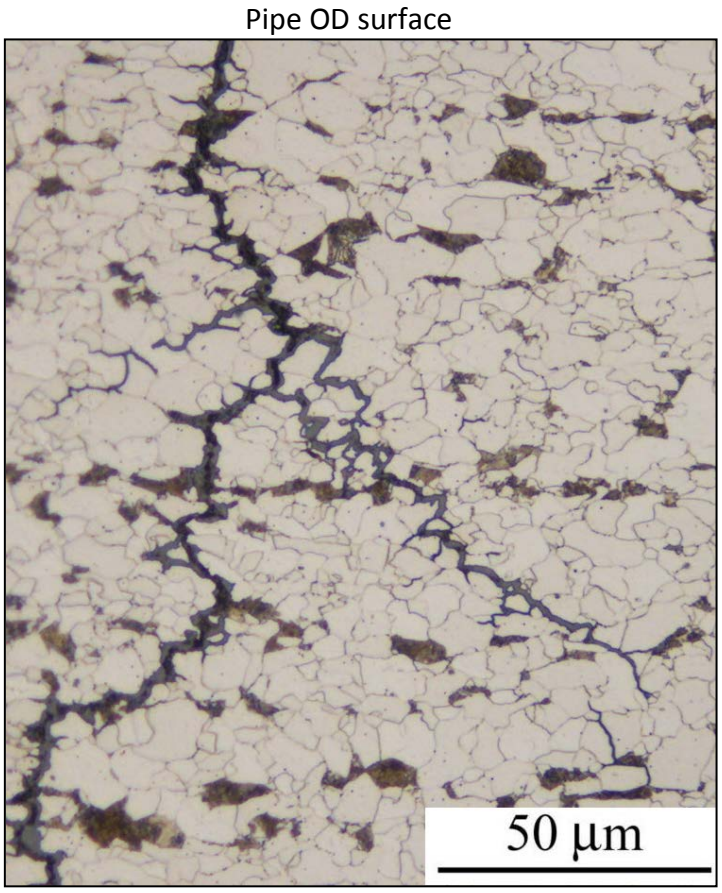

Figure 6-1: IG SCC crack path through the pipe wall.

6.1.2. Colonies (Dense/Sparse)

There are two main types of colonies of SCC cracks: dense and sparse. These dense and sparse classifications are dependent on the circumferential spacing between the cracks in the colony. Leis and Colwell (1997) explored these two types of crack colonies and concluded that the sparse colonies (colonies with larger circumferential spacing) contained,

or had the potential to contain, deep cracks. On the other hand, dense colonies (colonies with smaller circumferential spacing) tended to contain more shallow cracks. Analysis of field failures have shown that sparse colonies of cracks are associated with the locations of failures in a pipeline. Dense and sparse colonies are classified in terms of circumferential spacing (Table 6-1).

Table 6-1: SCC colony classification (CEPA 2007)

SCC density	Approximate circumferential spacing
Dense	< 0.2 wall thickness
Sparse	> 0.2 wall thickness

This current study studied five colonies of cracks. These colonies were labelled arbitrarily and were obtained from the same pipe. They were taken from various positions over a 59m segment of the ex-service pipeline. Measurement carried out on the majority of cracks in each colony revealed the average circumferential spacing between the cracks. This average value was used to find the ratio of circumferential spacing to wall thickness. The results from these measurements and the resultant colony classification for the crack colonies investigated in this study are shown in Table 6-2.

Table 6-2: Classification of each colony

Colony	CC-1	CC-2	FC	LC	TC
Classification	Sparse	Sparse	Sparse	Dense	Dense

Based on observations in the literature (Lies & Colwell 1997), it could be inferred that the depth of cracks in the dense colonies (LC and TC) are shallower than the cracks in colonies CC-1, CC-2 and FC, which were more sparsely separated. In order to obtain significant results, all of the cracks investigated were taken from the sparse colonies. The total number of cracks fitting into this category was 120.

6.1.3. Percentage Inclined

It was necessary to ascertain the likelihood of a crack being inclined or straight in nature. This can influence the estimated total depth of a crack, and the area of influence under an

actual 'typical' SCC crack. Examination of the sample available from the ex-service pipeline revealed that 81% of the cracks were inclined (Table 6-3).

Table 6-3: Percentage of total crack inclined

Classified	Percentage of total cracks
Inclined	81
Straight	19

Based on the large sample size and the high proportion of inclined cracks existing in the sample, it is highly probable that the other instances of SCC at various points in this pipe will display similar inclined crack path trends.

Metallographic observations conducted through etching and systematic hardness testing (HV0.1) revealed no clear cause for the inclination of the SCC cracks. No microstructural features e.g. grain size, presence of inclusions, segregation or decarburised layer, were observed that could explain this inclined crack path.

6.1.4. Inclination Direction

For consistency, all cracks were analysed looking in the downstream direction of the pipe when it was in service. This enabled the study of the direction of inclination to determine the presence of any significant trends.

Table 6-4: Direction of inclined cracks

Direction	Colony LC	Colony FC	Colony CC	Colony TC
% Clockwise	43	44	74	--
% Counter clockwise	57	56	26	--
Total number of cracks	9	9	77	

Of the 81% of the total cracks which were found to be inclined, the percentage of cracks in each colony inclined in each direction is shown in Table 6-4. For colonies LC and FC the proportion was approximately equal. However, for Colony CC, the majority of cracks investigated leaned in the clockwise direction. Colony TC was made up of non-critical (i.e. small) cracks or straight cracks and therefore no cracks in this colony were analysed. Due to its large crack population the majority of inclined cracks analysed came from Colony CC. It is

important to note also that colonies CC, LC and FC were taken from the same 4.1m segment of pipe. The only colony located on a separate section of the pipe was TC which was approximately 56 m away from Colony CC. As previously stated TC contained small non-critical cracks that were not analysed.

Approximately 69% of the total number of inclined cracks analysed were inclined in a clockwise direction when looking downstream. All of these analysed cracks were taken from same pipe segment. Table 6-5 shows the location of the crack colonies from the weld seam. The angle is measured from the longitudinal weld seam for the pipe section and it can be seen that colonies FC and LC are on the opposite side of the weld seam to that of colony CC. The arc distance shown is the distance between the longitudinal weld seam and the top or initiation point of the crack colony.

Table 6-5: Location of crack colonies from the longitudinal weld seam.

Colony	Angle (deg)	Arc Distance (mm)	Colony Circumferential Travel (mm)	Colony Axial Travel (mm)
CC	358	-30	1187	421
FC	22	332	638	880
LC	12	181	771	584

In colony CC, the majority of inclined cracks (74%) tended towards one direction. Such consistency could suggest that the direction in which the crack inclined is related to the plate rolling process or manufacture of the pipe. However, the percentage of inclined cracks in the other two colonies (LC and FC) does not show this weighting, even though they are from the same pipe segment. They are, however, on the opposite side of the weld seam to that of colony CC and metallurgical differences could be responsible for the observed trends. Examination of a greater number of cracks would need to be carried out on a different colony (on the same side of the weld seam) to confirm the clockwise bias of colony CC on the same side of the weld seam.

It can be suggested that two cracks do have a reasonable chance (31% which is the minority percentage of cracks tending counter-clockwise) of growing towards one another subsurface. Observations from the cracks analysed in this study have not found cracks that have grown towards one another within a distance where the cracks could feasibly be

interacting. The determination of cracks feasibly interacting was obtained from the Canada interaction guidelines (CEPA 2007). Stress shielding could be one possible explanation for this observation, although other more complex mechanisms (e.g. microstructural or electrochemical) could be at work.

6.1.5. Length to Depth Ratio

The effective crack depth was plotted as a function of the crack length. The term 'effective' refers to the perpendicular displacement from the surface of the pipe where the crack is located. This is best illustrated in Figure 6-2, where the theoretical crack is inclined and the total effective depth is shown (Sutherby & Chen 2004).

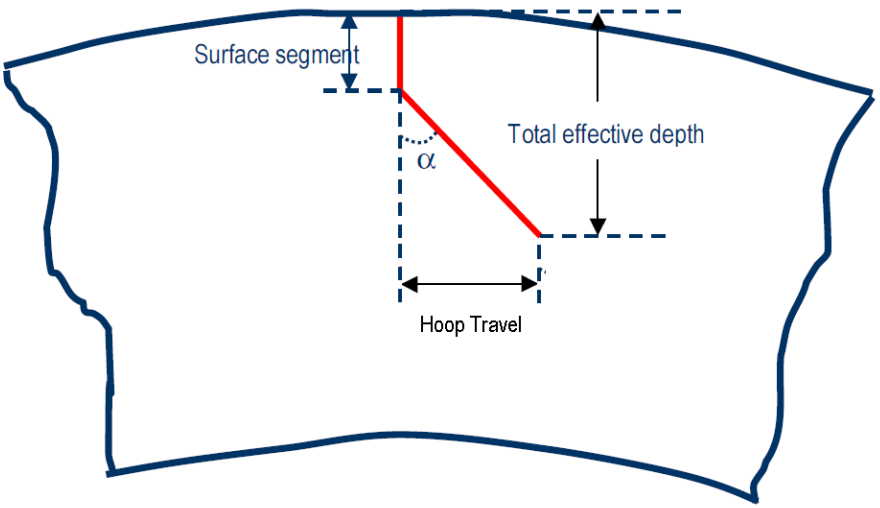

Figure 6-2: Illustration showing measured crack dimensions, (Adapted from Sutherby & Chen 2004).

The aspect ratio has been shown to correlate closely with the type of colony in which the cracks exist. As has been stated, failure location in pipelines is associated with sparse colonies (Leis & Colwell 1997).

Figure 6-3 is a plot of the crack length versus the maximum effective depth for every crack analysed in this investigation.

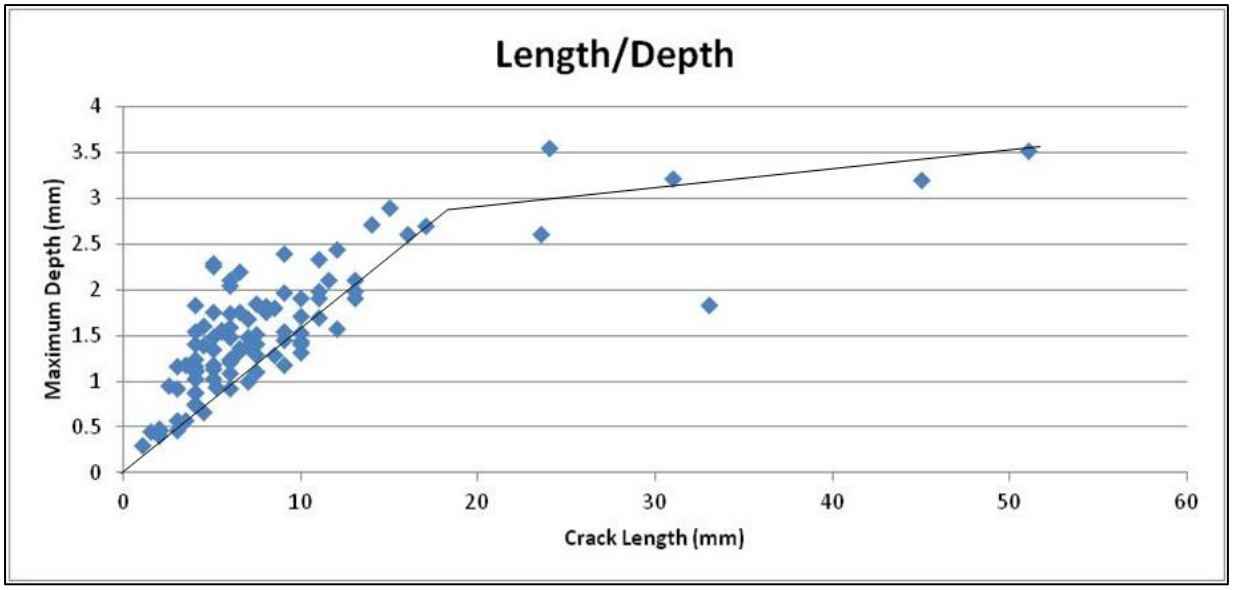

Figure 6-3: Length to depth ratio for all SCC cracks analysed.

The relationship depicted appears to have two aspect ratios. For cracks shorter than 18 mm, the aspect ratio is 0.21 and for cracks greater than 18 mm, the aspect ratio is 0.03. This change in aspect ratio corresponds to a crack depth of approximately 2.8 mm. Crack surface lengths were measured with an error of up to 1 mm on the outer pipe surface. This error was due to the rough MPI characteristics. The crack depths for each cross sectional slice were measured to an accuracy of ±50 µm.

The sudden change in the aspect ratio for cracks greater than 18 mm in length is attributed to smaller cracks having coalesced where there is a significant increase in the crack length but little deviation in the maximum depth. This effect of coalescence on aspect ratio has been identified in a previous work (Baker, Rochfort & Parkins 1987b) that examined the aspect ratio of merged cracks. This trend of the aspect ratio to change at 18 mm could also be influenced by the inclined angle of the cracks. Overall, for crack of length less than 18 mm, the results for the aspect ratio agree with the literature (Sutherby & Chen 2004).

6.1.6. Straight Section

Previous studies have shown that the majority of inclined SCC has a small segment of the crack from the initiation point that is perpendicular to the pipe surface before deviating

(Sutherby & Chen 2004; Xie et al. 2009). Figure 6-4 shows a transverse view of the wall thickness, revealing two cracks, one of which shows significant branching of the main crack path (illustrated). In the cross section, the 'straight section' can be seen on both cracks as the small perpendicular segment of crack from the initiation point before the crack deviates. The straight section is defined as the small segment of crack where the crack is travelling perpendicular to the pipe wall from the initiation point to the point of inclination. The method by which the morphological parameters of the cracks, in terms of the inclination angle and total effective depth, are measured is illustrated in Figure 6-4. Of interest is the very large distance that the cracks travel in the hoop direction underneath the surface (approx. 2.5 mm for the crack on the left and 1.8 mm for the crack on the right).

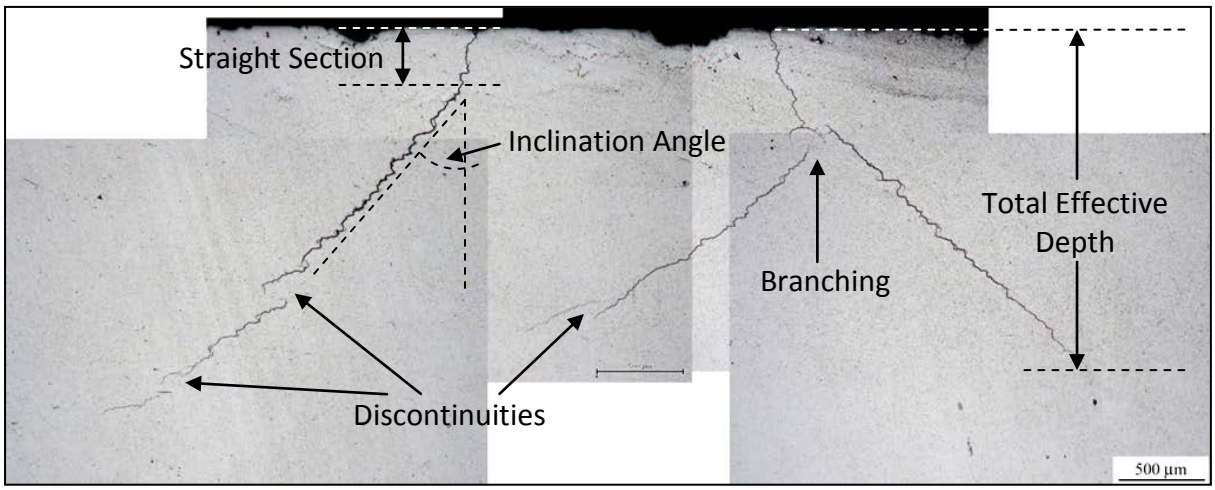

Figure 6-4: Transverse view illustrating SCC cracks with typical straight sections and defining the inclination angle.

The straight section was measured for each metallographic slice of all cracks and the typical depth was found to be in the range of 200–900 µm. Figure 6-5 shows the typical range of straight sections observed. The straight section was consistently measured to an accuracy of ±5 µm or better. It is also important to note the discontinuities present in the cracks shown. Many were observed in the study and were probably a result of crack interactions, however, these discontinuities also occasionally occurred around inclusions.

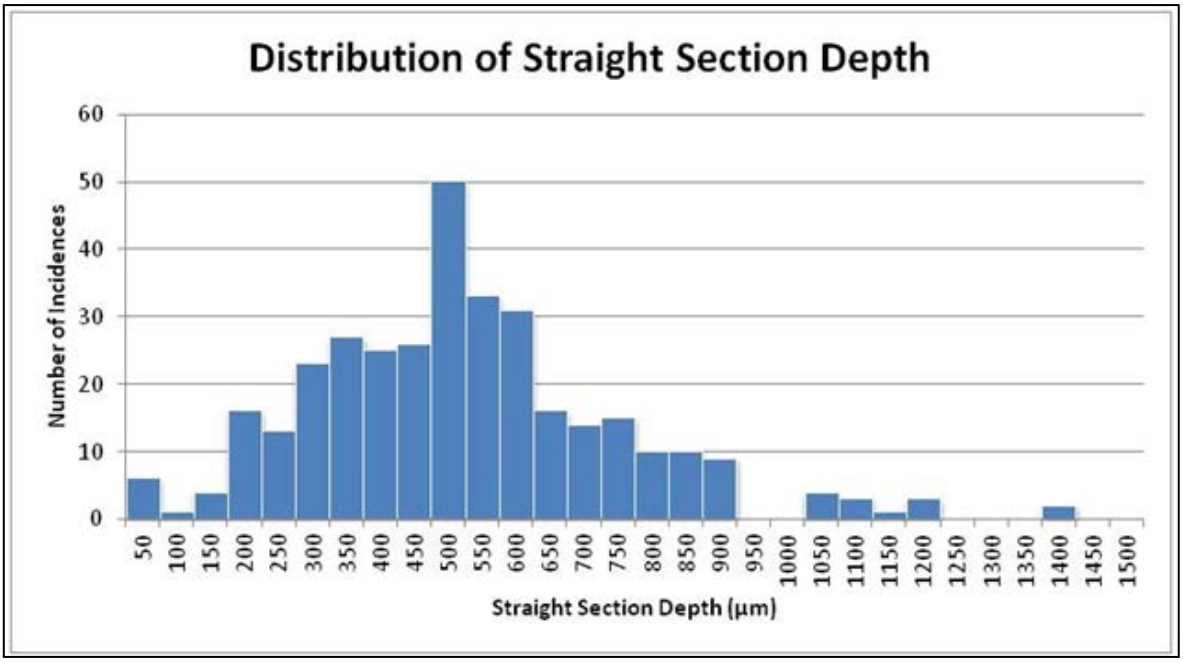

Figure 6-5: Straight section depth distribution for all cracks.

It is important to note that each SCC crack had different straight section depths for each cross sectional slice measured. Therefore, for this study, the straight section depth for each cross sectional slice was plotted, instead of the average straight section depth of each crack. Importantly, the variation in straight section profile for each crack did not follow a specific pattern and therefore no hypothesis on the probable straight section depth could be proposed.

6.1.7. Inclination Angle

During the analysis of each crack length, a large number of cross sections were analysed and it was found that; each inclined crack showed variations in the inclined angle for each slice. Figure 6-6(a) and Figure 6-6(b) illustrate this variation. The two images correspond to the same crack with a 1 mm separation between the cross sectional slices and the radical change in the appearance of the crack path as well as direction is visible.

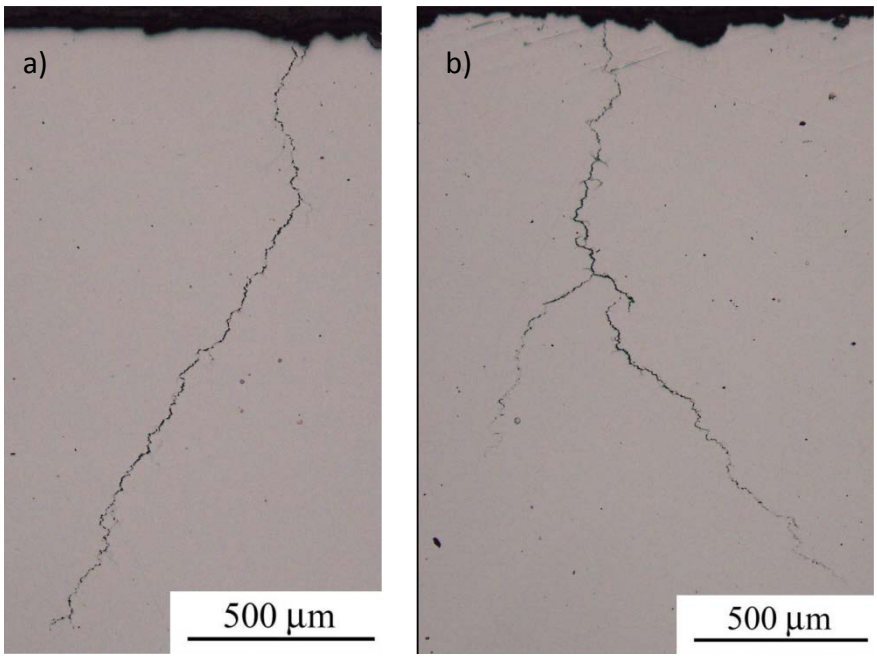

Figure 6-6: Unetched sections (a) and (b) 1 mm apart in the main axis direction. (MPI) of the surface appearance of this crack was straight in the longitudinal pipe direction.

Distinct changes in morphology are evident in the above images. The observable straight section has increased significantly in Figure 6-6b. The main inclined section of the crack has changed direction along with a change in angle. The branching is evidence of potential for a collinear interaction of cracks that are inclined in different directions. Figure 6-6 reveals the complex geometry of paths for each individual crack, even in cross sections only 1 mm apart. The inclination of the cracks represented is typical of the SCC observed, which has a straight section from the initiation at the surface leading to an inclined section.

For all cracks with lengths less than 18 mm or depths less than 2.8 mm, the inclination angle was in the range 30–45 degrees from the perpendicular. The relationship measured between the crack length and inclination angle is shown in Figure 6-7. The error in the results produced in Figure 6-7 is +/- 1 degree. The graph demonstrates the average inclination angle for each inclined crack analysed with many of the cracks less than 18 mm having approximately the same angle (data points overlapping).

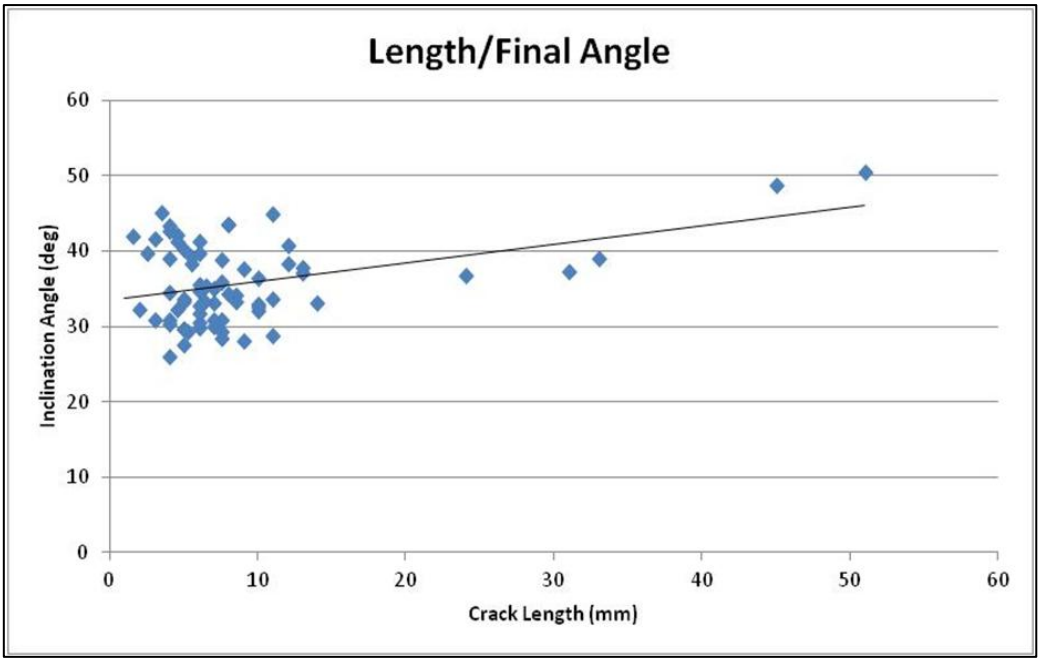

Figure 6-7: Relationship between crack length and inclination angle for all inclined cracks.

The range of 30–45 degrees is not inclusive of cracks greater than 18 mm in length. For the small number of results for cracks greater than this length, the trend observed was that the angle increased at the crack tip. Observation showed that the longer the crack grows across the pipe surface, the steeper the crack angle at the tip. As a result, the crack travelled considerable distances in the hoop direction. The inclination angle was observed as being between 45 and 60 degrees for cracks exceeding 18 mm in length. As a result, the rate of increase in the crack depth reduces and this was shown in Figure 6-3, where the aspect ratio changed at an approximate crack length of 18 mm.

Figure 6-8 is a montage of images of a transverse section through the pipe wall. Solid arrows highlight the initiation points of the three cracks at the pipe free surface. The two surface cracks on the right coalesced at a depth of approximately 500 µm beneath the pipe free surface (dashed arrow). The remaining crack and the coalesced crack grew into the material in directions inclined away from one another. As described above, the crack angles increased the deeper they grew, as illustrated by the black lines drawn parallel to the crack at various locations along the crack path. Of particular importance is that the left hand crack grew 3.5 mm under the surface in the hoop direction and reached a depth of 3 mm in the

through-wall direction. The ratio between the travel distance in the hoop direction and the total effective crack depth has been termed the 'inclination factor'.

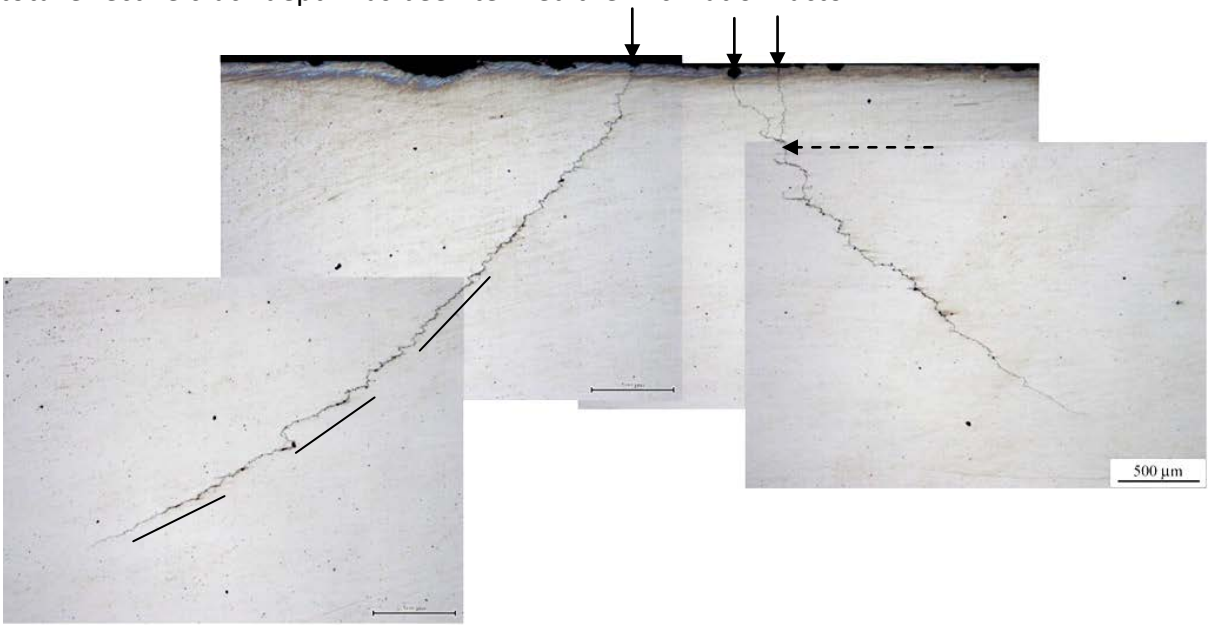

Figure 6-8: Angle changes as the crack grows in the through-wall direction (scale bar is 500 µm).The two cracks on the right have coalesced.

6.1.8. Hoop Travel to Length Ratio

Based on the results obtained for the aspect ratio and inclination angles of the SCC cracks investigated, the relationship between the maximum measured hoop travel and the length of the cracks was expected to be approximately linear, with a steady increase in the hoop travel as the crack length increased. This trend was expected to apply only to the inclined cracks as straight cracks have very little hoop travel for a given depth. This relationship is confirmed in Figure 6-9.

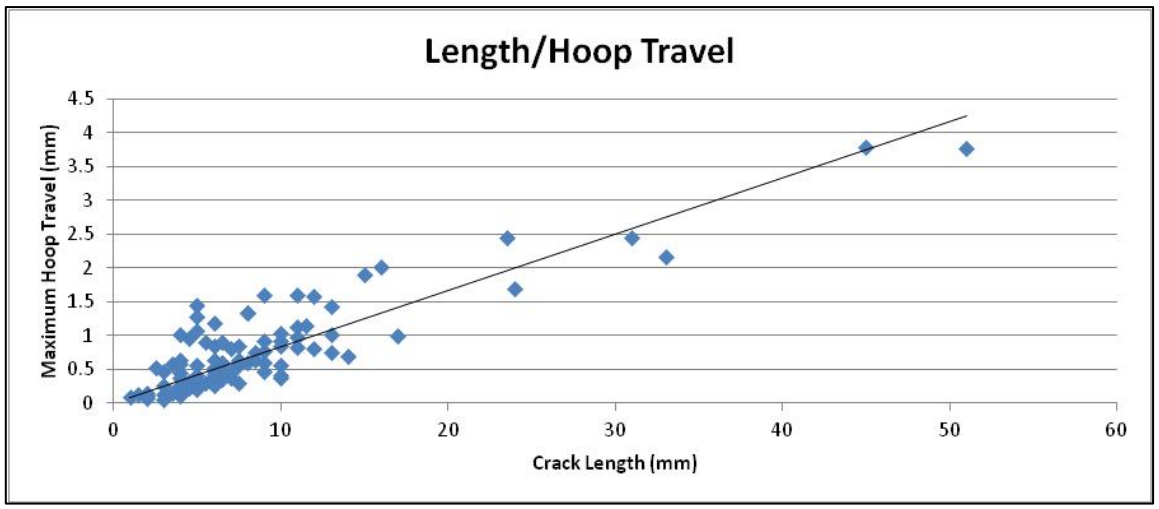

Figure 6-9: Maximum hoop travel plotted as a function of the crack surface length.

The relationship shown in Figure 6-9 leads to the definition of an 'inclination factor'. The linear trend line in this graph is tentative and has been superimposed for discussion purposes. The inclination factor is defined as the maximum hoop travel divided by the surface crack length. This factor aids in identifying a typical or worst case situation with regard to the hoop travel for an inclined crack. The inclination factor obtained for the SCC existing in the Australian pipeline examined is 0.075.

To illustrate the observed increase in angle as the depth increases, the maximum hoop travel was plotted against the maximum depth as shown in Figure 6-10. The large scatter within the few data points obtained suggests the relationship may be more complex than a linear relationship but the general trend is evident. However, more data for longer cracks is required to establish a more precise relationship.

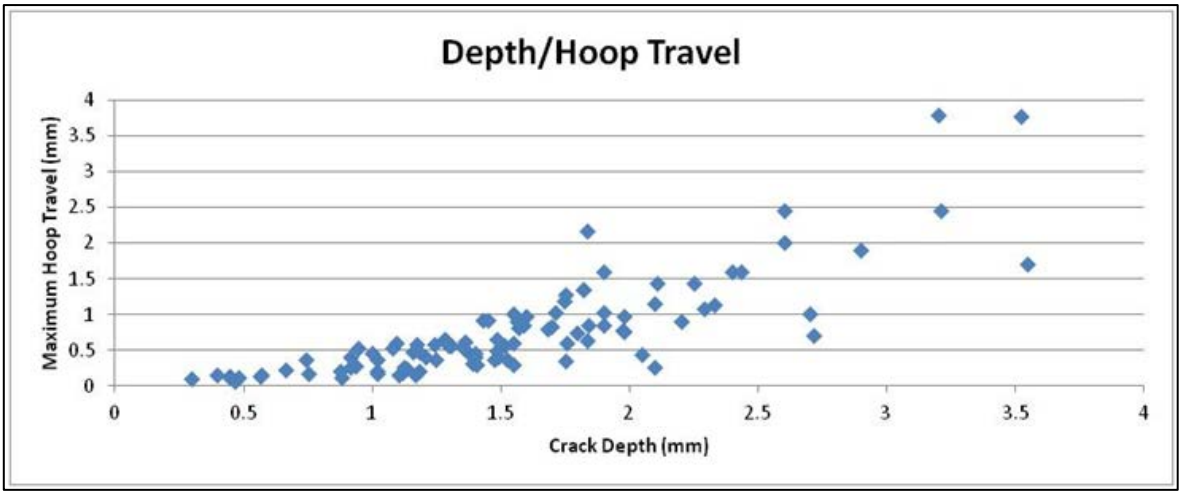

Figure 6-10: Relationship between maximum crack depth and hoop travel.

6.1.9. Branching

The phenomenon of crack branching was observed in the Australian pipeline and has also been reported in the SCC analysed in Canada. For a significant proportion of the cracks analysed branching initiated at the point where the crack deviated from the perpendicular, or along the inclined segment of the crack towards the crack tip.

A large proportion of branching from the main crack path was due to two or more cracks coalescing at the pipe surface as illustrated with the following example. Figure 6-11 is a transverse view of a crack located in the Australian pipeline and shows a crack with branching occurring along the inclined segment of the crack. This phenomenon has been previously observed on another SCC affected pipe sample (Wang & Atrens 2003).

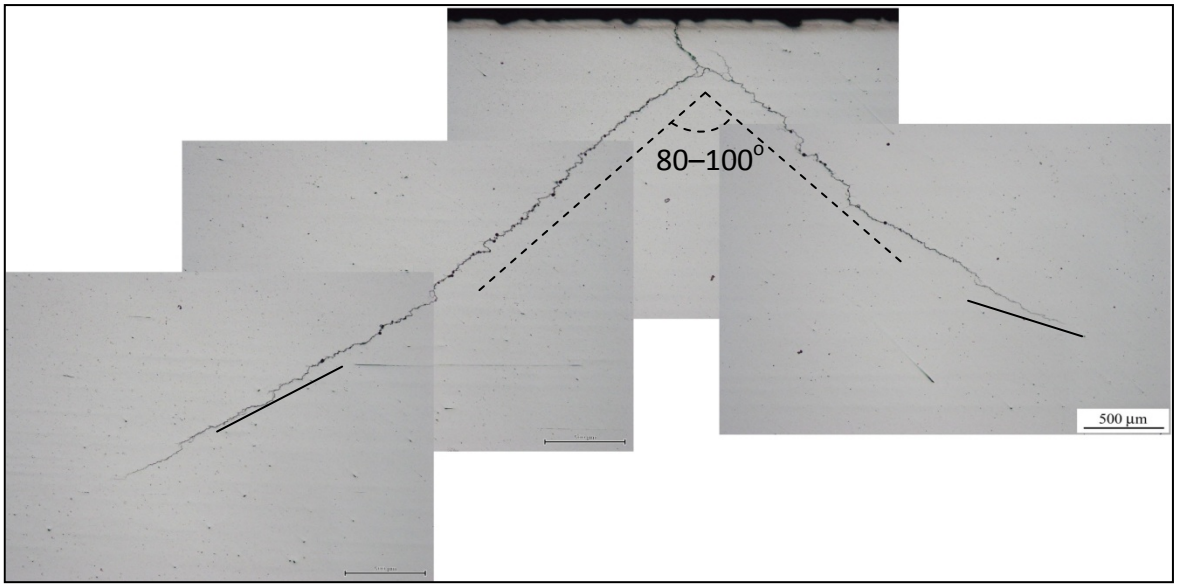

Figure 6-11: Inclined crack with significant branching at a perpendicular angle to the inclined crack path.

The crack branching shown in Figure 6-11 formed as the result of two cracks which were inclined in opposite directions coalescing to form one initiation point. Figure 6-8 shows the slice taken 3 mm before the transverse view shown in Figure 6-11 where the two primary cracks had not yet coalesced. The two separate cracks coalesced to form one initiation point. In the study of the Australian pipeline, branching off an inclined SCC crack typically travels at an angle of between 80 to 100 degrees to the main crack path. Figure 6-11 (above) illustrates this approximate perpendicular path effectively. It is interesting to note that for the crack presented in Figure 6-11 the inclination angle of the main crack and the branched crack increases slightly as the crack depth grows (shown with the solid lines). This means that the angle between the branch and the main crack path is growing and not staying in the defined 80–100 degree range.

6.1.10. Inclusion Interactions

Through the analysis of many cracks in the ex-service pipeline in Australia, many instances of non-metallic inclusions (NMI's) were found. Elongated manganese sulphide inclusions were found in the banded regions of the steel as a result of the pipe rolling operation The chemical composition of the inclusions was determined by EDAX and the normalised results are shown in Figure 6-12.

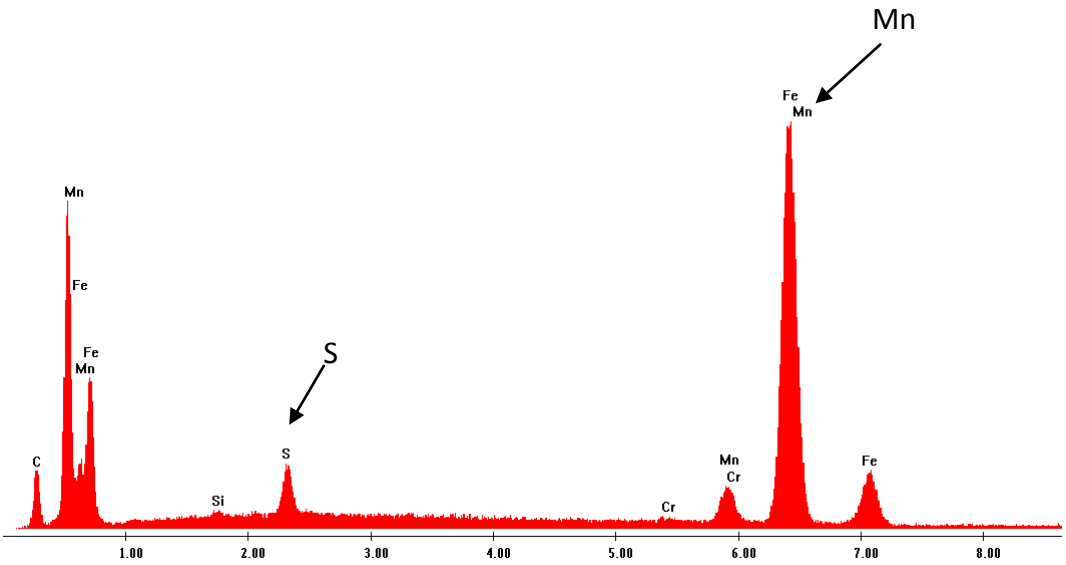

Figure 6-12: Chemical composition of the existing inclusions.

The inclusions were observed to exist at a depth typically greater than 2 mm from the pipe outer surface. As a result, cracks penetrating at least 2 mm into the pipe wall had the potential to interact with the inclusions present. Figure 6-13 illustrates a SCC crack that has interacted with an inclusion present in the pipe wall. The inclined segment of crack is shown entering the inclusion (solid arrow) and then exiting from the inclusion (dashed arrow) and continuing along the inclined crack path.

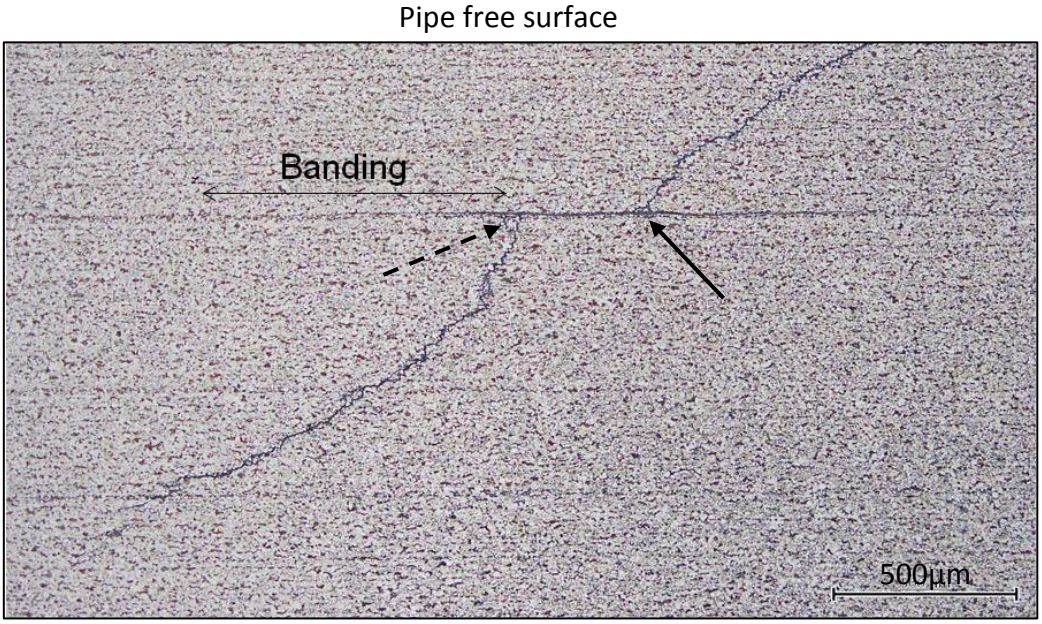

Figure 6-13: 2% Nital etched image of SCC crack interacting with an inclusion.

No evidence could be found to provide a reason for the crack exiting the inclusion at a particular point (Figure 6-13). However, the crack does have a small straight section before inclining in a direction parallel to the inclined crack entering the inclusion. It is important to recognise that this is only a single cross sectional representation of a three dimensional interaction where the inclined crack is continuous either side of the inclusion.

6.1.11. Longitudinal Subsurface Extension

The existence of axial subsurface travel was observed for a small number of the SCC cracks analysed. This axial subsurface travel occurs when a crack extends axially further beneath the pipe free surface than can be observed on the pipe free surface. This was revealed in cross sections. This phenomenon was only found in two cracks, with the maximum subsurface extension recorded to be approximately 1.5 mm. One of the cracks where this was observed is shown in Figure 6-14. The arrow shows the point where the crack first presents itself beneath the pipe outer surface. A section at 2 mm beyond MPI did not show any evidence of this crack continuing.

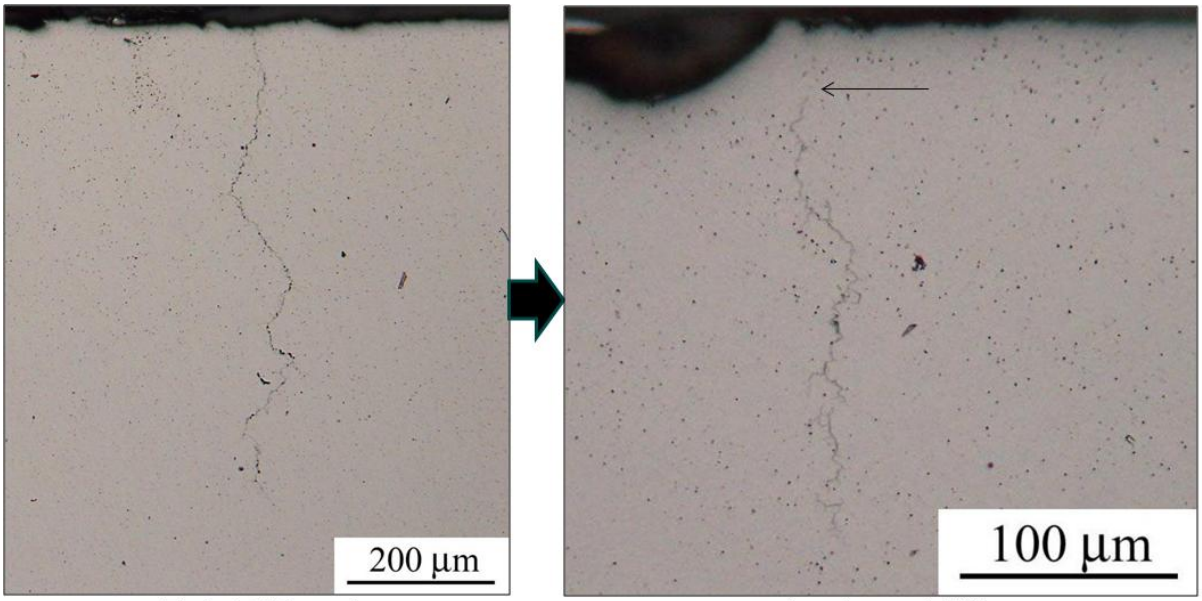

Figure 6-14: Longitudinal subsurface extension.

6.1.12. Crack Interactions

Due to the large spacing between cross sectional slices (1–3 mm) the metallographic process is neither ideal for analysing nor confirming predicted crack interactions. However, throughout the analysis all observed interactions were recorded and classified according to whether they were collinear or non-collinear interactions. A non-collinear interaction is when two offset separate cracks coalesce at the pipe free surface to become a single crack (Figure 6-15a). A collinear interaction is when an interaction of some nature observed in the cross section beneath the free surface of the pipe wall (Figure 6-15b) and there is only one observed initiation point or a very small deviation in initiation points These observed features suggest the cracks are collinear. This work has shown very complex crack paths and interactions, so there is some overlap in these classifications.

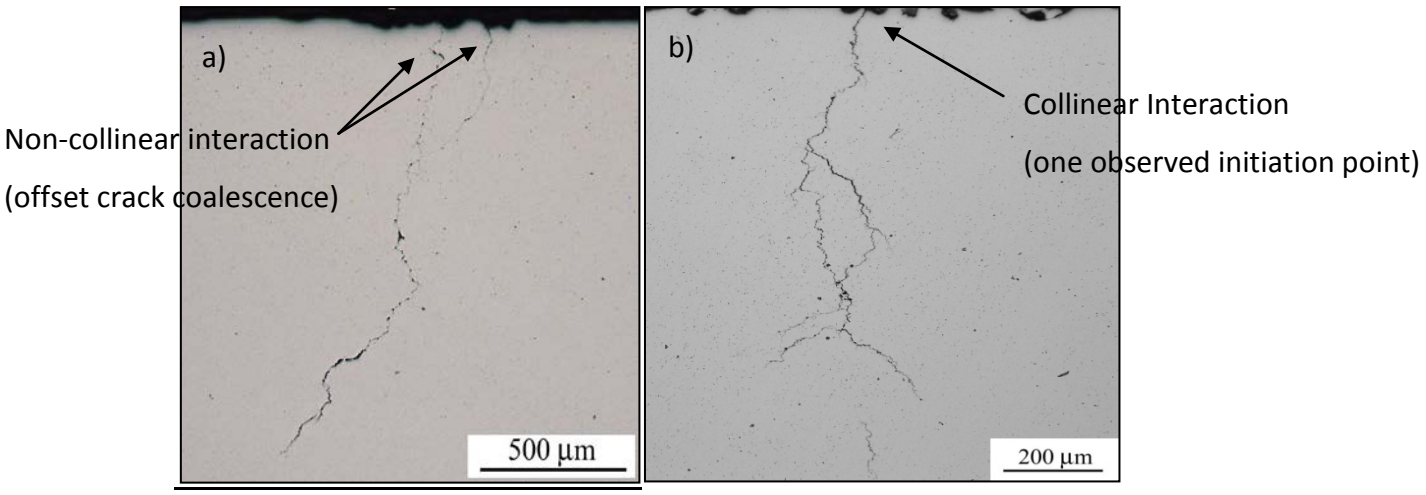

Figure 6-15: Cross sectional observations of a) non-collinear interaction and b) collinear interaction.

Approximately 32% of the cracks analysed in the study revealed some form of non-collinear or collinear interaction. This is a significant percentage of observed interactions. The largest circumferential separation of cracks, which were observed to be interacting, was 2 mm for cracks of lengths 19 mm and 36 mm respectively. Due to the long crack lengths, the two cracks would be expected to be interacting according to the interaction guidelines (CEPA 2007). If metallographic slices were taken at shorter intervals on seemingly 'straight' cracks used in this study, the percentage could be expected to be higher.

6.1.13. Hardness Profile

To determine any potential relationship between the hardness profile of the microstructure through the pipe wall, and where the crack deviates from the perpendicular, a Vickers hardness test was conducted along an inclined crack. The hardness measurement was taken along the SCC crack and either side of the crack providing three data points for each depth the hardness measurement was taken, intended to provide accurate results by removing random or faulty measurement. The error in the results was estimated at ±10HV0.1, considering the precautions taken to ensure accurate data was obtained. A 100gf was used for each hardness measurement. The red line in Figure 6-16 shows how the hardness varied at 50 µm intervals in the through-thickness direction of the pipe wall. For comparison, the blue line in Figure 6-16 is included for comparison and shows the results obtained from work completed on an SCC crack on a pipeline in Canada (Xie et al. 2009).

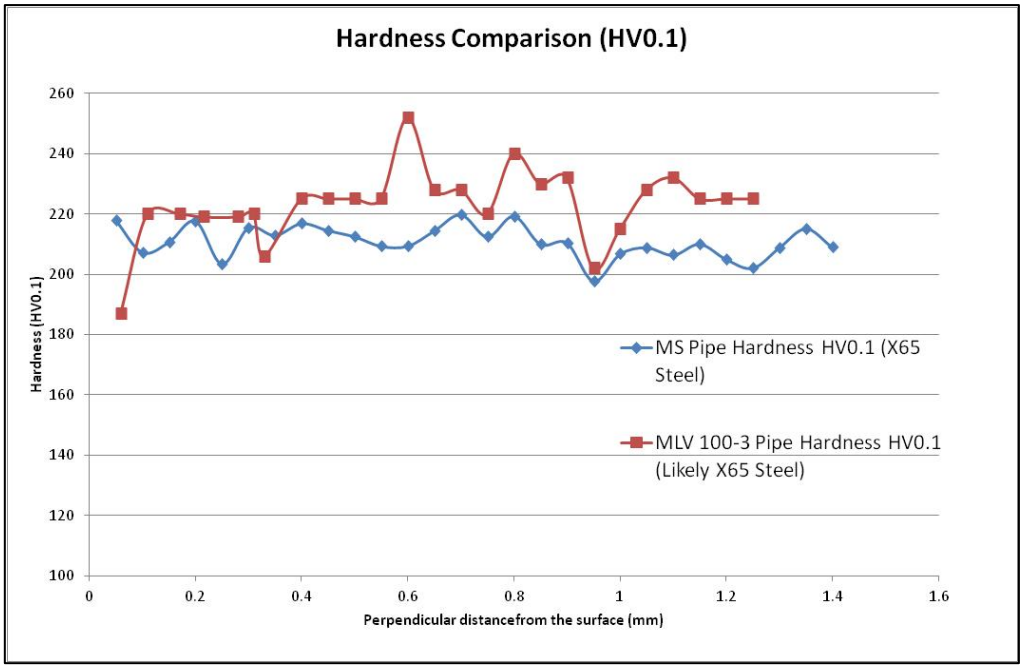

Figure 6-16: Hardness in the through-wall direction of investigated pipelines in Canada (red line) and Australia (blue line), adapted (Xie et al. 2009).

These results show variations in the hardness through the pipe wall but show no indication of any significant change at the point where the crack deviates. This means that where the deviation in the crack occurred (600 µm) there was no spike or change in the hardness profile in that zone.

6.2. Summary of Results

Examination of an ex-service Australian gas transmission pipeline sample has shown that 81% of stress corrosion cracks incline to the perpendicular. Based on this study, and anecdotal evidence from the field, it is highly likely that other instances of SCC in this pipeline will also display an inclined crack path. Metallographic observations of the cracks did not show a clear reason for the inclinations of the SCC cracks.

All cracks were examined looking in the downstream direction of the pipe to maintain consistency of results. Three colonies (CC, FC, and LC), were located in the same section of the Australian pipeline investigated. For Colonies FC and LC, the proportion of cracks inclined in a clockwise or counter clockwise direction was approximately equal. However, for Colony CC (sparse), the majority of cracks investigated (74%) inclined in a clockwise

direction. This colony also contained the vast majority of inclined cracks investigated. This significant percentage suggests that the inclination direction of the SCC cracks could be related in some way to the plate rolling process or manufacture of the pipe piece rather than environment or operation of the pipe.

The crack aspect ratios measured in this study agree with the previously reported literature on cracks up to 18 mm in length. However, the aspect ratio for cracks longer than 18 mm was found to decrease, due to the crack growing at a larger inclination angle the deeper it grows, slowing the through-wall penetration. Examination of the crack aspect ratios shows a bi-modal trend with cracks less than 18 mm having an aspect ratio of 0.21, and cracks larger than 18 mm having an aspect ratio of 0.03. This sudden change in aspect ratio corresponds to a crack depth of up to 2.8 mm. This change in ratio can be attributed to smaller cracks coalescing and concurs with previously published work (Baker, Rochfort & Parkins 1987b).

After an initial perpendicular crack path of approximately 500 microns, the majority of inclined cracks had an inclination angle of between 35–45 degrees from the perpendicular, until they grew to a depth of approximately 2.8 mm. As the crack deepened further, the inclination angle increased to between 45 and 60 degrees. This steep inclination implies that the longer a crack grows along the surface, the larger the inclination angle at the crack's tip, causing the crack to travel considerable distances below the surface in the hoop direction. The ratio between the travel distance in the hoop direction and the total crack depth has been termed the 'inclination factor'.

An important outcome of this work was the identification of a relationship between the maximum hoop travel and the crack length for each of the inclined cracks. This relationship was analysed and the trend was observed to be approximately linear for all cracks. The relationship has the potential to be refined as there was a limited amount of data investigating cracks longer than 18 mm.

Approximately 32% of the cracks analysed in this report revealed a form of non-collinear or collinear interaction. Metallography is not an ideal method for analysing crack interactions, and taking cross sections at significantly shorter distances would improve the results. However, the process can be used to suggest that, in a colony of SCC cracks, a large number

of cracks will interact whether the appearance of the cracks on the surface is collinear or non-collinear.

Analysis of the cracks revealed the existence of axial subsurface travel of a small proportion of the cracks. This subsurface travel occurs when a crack extends axially without having a surface initiation point present. This phenomenon was observed for two of the cracks with a maximum observed extension of approximately 1.5 mm. This result could have important implications when determining SCC crack interactions using the CEPA (CEPA 2007) guidelines.

Cracks were observed to travel in the hoop direction along manganese sulphide inclusions, exiting at seemingly random points along the inclusion. On exiting the cracks start in a perpendicular direction but quickly (less than 100 µm) resume the same inclination angle at which they entered the inclusion.

6.3. Assumptions

Through the process of metallography, several assumptions were made regarding the crack path between transverse slices for some cracks. Before analysing the SCC cracks, crack lengths were measured on the surface of the pipeline sample using MPI. The surface image did not always locate cracks interacting collinearly. As a result, there was potential for the two collinear cracks to be measured and recorded as one crack. This was evident in a small number of the cracks where the initiation point varied between two transverse views. In addition, the morphology of the crack had either changed significantly or revealed subsurface evidence that an interaction was taking place. These cracks, assumed to be single cracks from the surface, were actually a combination of two cracks that had interacted. Further support came from the depth profile of some of the cracks, which showed changes that suggested two cracks were present.

6.4. Limitations

It is important to highlight again that the fundamental limitation in the method used in this project was the distance between transverse sections of the SCC cracks. With this in mind, the morphology of each SCC crack analysed was accurate, and any inaccuracies primarily impacted on observations relating to crack interactions, which can occur over very small distances (<1 mm).

6.5. X-ray Tomography Results

All samples analysed by X-ray tomography using the equipment at Adelaide Microscopy needed to be 4 mm in diameter. The images produced by the machine had a minimum pixel size of 6µm. The effectiveness of tomography using the equipment available can best be described through a case study of one of the samples analysed.

6.5.1. Case Study (CC Colony)

To illustrate the constraints present in the available equipment, the results obtained from a 4 mm diameter sample with a 4 mm long SCC crack present were used. The sample was obtained from Colony CC. The best method of illustrating the limitations of the equipment was to analyse the sample using the metallographic process after X-ray scanning of the sample . The cross section corresponding to the midpoint of the crack was extracted from the tomographic data and was mounted and polished for analysis using metallography. Figure 6-17 displays the transverse image as obtained from the scanning, with a pixel size of 6µm (left), versus the equivalent transverse view of the same SCC crack using metallography. It is evident from this comparison that the resolution and clarity of imaging through this particular CT scanner with these settings makes it difficult to observe the crack clearly. With careful scrutiny, and by displaying consecutive images, the crack can be seen. However, the quality after post-processing could not provide an accurate assessment of the crack's morphology.

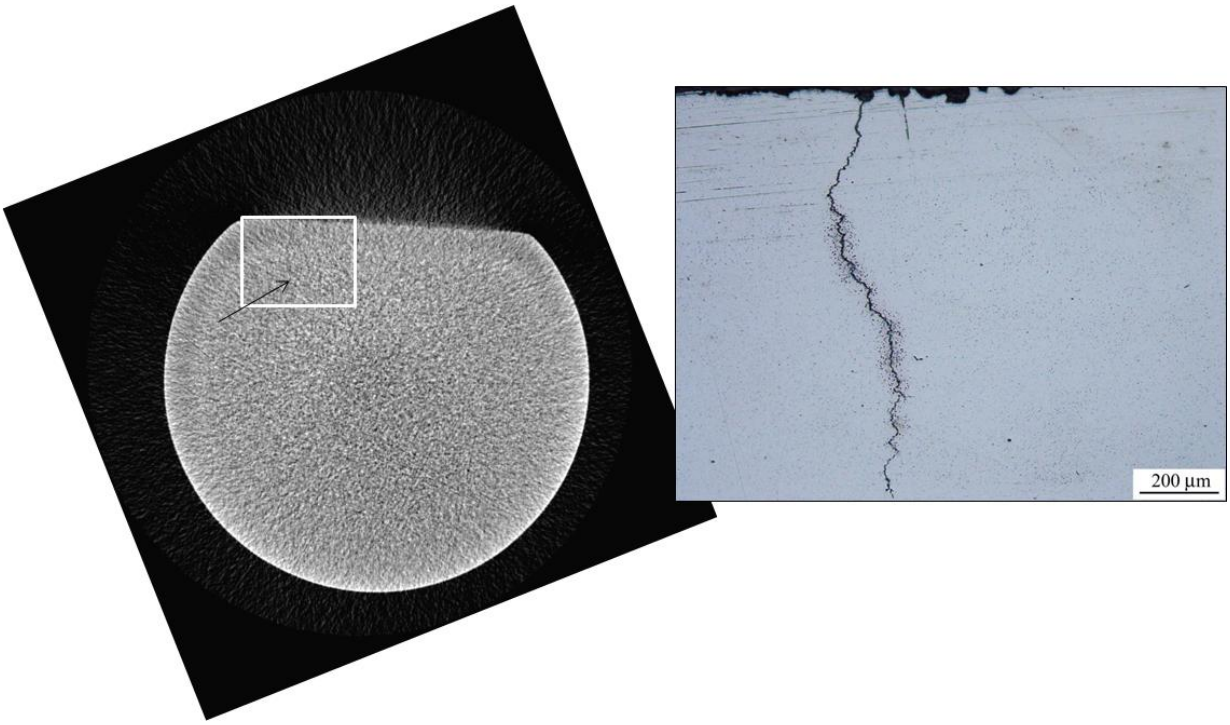

Figure 6-17: Cross section of SCC affected sample using X-ray scanning (left) and metallography (right).

The comparison shown in Figure 6-17 demonstrates the need for the process of tomography to be optimised to a point where crack visualisation is clear. This optimisation is being undertaken currently at the University of Adelaide (Giuliani 2013).

6.5.2. Limitations

The following limitations existed with the available X-ray CT equipment:

- Radiation exposure of the specimen.

  This was primarily due to the voltage, current and exposure time. The equipment limited the exposure time to 10s. Other factors affecting the radiation exposure were the physical size of the sample, the distance between the source and detector, the filter thickness and its composition, and the efficiency of the detector.
- Number of projections from which images could be taken had a machine limitation of 800. The software was therefore required to interpolate between pixels, rather than the correct pixel value being known.

- The detector was 10 years old and possibly had a number of defective pixels. This could result in a false image and incorrect photon count.
- It was difficult to mount the specimen in the machine and the sample was seen to wobble whilst being rotated during data collection.
- No motor control of the horizontal axis (difficult to centre the specimen).

6.5.3. Conclusions

The potential application of tomography was evident through this study. However, the limitations of the available equipment hindered the production of clear results that accurately described crack morphology and visualised crack interactions.

A concurrent study was initiated in conjunction with this project, aimed at sourcing equipment that had more appropriate capabilities. Figure 6-18 shows an SCC crack in a 4 mm sample using improved and more powerful equipment (Giuliani 2013).

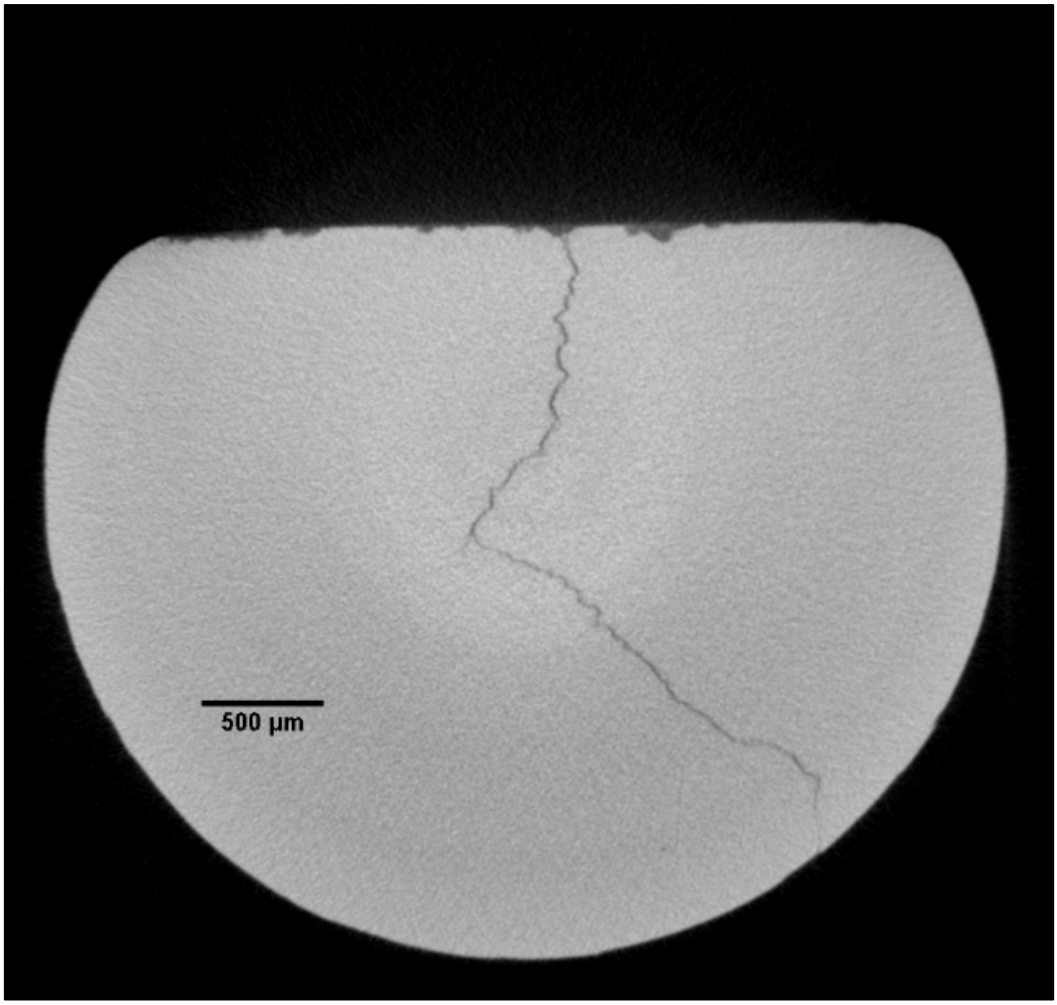

Figure 6-18: 4 mm SCC sample using tomography (source Michael Giuliani).

This study is continuing with this more appropriate equipment and is providing an effective means for crack visualisation. With the aid of more suitable equipment and further development of the technique, it should be possible to gain accurate data regarding crack interactions.

7. Comparison

Up to this point, the results presented in this report have been focussed on the current study of the Australian pipeline. Similar studies on morphological appearance were conducted on cases of inclined SCC found on a pipe in Canada. This chapter examines these differences.

7.1. Aspect Ratio Comparison

Previous work on a pipeline in the TransCanada pipeline system (Sutherby & Chen 2004) analysed a number of cracks, and from the analysis was able to plot the effective crack depth against the crack length. Figure 7-1 shows the linear relationship obtained from that work.

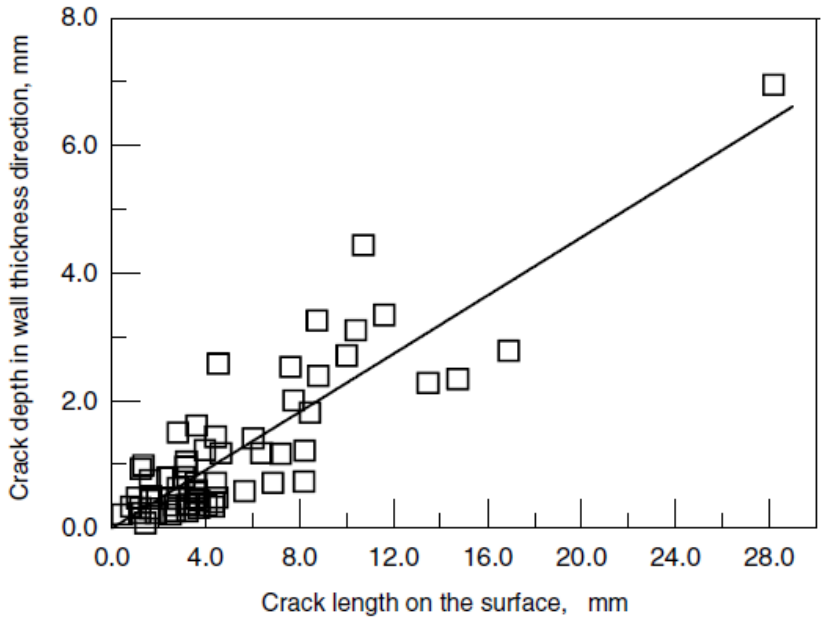

Figure 7-1: Crack depth plotted as a function of the crack surface length (Sutherby & Chen 2004).

From Figure 7-1, the reported aspect ratio was approximately 0.18 (Sutherby & Chen 2004). Using the same approach and geometrical definitions, the same aspect ratio relationship was found on the Australian pipeline containing SCC. Unlike the results from this current work there was no recorded bi-modal trend found in any of the cracks analysed in the Canadian pipeline investigation (Sutherby & Chen 2004). From Figure 7-1, it can be seen that

with the exception of one crack the SCC cracks available for the study on the Canadian pipeline were below 18 mm in length.

All cracks of length greater than 18 mm investigated on the Australian pipeline had evidence that they were comprised of more than one crack. This observation concurs with previous works examining 'typical' SCC cracks (Baker, Rochfort & Parkins 1987b; Parkins & Singh 1990). An interesting point is that a changing inclination angle (mentioned earlier) could be a factor in retarding the crack growth in the through-wall direction.

7.2. Straight Section Comparison

The reported cases of inclined SCC observed on the Canadian pipeline revealed that straight sections were generally in the range of 200 to 600 µm in length. This is supported by an earlier work (Sutherby & Chen 2004) which indicated that the range for the straight section depth was 200 to 800 µm as shown in Figure 7-2. This figure (Figure 7-2) also shows that the straight section may grow significantly deeper than this range on occasions.

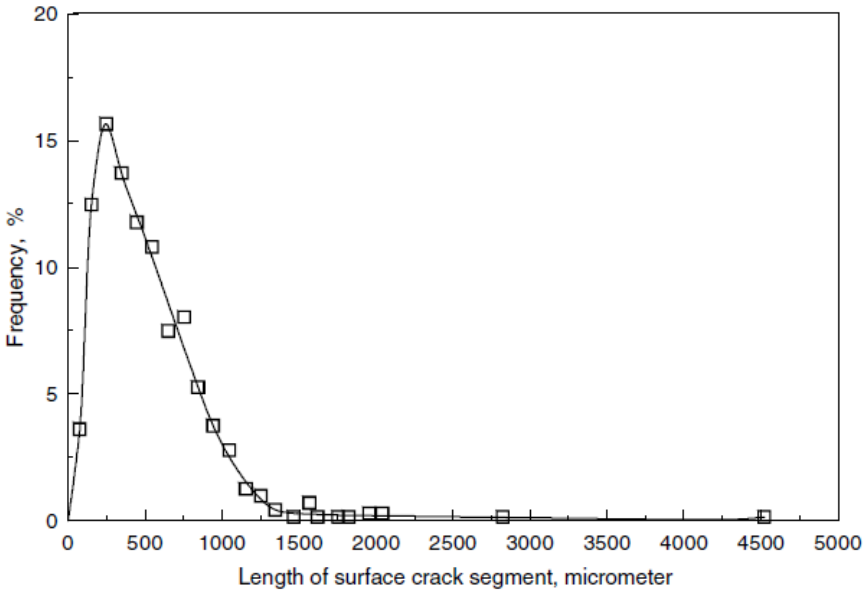

Figure 7-2: Distribution of straight section depths (Sutherby & Chen 2004).

The reported straight section ranges for the pipeline in Canada were similar to those in the pipeline in Australia which are recorded as 200–800 µm. Therefore there is general agreement that the depth of the straight section of the inclined cracks is in the range of

200–800 µm. In some occasional cases from the Australian pipeline, no straight section for the inclined cracks was evident as the cracks were inclined crack from the initiation point.

7.3. Inclination Angle Comparison

For all inclined cracks observed on both pipeline reports on Canadian SCC, the inclination angle was recorded. Figure 7-3, taken from the earlier report (Sutherby & Chen 2004), shows that the typical range of inclination angle is 30–60 degrees from the perpendicular.

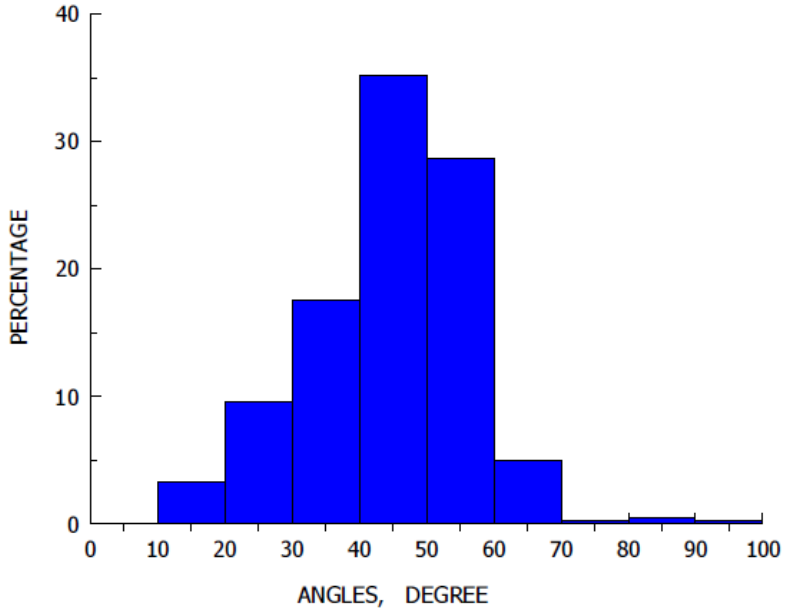

Figure 7-3: Distribution of the inclination angle (Sutherby & Chen 2004).

The more recent report from a different site on the pipeline in Canada (Xie et. al. 2009) confirmed these findings of the typical range 30–60 degrees which are again consistent with those previously presented earlier in this report for the Australian pipeline of 30–60 degrees.

The published work (Xie et al. 2009) from the pipeline sites in Canada did not suggest that the inclination angle increased with greater crack depth. However, this was observed in the current study on the Australian pipeline. As the inclination angle results from the two studies are in close agreement, this trend either may have gone unnoticed or was not included in the report. As a consequence of pipe maintenance procedures any cracks of significant length would have been removed and therefore for all studies, cracks of length

greater than 18 mm have been scarce and no strong conclusions can be made about the observed trends.

An observation made through a recent study on a pipe in Canada (Xie et al. 2009) showed that SCC cracks with a total effective depth of less than 400 µm were typically straight cracks without inclination. This has also proven to be the case in the present study although some cracks of total depths of less than 400 µm were found to be inclined.

7.4. Crack Branching Observations

Crack branching has been observed in a number of cracks on the Canadian pipeline(Xie et al. 2009). The angles between crack branches were reported to be approximately 90 degrees from each other. In that study branching existed at the point where the crack deviated from the straight crack path or at a position near the crack tip. This trend was observed in the present study on the Australian pipeline; however it was also found that branching resulting from crack interaction occurred at different points along the inclined segment. The angle at which the branch deviated from the main crack path was between 80 and 100 degrees. No significant branching off any straight cracks was observed.

7.5. Hardness Comparison

Vickers hardness was conducted along the crack path for the studies on the pipeline sites in Canada (Sutherby & Chen 2004; Xie et al. 2004). The purpose of this test was to determine any possible relationship between the hardness and the deviation of the existing cracks. This study was also conducted on the Australian pipeline using the standard procedure of recording three sets of points and reporting the average. The results from one of the Canadian studies (Xie et al. 2009) and the results from the current study on the Australian pipeline were presented in Figure 6-16. Neither study identified any relationship between the hardness profile nor inclined SCC cracks.

However Sutherby et al ((Sutherby & Chen2004) concluded that there was a relationship between hardness and the location of the crack deflection. In that work, the hardness profile was found for the entire through-wall thickness as shown in Figure 7-4.

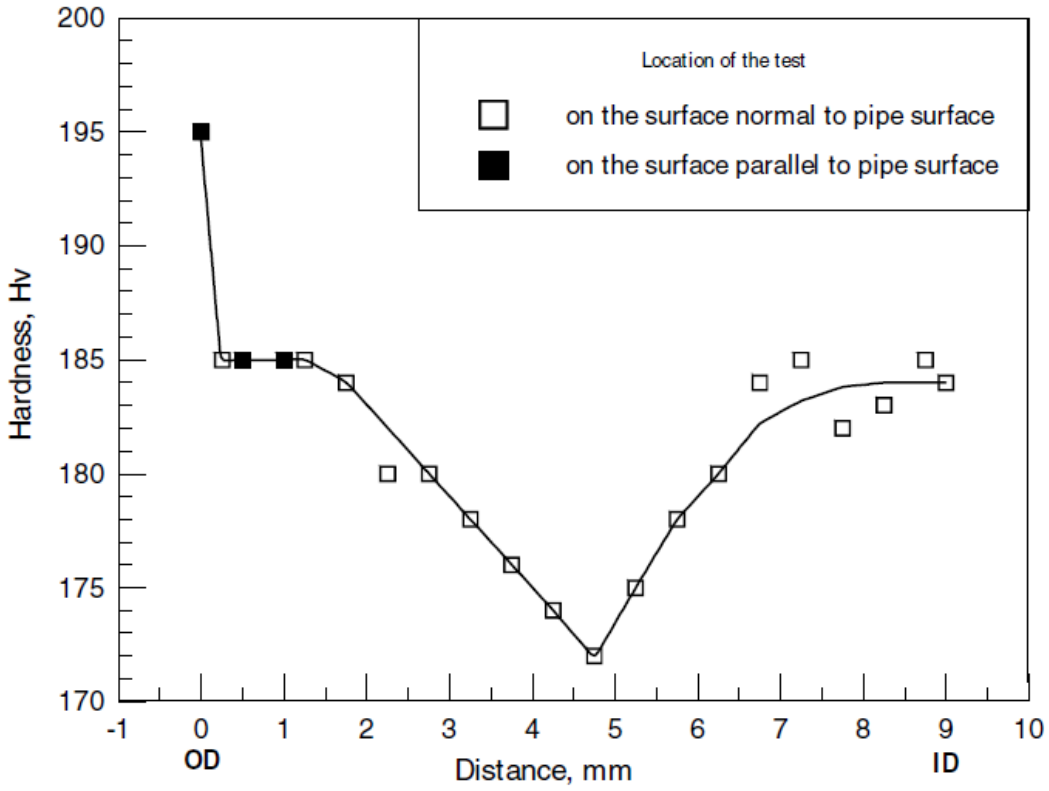

Figure 7-4: Variation of the hardness across the pipe wall (Sutherby & Chen 2004).

Figure 7-4 indicates a hardened layer of approximately 1.5 mm on both the inner and outer surfaces of the pipe wall. This study noted that the transition period between the hard material on the outer surface and the softer material at mid wall thickness coincided with the position where the cracks deviated from the perpendicular.

7.6. Summary

Examination of an ex-service Australian pipeline has produced results that can be compared to previous studies on an ex-service pipeline in Canada (Sutherby & Chen. 2004; Xie et al. 2009). All SCC cracks investigated in the studies were IG in nature, indicating a 'classical' high pH SCC mechanism.

The length to depth ratio for SCC existing in an ex-service pipeline in Australia reveals a likely bi-modal relationship (shown in Figure 6-3). The critical length where the change in relationship occurs is 18 mm. This relationship has been reported previously (Baker, Rochfort & Parkins 1987a) and suggests that the longer a crack is on the surface, the more

likely it has merged with other cracks. This results in cracks of greater length but little increase in depth. All of the studies were in good agreement for cracks up to 18 mm in length.

The straight section depth range recorded for the Canadian pipeline was between 200–600 µm in which compares favourably with the straight section depth of 300–800 µm measured in the current investigation for the ex-service Australian pipeline.

The inclination angle of the inclined cracks investigated on Canadian pipelines revealed a range of 30–60 degrees. This was for all inclined cracks investigated. The present study on the Australian pipeline indicated that for cracks less than 18 mm in length, the typical inclination angle ranged between 30–45 degrees. With longer cracks, the inclination angle range extended up to 55 degrees from the perpendicular. These figures demonstrate similarities in observed inclination angles across all studies.

Hoop travel is defined as the maximum distance an inclined SCC crack travels along the pipeline in the circumferential direction. The relationship between the maximum hoop travel and the crack length was approximately linear for the SCC cracks investigated on the Australian pipeline. From this relationship, the inclination factor was defined as the maximum hoop travel divided by the surface crack length. The inclination factor found for the Australian pipeline was 0.075.

Branching from the main crack path of an inclined crack was observed in many instances on the Australian pipeline. It was found that branching was often the result of crack interactions and occurred between 80–100 degrees from the main (inclined) crack path. This was in good agreement with the work on the pipeline with SCC in Canada, which reported branching to be approximately 90 degrees to the main crack path.

In Australia, for cracks with a depth of 3 mm or greater, instances of SCC cracks interacting with manganese sulphide inclusions in the pipeline steel were observed. The inclined crack entered and exited the inclusions at the same angle but travelled axially along the inclusion. The effect of inclusions on the path of inclined cracks has not been reported in the Canadian studies on inclined SCC.

An evaluation of the possible relationship between the hardness of the pipe material in the through-wall direction and the deflection of the cracks was completed for the pipeline in Australia. This, as was also the case from one work on the pipeline from Canada (Xie et al. 2009), showed no indication of any strong relationship. However, this is not conclusive as the other study (Sutherby & Chen 2004) did conclude there was an existing relationship. Therefore, any correlation potentially present would not be clearly visible using optical microscopy.

This study has shown that there is a good correlation between the results from the present study and those from previous Canadian studies. The results are comparable for inclined SCC crack morphology in terms of aspect ratio, straight section, inclination angle and typical branching.

However, additional details relating to inclined SCC have been revealed in the present study. It has been ascertained that the inclination angle increases with crack depth and an has been defined to describe the hoop travel of an inclined crack. The crack path for inclined SCC has also been observed to be affected by inclusions, which exist in the pipeline steel from manufacture.

8. Review of Existing Theories

Data cited in this report from previous studies together with the data collected during the current investigation can be used to describe the morphology of inclined SCC, in particular the aspect ratio and hoop travel of a crack of a given length. This section examines existing theories explaining the mechanism of SCC and the modelling of a typical SCC crack and its growth to evaluate these models.

8.1. Crack Depth Profiling

The aspect ratio for the SCC analysed in the present study has been determined and is in good agreement with results from studies on a Canadian pipeline (Sutherby & Chen 2004; Xie et al. 2009) for SCC cracks up to 18 mm in length. A previous study (Baker, Rochfort & Parkins 1987b) on the same Australian pipeline analysed in the present study is also in agreement for SCC cracks less than 20 mm. That study also recognised that for some cracks greater than 20 mm in length the aspect ratio decreased. This again is in agreement with the findings of the present study. However, as shown in Figure 2-8 it can also be concluded from the work of Baker et al (Baker, Rochfort & Parkins 1987b) that if there were no crack interactions a single crack could remain active and continue to grow with the same aspect ratio beyond 20 mm in length. This could not be confirmed in the present study because all cracks greater than 18 mm were the result of crack coalescence, which suggests that it is unlikely that circumstances would exist where a single crack would exceed 20 mm in length and remain active.

For each crack investigated in this study, an associated depth profile together with a straight section and hoop travel profile were created. Figure 8-1 shows the depth profile (blue line) plotted for an SCC crack that had a recorded length of 51 mm. On the surface, this crack had indicators that suggested it was comprised of a number of cracks that had coalesced to form one large crack. Analysing the transverse sections of the crack confirmed this assessment. The profile of the straight section has been included on the figure to demonstrate the typical change in straight section that occurs along the length of each crack characterised. In this particular case, the straight section depth ranged from 0mm to almost 800 µm in depth. It is interesting to note that a typical crack depth profile has a semi elliptical shape, this crack depth profile has many anomalous points along its path.

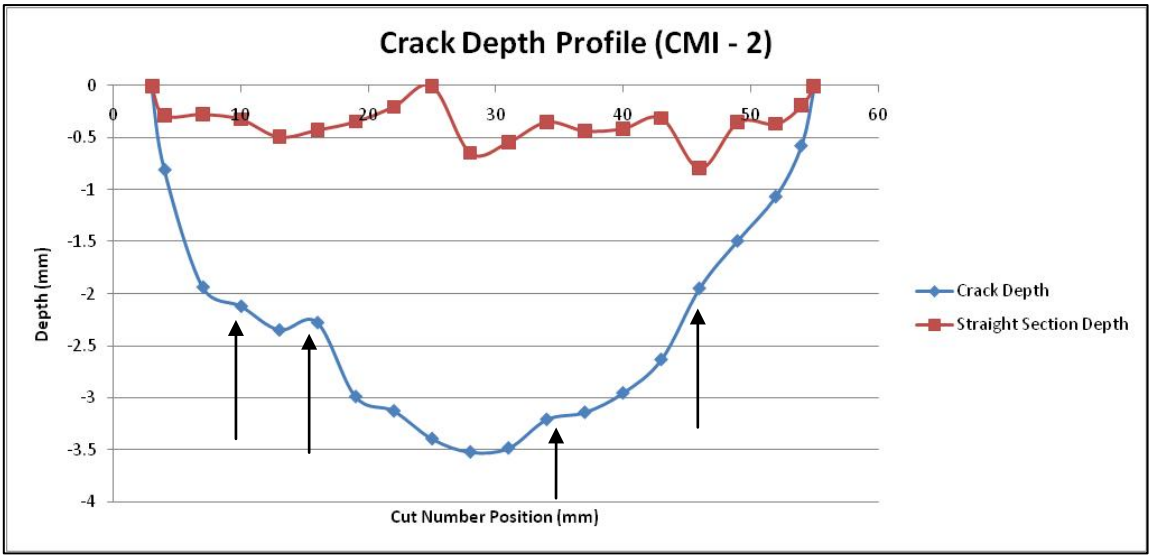

Figure 8-1: Crack depth and straight section depth profile for sample CMI-2.

Inconsistencies in the depth profile arrowed in Figure 8-1 suggest some form of crack interaction could be occurring. It is unlikely that these are due to microstructural features resisting the uniform growth of the crack front. This was confirmed when analysing the transverse sections of the SCC crack. Figure 8-2 is of the outer surface of the pipe and shows the crack that was analysed. The lines etched on the surface indicate the positions at which the transverse cross sections of the crack were taken and the predicted points of crack interactions identified and arrowed on the image.

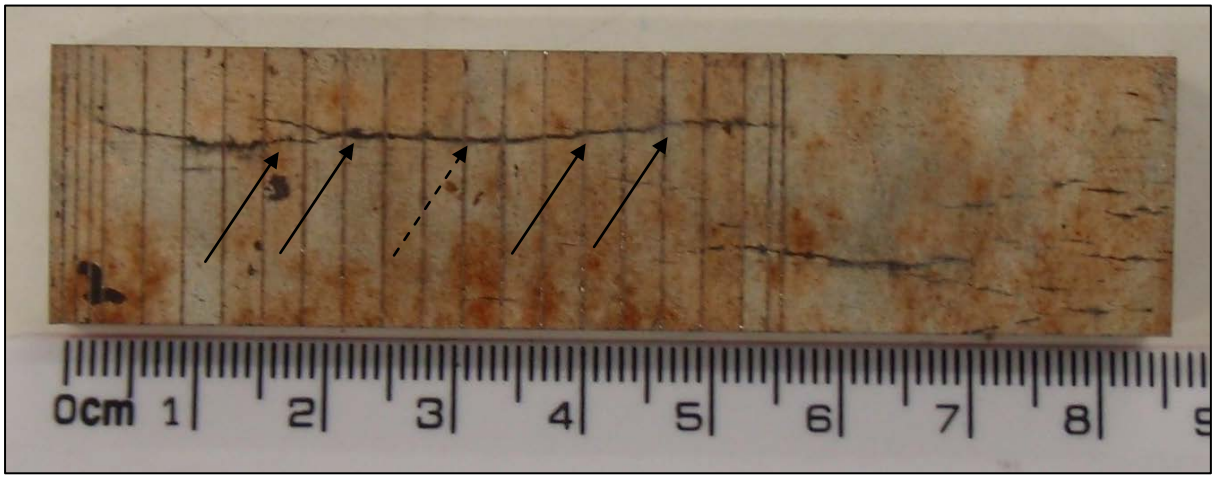

Figure 8-2: Sample CMI-2 as photographed before analysis.

The crack shown in Figure 8-2 reached a maximum depth of 3.5 mm at the location indicated by the dashed arrow (approximately the midpoint of the crack). Interestingly, the maximum hoop travel attained for this crack was about 3.8 mm from the initiation point and this was the largest observed hoop travel by any crack in this study.

This one example was typical of all the cracks exceeding a surface length of 18 mm analysed in this study where the deepest point of the cracks occurred at the midpoint of what appeared to be the longest 'single' crack in the cracks' lengths. Analysis of more samples of 'single' SCC cracks longer than 18 mm from sparse colonies are needed to give greater confidence in this conclusion and for comparison with the older study done on the same pipeline (Baker, Rochfort & Parkins 1987b).

8.2. Impact on CEPA

Based on the results of this study an inclination factor has been determined which relates the hoop travel to the surface crack length for the Australian pipe analysed. This enables the calculation of the worst-case hoop travel length and allows a comparison with the CEPA guidelines for the minimum crack separation. It is important to realise that the observed longitudinal subsurface extension may also have an impact on the conservative nature of the axial measurement of crack interactions taken from CEPA.

Based on the circumferential and axial spacing between cracks in a colony it is possible to assess the likelihood of crack interactions according to CEPA guidelines. To best illustrate the potential impact of this project's results on the conservative nature of these calculations, see the following example. Figure 8-3 shows two random cracks taken from CC Colony (a sparse colony) that were analysed in this study. Crack 1, shown in Figure 8-3, was 5.5 mm in length and Crack 2 was measured at 4 mm in length. After analysis, the maximum hoop travel for Crack 1 was measured as 0.3 mm and the maximum hoop travel for Crack 2 was measured as 0.18 mm. Both cracks are inclined and have the potential to incline towards each other. The black rectangle in Figure 8-3 illustrates the measured maximum hoop travel superimposed on either side of the initiation points of both cracks.

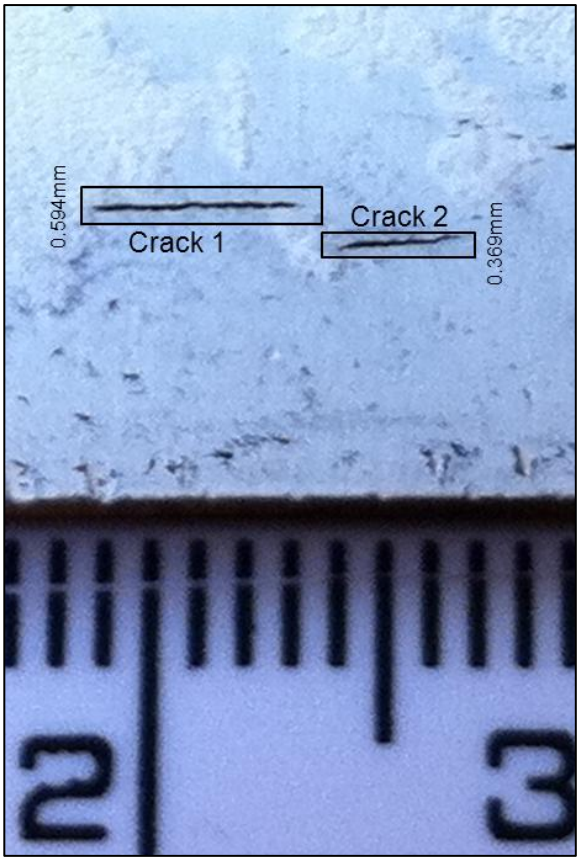

Figure 8-3: Two cracks in a sample not expected to interact (measured hoop travel).

The circumferential spacing between both cracks in Figure 8-3 was measured as 1 mm. Recalling that both circumferential and axial conditions must be satisfied for two cracks to be deemed as interacting, the 'cut-off' circumferential condition can be calculated from CEPA to determine if interaction is expected.

$$Y = 1 \leq \frac{0.14(5.5 + 4)}{2} = 0.665\ mm$$

The above equation shows that 1 mm is larger than the minimum separation of 0.665 mm and therefore the cracks would not be considered to interact from the OD surface. However, inclined SCC introduces the possibility of the crack tips actually existing in closer proximity than is measured on the surface of the pipe sample (axially and circumferentially).

In Figure 8-4, the dashed regions denote the same calculated range of the potential crack tip locations if we take an absolute worst case scenario. This worst case exists if both cracks were inclined towards each other and the hoop travel existed towards each other. Using the

known hoop travel distances for both existing cracks, the potential distance between the crack tips is calculated to be 0.52 mm, which is less than the minimum allowable circumferential distance calculated from the CEPA guidelines. Therefore there is a degree of uncertainty whether these cracks could interact and whether the CEPA guidelines are conservative enough when inclined SCC is involved. Future work is required to address this potential problem. It is worth noting that when these cracks were analysed it was found that they were not interacting and were both inclined in the same direction towards the top of the figure.

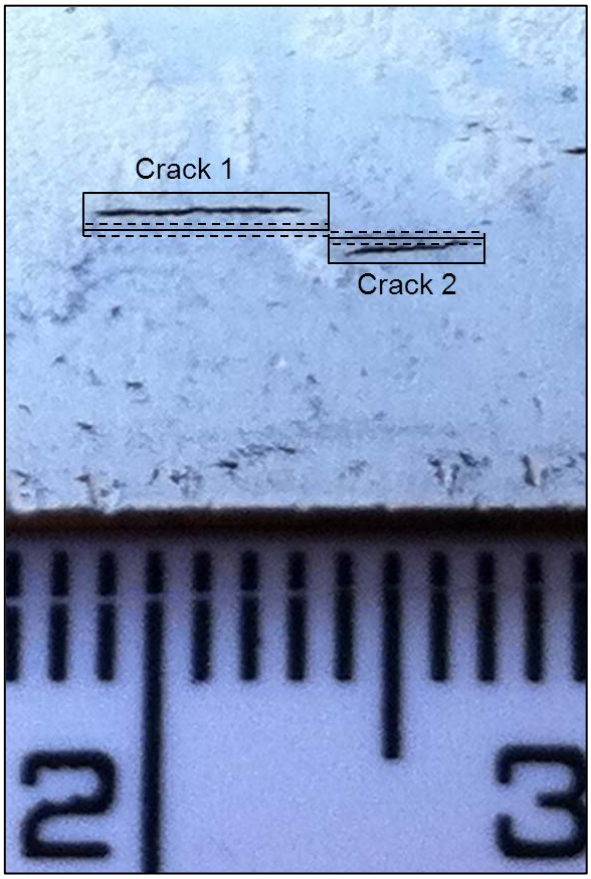

Figure 8-4: Two cracks that may be interacting when approaching the CEPA calculation from a 3D perspective.

This particular example was a worst-case inclination scenario for these two cracks, and would need ideal conditions for crack interaction to occur.

However, it does demonstrate that the issue of crack interactions is a three dimensional problem. It is likely that the CEPA guidelines are sufficiently conservative for crack

interactions to be determined solely from their examination on OD surface of the pipeline (as shown by many years of incidence free maintenance), but the margin of safety may be less than anticipated.

An important point to note is that this “worst case interaction scenario” has been applied to several crack pairs on pipes samples in this project where the two cracks were observed to be close to each other, but not assessed to be interacting according to CEPA guidelines.

8.3. Active or Dormant

An important variable in assessing the threat an SSC crack colony poses to an affected pipeline is the question of whether the existing cracks are active or dormant. A previous study (Wang & Atrens 2003) used existing SCC in an ex-service pipeline, and laboratory samples of induced SCC, in samples known to be active. The study concluded that it was reasonable to compare the crack tips of both samples to determine if the SCC existing in the ex-service pipe sample is active or dormant.

The study (Wang & Atrens 2003) concluded that if the crack tips of the ex-service samples were similar to that of the induced cracks, the pipe crack was active. To this end, an induced SCC crack was produced in the laboratory at the University of Adelaide in a sample from the same ex-service Australian pipeline examined in the current study. The crack is shown in Figure 8-5. The crack tip (arrowed) is that of an active crack.

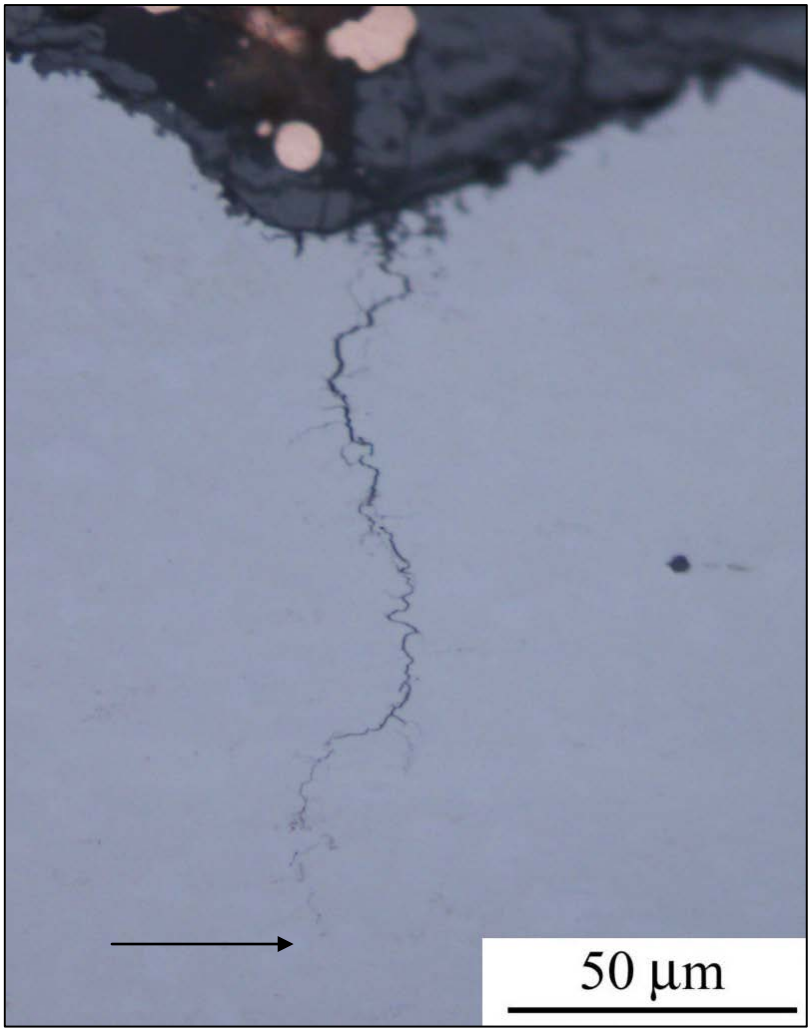

Figure 8-5: Induced SCC crack in pipe sample (active), (courtesy of Olivier Lavigne, UoA).

The crack tip shown in Figure 8-5 was compared with a typical crack tip taken from the ex-service pipe sample shown in Figure 8-6. The crack tips in both figures show similar characteristics, being fine and having little oxidation indicating that the crack tip in the ex-service pipeline sample shown in Figure 8-6 is also active.

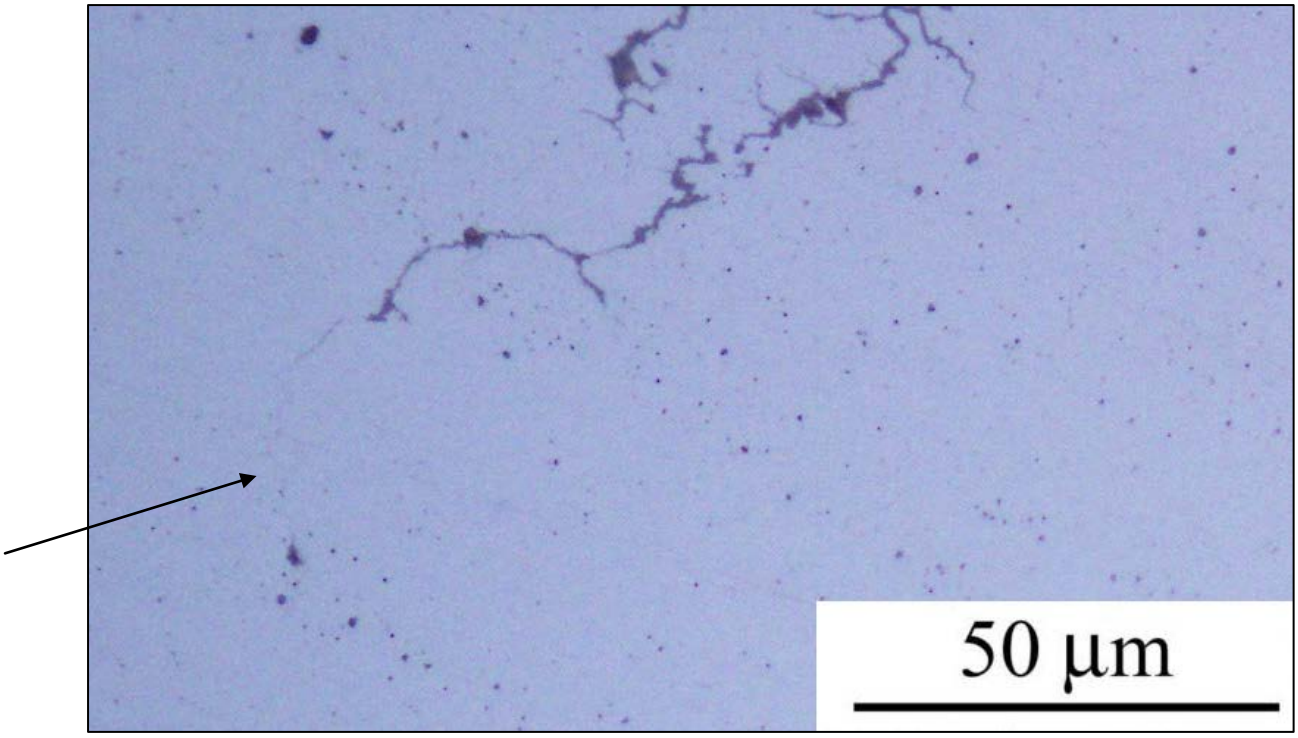

Figure 8-6: SCC crack tip taken from ex-service pipe sample showing a very fine structure near the tip.

As the crack tip in Figure 8-6 is typical of those analysed in this project, it can be deduced that the cracks were active when removed. This is a tentative conclusion, since an ideal investigation would determine the active nature of a crack tip by examining the oxide layer profile at the crack tip and analysing the crack tip at a greater magnification.

8.4. Crack Growth Rates

Modelling crack growth rates has been identified as an important part of SCC analysis, in particular with the application of predicting the residual life of SCC affected in-service pipelines (Parkins 1980). SCC in many cases has been noted to approach dormancy when isolated from surrounding SCC cracks; in this case, the cracks are not critical (Parkins 1987). However, SCC occurs in colonies where the nucleation of cracks encourages coalescence and, in some cases, re-activates otherwise dormant cracks.

Crack coalescence, particularly in environment-sensitive cracking, has been reported as a major factor responsible for leaks or ruptures in pressurised environments such as gas pipelines (Parkins 1987; Parkins 1989). This is primarily due to the damaging effect it can play in crack growth kinetics (Parkins 1989), increasing the crack growth rate. Crack interactions change the SIF, which is related to the crack growth rate.

8.4.1. Stress Intensity Factor

The SIF of the crack tip is important in determining the growth of a crack and the way cracks interact. In its simplest form this factor, represented mathematically by 'K' is given by:

$$K = Y\sigma\sqrt{\pi a}$$

Where Y is a dimensionless parameter, σ is the applied stress and 'a' is the length of the crack in the longitudinal direction (Callister 1994). This fundamental formula represents the simplest Mode I critical case. Using SIFs is important for crack analysis and data treatment (Baker, Rochfort & Parkins 1987a).

The SIF is a description of the stress state at the tip of a crack based on a single or a group of cracks, the tensile stress (applied and residual) and crack geometry. For SCC, when certain environmental cracking conditions are present, and the stress state becomes critical or exceeds the critical value, the crack will grow. The SIF can be used to assist in creating criteria for pipe failure, crack propagation and environmental behaviour. The load that causes the material failure is known as the 'fracture strength' of the material (Hertzberg 1996).

There are three loading types and therefore three failure modes that are characterised by Mode I, Mode II, or Mode III. The three modes are shown in Figure 8-7:

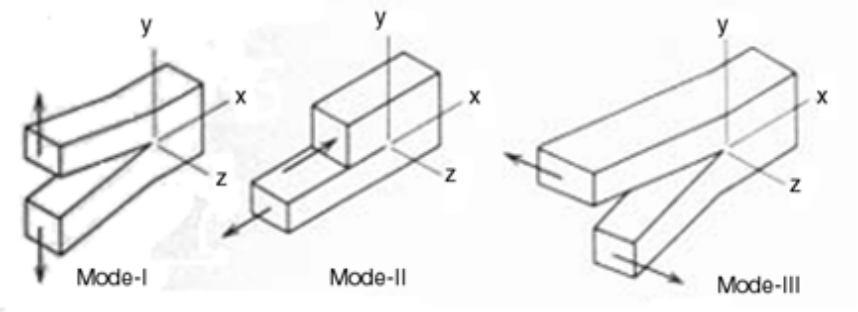

Figure 8-7: The three basic modes involving different crack surface displacements (Hertzberg 1996).

The first mode is the most common among cracks and is the tensile mode where the crack surfaces move directly apart from one another. The second mode is the sliding or the in-plane shear mode where one crack surface slides over the other crack surface in a direction normal to the leading edge of the crack. The third mode is the tearing or anti-plane shear mode where the crack surfaces move with respect to each other and in a direction parallel to the leading edge of the crack.

The SIF for neighbouring cracks can change as the cracks grow and interact with each other. SIF is evaluated at the tip of each crack in the position where the tips from opposing cracks are closest. It is important to note that cracks will grow at different SIF values depending on the driving mechanism. For example, the SIF required for fast brittle fracture is different to that required for SCC crack growth (assuming environmental and electrochemical conditions are satisfied).

As two crack tips approach each other, Wang et al have established (1996) that the Mode I SIF increases. As soon as the crack tips pass each other, the Mode 1 SIF decreases and the Mode II SIF begins to increase (Wang et al. 1996). The mathematical sign of the Mode II SIF changes as the tips pass one another when the two cracks were originally offset. The greater the offset distance, the less the SIF will change as the cracks move. This also means that the stress intensity values experience a mixed-mode condition as the cracks move past and interact. A mixed-mode loading condition would be expected as the cracks either interact or come together.

A recent study (Lam & Phua 1991), observed that the influence of crack interactions is dependent on the relative position of the cracks to each other. As a result, the crack interaction influence was classified as either accelerating or suppressing crack growth (Lam & Phua 1991). SCC exists in colonies of many cracks that typically all travel axially along the surface of a pipe wall. The observation of inclined cracking changes the problem of multiple cracks interacting into a three dimensional problem. This is an area for further work.

The relative length of the cracks present also influences crack interactions. When the crack lengths are equal, the influence these cracks have on each other is strongest (Kamaya & Totsuka 2002). A greater difference between the crack lengths results in a decreased influence. If the difference between the crack lengths is significant, it has been reported that the influence of the interaction on the behaviour of the crack growth is negligible (Kamaya & Totsuka 2002).

Throughout this study, definitive observations of crack interactions were not possible due to the metallographic method of crack analysis used. However, observations regarding crack interactions were made from the MPI results of the surface of the pipe before sectioning and metallographic processing. In the post-processing procedure, the crack depth profiles of all cracks and coalesced cracks were analysed. With interacting cracks, the crack depth profile would show this interaction through a variation in the crack depth. This factor explained why many of the crack depth profiles created were not a semi-elliptical shape.

Figure 8-8 shows the depth profiles of two cracks. Figure 8-8 (top) shows a smaller crack that was analysed and was clearly shown to be a single crack with no interactions taking place. As can been seen, the profile of this crack is semi-elliptical and shows a typical crack depth profile. Figure 8-8 (bottom) is made up of at least two cracks observed to be interacting on the surface of the pipe and this is evident in the depth profile.

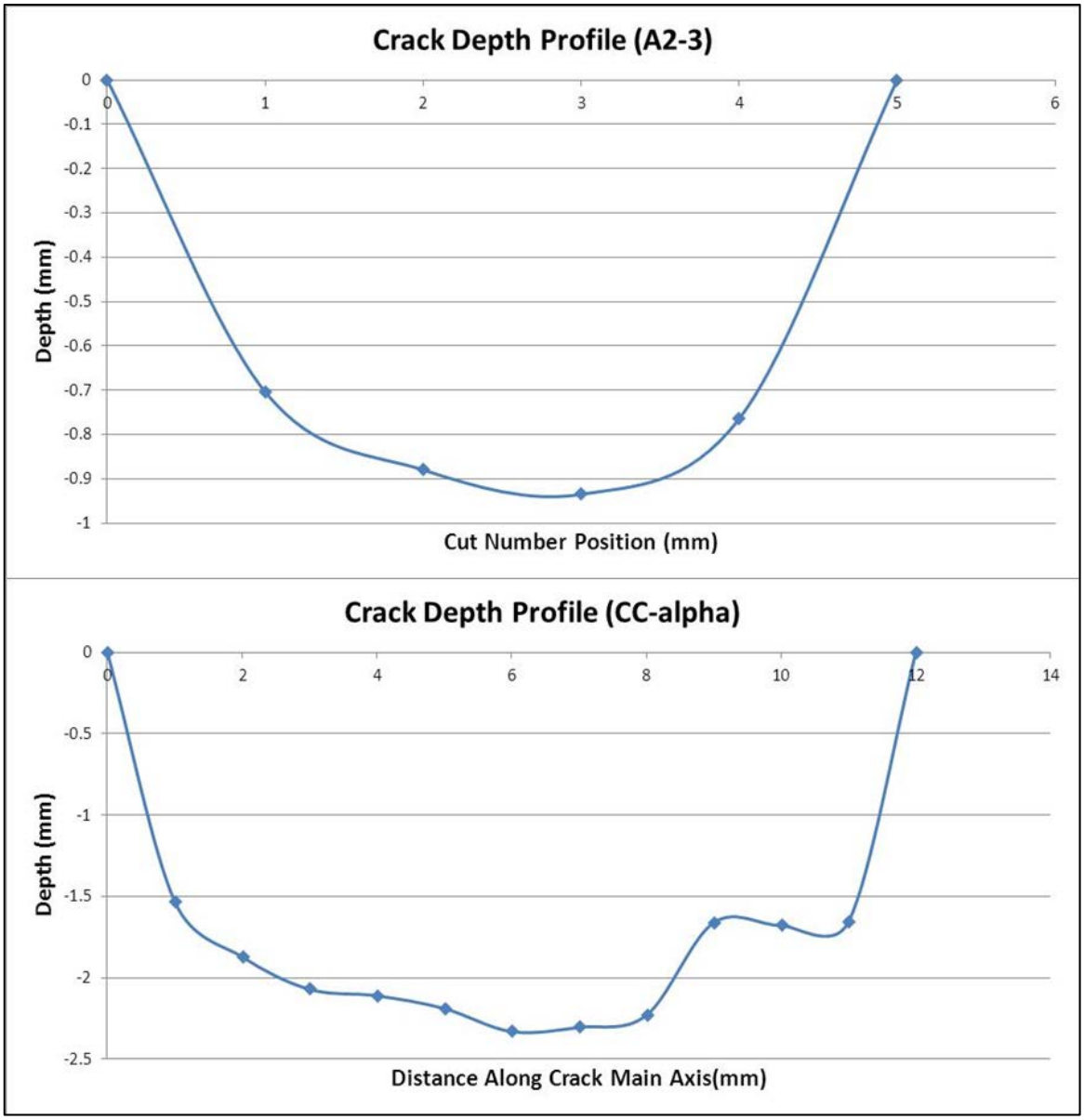

Figure 8-8: Depth profiles of a single 5 mm crack (top) and 12 mm coalesced cracks (bottom) (purposed for profile only).

8.5. Residual Stress Impact

Comparing the cases of inclined SCC studied in Canada and Australia, the morphological and metallurgical results presented do not provide a clear reason, nor indicate strongly why some SCC cracks are inclined and why the inclination angle of inclined SCC is variable and not a fixed angle.

Both of the pipes analysed in Australia and Canada were manufactured in a similar way and experienced similar service conditions. This implies that the applied operational stresses are

unlikely to be responsible for the inclination angle itself, as they cannot account for variations in the angle and the direction in which the inclined crack is directed in very close proximity. Hydrostatic testing that occurs on the pipes does apply a pressure larger than the typical operating pressure, but only over a short period (order of hours or days) and therefore is unlikely to be responsible for the differing inclination angles.

To illustrate the variation in inclination angles that can occur over short distances, Figure 8-9 shows an SCC crack shown with a 1 mm space between the cross sections. These two transverse views of the same crack show a distinct change in both the inclination angle and the crack direction.

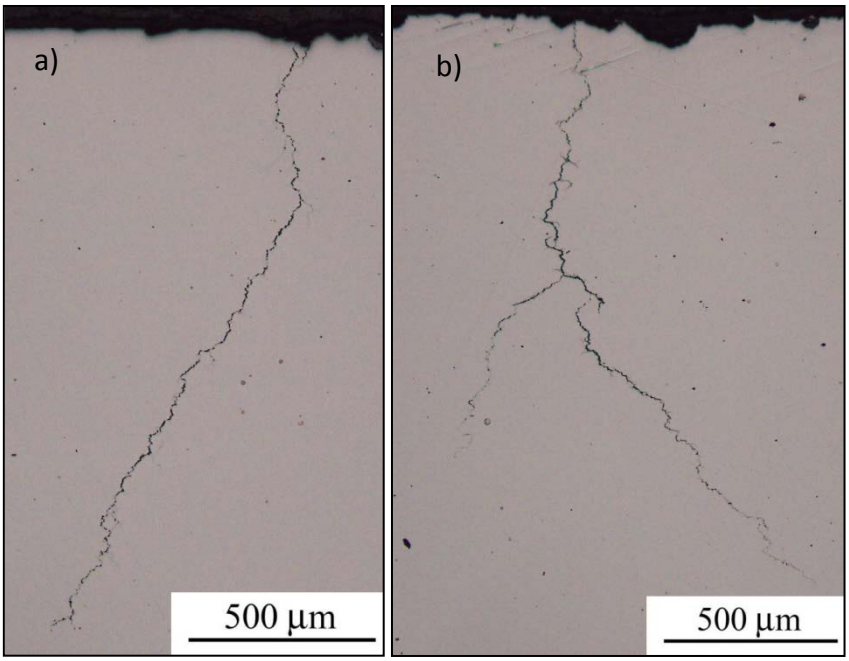

Figure 8-9: Observable change in inclination angle and direction of a single crack with a) and b) cross sectional slices 1 mm apart.

The two transverse views shown in Figure 8-9 do have the potential to be collinear inclined SCC cracks interacting while inclining in different directions. As the inclination angle and direction are different over such a small separation, it is unlikely this difference occurred because of residual stresses. . Previous work (Linton, Gamboa & Law 2007) has found that the residual stresses existing in the pipeline are less than 40MPa and over the small distance

between the cracks, the residual stresses are not likely to change significantly and therefore it is unlikely that these stresses play a major role in defining the inclination angle.

Based on these results, as well as previous work done on the Australian pipeline, it appears that microstructure rather than residual stresses is a more important factor in determining the crack path. Current work being done in parallel is aimed at relating other studies (Lozano-Perez, Rodrigo & Gontard 2011; Song 2008) to the results of the current of study inclined SCC.

8.6. 3D Model Significance

In the current work, metallography has been the primary method used for acquiring data to characterise SCC in the Australian pipeline under analyses. A recent study concluded that understanding SCC initiation and propagation is critical to understanding the mechanisms of SCC (Lozano-Perez, Rodrigo & Gontard 2011). The method of taking two-dimensional transverse slices to characterise SCC using metallography is inadequate for understanding what is fundamentally a three dimensional phenomenon, particularly crack interactions.

Three dimensional crack visualisation using X-ray tomography has been identified as a technology with the capability to provide data for characterising SCC in addition to crack interactions within a colony of SCC cracks (Lozano-Perez, Rodrigo & Gontard 2011 and hence the potential to provide information that could be used to improve the understanding of SCC mechanisms and crack interactions.

The current study identified that the CT equipment available at Adelaide Microscopy was not adequate to clearly image SCC cracks in a 4 mm sample. Work has proceeded in a concurrent study at the University of Adelaide using different, more powerful X-ray tomography equipment for successfully characterised SCC in samples ranging from 1.5 mm to 8 mm diameter.

8.7. Subsurface Extension

Two cases of longitudinal subsurface extension have been observed during this work. Reviewing many of the other reported occurrences of SCC, there is a very little information or data accounting for this observation.

During the current research, cracks were observed interacting with elongated manganese sulphide inclusions. The cracks entered the inclusions at one point, propagated along the inclusion and exited at another point further along the inclusion. This could explain subsurface extension in some cases. The crack appeared to be able to propagate more easily along the inclusion than on the free surface. The impact of subsurface extension on crack interactions, and the mechanism when there were no inclusions present, however, is unknown. This is an area for future work.

9. Implications for Australian Industry

Currently, the CEPA guidelines are used to assess SCC cracks on Australian in-service pipelines. These guidelines were formulated from data and information gained from SCC that existed on Canadian and USA pipelines. As such, the guidelines have been critical for the identification and remediation of potentially dangerous SCC cracks and thus ensuring safe pipeline operation.

It is in the best interest of the Australian pipeline industry to ensure that all pipelines affected by SCC do not present a danger to any of the operational team or to the general public. The results obtained during this work have shown no breaches of the current industry guidelines and hence suggest that these guidelines are still adequate for the assessment of crack interactions. An important point to note is that for some non collinear cracks, CEPA guidelines suggested that they are not interacting by a reasonable margin. However, 3D subsurface crack morphology showed that the minimum distance between the cracks was less than what was measured on the pipe surface. As a result, the level of conservativeness was reduced.

Through this study, current SCC critical assessment techniques (CEPA guidelines) have been shown to remain suitable for assessing crack interaction. This increases the confidence in this previously unproven taken from pipeline management internationally. This increases the confidence for the Australian industry that a guideline adopted from overseas is applicable domestically. As a result, the current assessment strategy is a safe and worthwhile technique providing confidence in cost effective management and remediation strategies.

Through this study, the existing SCC in the extracted ex-service pipeline section has been characterised and this provides industry with a strong indication as to what the expected crack morphology is inside the pipe wall when an SCC colony is found on the pipe surface.

10. Future Work

This project characterised the morphology of existing SCC in an ex-service Australian pipeline segment. As a result, a library of data was generated describing the morphological features of each crack analysed. This data has the potential to be used to build improved understanding of SCC crack initiation, growth, interaction and management.

This data can be used to develop a model designed for understanding crack growth in 3D and how cracks interact. This model could be used to determine whether complex 3D cracks could breach CEPA guidelines and under which conditions. This model could predict how SCC will grow within a colony to determine whether the colony should be classified as critical for further action to be taken. Easily measured inputs such as crack length and spacing would be the main required feedbacks for the colony classification.

Another question is whether inclined SCC cracks take longer to grow to critical dimensions that could lead to catastrophic failure. They have been observed to increase in inclination angle with respect to depth, but this poses the question of whether these types of SCC cracks will eventually stop growing in the through wall direction altogether.

Further work needs to be done to understand the main driving mechanism behind crack inclination. It is expected the residual stresses play a role. However, a detailed understanding of the mechanism could aid pipe operators in managing SCC, and pipe manufacturers in producing SCC resistant pipe.

SCC is a real problem to steel pipelines and comprehensive management mechanisms are vital to ensure the maximum pipeline lifetime is reached. Understanding the mechanism of inclined SCC will help ensure in the future instances of SCC can be more easily managed.

Through this study, a small number of SCC cracks greater than 25 mm in length were analysed. To confirm and provide an increased confidence level of these results (especially of critical sized cracks), a much greater number of significantly large cracks are required to confirm the results presented in this thesis.

11. Conclusion

Through this investigation, 120 existing SCC cracks, extracted from a segment of the Moomba–Sydney pipeline, were characterised primarily in relation to each individual crack's morphology. This characterisation formed the 'survey' that has quantified the crack morphology of the SCC existing in the Australian pipeline.

From the results it was determined that 81% of all the cracks analysed with a crack length greater than 4 mm, were inclined and had a depth greater than 200 µm. The typical straight section of the cracks from the initiation point at the surface was in the range of 200–900 µm. The inclination angle for the majority of cracks less than 18 mm in length was in the range of 30–45 degrees away from the perpendicular. However, for cracks greater than 18 mm the range was between 45–60 degrees.

For crack less than 18 mm in surface length, the aspect ratio was found to be 0.21. Cracks exceeding this length did not add much in depth (aspect ratio of 0.03) and were typically a result of coalesced cracks. This change in aspect ratio corresponded to a crack depth of 2.8 mm.

The maximum crack depth observed was 3.5 mm for a crack of length 24 mm. The maximum hoop travel observed was 3.8 mm for a crack of 45 mm in length.

During the analysis it was found that 32% of cracks showed some form of crack interaction. Approximately 44% of these interacting cracks were non-collinear cracks that had joined beneath the outer surface of the pipe and approximately 47% were observed to be collinear crack interactions. The remaining 9% had both collinear and non-collinear interactions occurring along the crack path. The largest circumferential separation of cracks, which were observed to be interacting, was 2 mm for cracks of length 19 mm and 36 mm respectively.

Longitudinal subsurface travel was observed for two cracks in the study. The greatest longitudinal subsurface travel observed was approximately 1.5 mm for a 5 mm long crack. The occurrence of subsurface longitudinal travel was supported by X-ray tomography may prove to be significant.

The majority of cracks observed on the surface of the pipeline were travelling axially along the pipe wall. Any deviations were generally due to crack interactions occurring which

altered a crack's path. Although numerous short-range crack interactions were observed, no cases were observed of large-scale crack interactions, which would have breached the CEPA guidelines. The level of the conservatism in the guidelines is not known and more data is required from large significant cracks to be able to ensure that the guidelines are adequately conservative for all situations involving SCC.

Inclined SCC is a 3D problem, which is difficult to measure and assess using traditional analytical metallography. Through the current research, it has been shown that X-ray tomography has the potential to enable these cracks to be visualised in 3D. This would provide considerable information and assistance in the understanding of this phenomenon.

No strong trends were found between microstructural features, micro hardness levels, residual or operational stresses and the incidence of inclined SCC. The present work and previous studies [REF] indicate that fine microstructural features are the major cause of inclined SCC rather than environmental or stress conditions.

12. References

Baker, TN, Rochfort, GG & Parkins, RN 1987a, 'Post-rupture analyses reveal probable future line failures', *Oil & Gas Journal*, 12 Jan, pp. 65–70.

Baker, TN, Rochfort, GG & Parkins, RN 1987b, 'Studies of line failure focus on cracking conditions', *Oil & Gas Journal*, 26 Jan, pp. 65–70.

Callister, W 1994, *Materials Science and Engineering*, John Wiley and Sons, New York.

Canadian Energy Pipeline Association 2007, 2nd edn, *Stress corrosion cracking: recommended practices*, CEPA, Alberta.

Connolly BF, Horner DA, Fox SJ, Davenport AJ, Padovani C, Zhou S, Turnbull A, Preuss M, Stevens NP, Marrow TJ, Buffiere JY, Boller E, Groso A, Stampanoni M 2006, 'X-ray microtomography studies of localised corrosion and transitions to stress corrosion cracking', *Materials Science and Technology*, vol. 22, no. 9, 1076–1085.

Conroy, GC & Vannier, MW 1984, 'Non-invasive three-dimensional computer imaging of matrix-filled fossil skulls by high-resolution computed tomography', *Science*, vol. 226, 456–458.

Elboujdaini, M & Shehata, MT 2004, 'Stress corrosion cracking: a Canadian prospective for oil and gas pipeline', CANMET Material Technology Laboratory, Ottowa.

Eslami A, Fang B, Kania R, Worthingham B, Been J, Eadie R, Chen W 2010, 'Stress corrosion cracking initiation under the disbonded coating of pipeline steel in near-neutral pH environment', *Corrosion Science*, vol. 52, pp. 3750-3756.

Fotheringham, IM 1983, 'Moomba–Wilton pipeline: corrosion protection in the Moomba area', Site report.

Gamboa, E 2011, 'SCC benchmarking of Australian pipelines', *Final Report for the University of Adelaide*, The University of Adelaide, Adelaide, pp. 10-16.

Gamboa, E & Linton, V 2010, 'Investigation of line pipe properties on SCC susceptibility of pipelines', *Final Report for the University of Adelaide*, The University of Adelaide, Adelaide, pp. 15-52.

Gamboa, E & Sneddon, G 2011, 'Metallographic comparison to tomography of inclined SCC cracks', *International Corrosion Congress (ICC)*, 20–24 Nov 2011, ICC, Perth, pp. 491–502.

Gan, F, Sun, ZW, Sabde, G & Chin, DT 1994, 'Cathodic protection to mitigate external corrosion of underground steel pipe beneath disbonded coating', *NACE International*, vol. 50, no. 10, pp. 804-816

Guiliani, M 2013, '3D Visualisation of Inclined SCC', M.A. thesis, Adelaide University, Adelaide.

Hertzberg, R 1996, *Deformation and fracture mechanics of engineering materials*, John Wiley and Sons, New York.

Ketcham, RA & Carlson, WD 2001, 'Acquisition, optimization and interpretation of X-ray computed tomographic imagery: applications to the geosciences', *Computers and Geosciences*, vol. 27, pp. 381–400.

Jayaraman, N & Prevey, PS 2005, 'An overview of the use of engineered compressive residual stresses to mitigate SCC and corrosion fatigue' Lambda Research, Ohio, pp. 1-11.

Kamaya, M & Totsuka, N 2002, 'Influence of interaction between multiple cracks on stress corrosion crack propagation', *Corrosion Science*, vol. 44.

Kim, BA, Zheng, W & Oguchi, N 2004, 'Experimental study of SCC susceptibility of X60 steel using full pipe sections in near-neutral pH environment', *International Pipeline Conference (IPC)*, 4–8 October 2004, Calgary.

Lam, KY & Phua, SP 1991, 'Multiple crack interaction and its effect on stress intensity factor', *Engineering Fracture Mechanics*, vol. 40, no. 3, pp. 585–592.

Lam, KY & Wen, C 1993, 'Interaction between microcracks and a main crack in a semi-infinite medium', *Engineering Fracture Mechanics*, vol. 44, no. 5, pp. 753–761.

Leis, BN & Colwell, JA 1997, 'Initiation of stress-corrosion cracking on gas transmission piping', *Effects of the Environment on the Initiation of Crack Growth, ASTM STP 1298*, American Society for Testing and Materials, Van Der Sluys, Piascik, pp. 34-58.

Leis, BN & Eiber, RJ 1997, 'Stress-corrosion cracking on gas transmission pipelines: history, causes, and mitigation', *First International Business Conference on Onshore Pipelines*, Dec 1997, Berlin (proceedings).

Linton, V, Gamboa, E & Law, M 2007, 'Fatigue of SCC Cracks in Gas Transmission Pipelines', *Final Report for the University of Adelaide*, The University of Adelaide, Adelaide.

Lozano-Perez, S, Rodrigo, P & Gontard, LC 2011, 'Three-dimensional characterizations of stress corrosion cracks', *Journal of Nuclear Materials*, vol. 408, pp. 289–295.

Marrow, TJ, Babout L, Jivkov AP, Wood P, Engelberg D, Stevens N, Withers PJ, Newman RC 2006, 'Three dimensional observations and modelling of intergranular stress corrosion cracking in austenitic stainless steel', *Journal of Nuclear Materials,* vol. 352, 62–74.

Parkins, RN & Fessler, RR 1978, 'Stress corrosion cracking of high-pressure gas transmission pipelines', *Materials In Engineering Applications*, vol. 1, pp. 80–98.

Parkins, RN 1980, 'Predictive approaches to stress corrosion cracking failure', *Corrosion Science*, vol. 20, no. 1, pp. 147–166.

Parkins, RN 1987, 'Localised corrosion and crack initiation', *Materials Science and Engineering*, A103, pp. 143–156.

Parkins, RN 1989, 'The application of stress corrosion crack growth kinetics to predicting lifetimes of structure', *Corrosion Science*, vol. 29, no. 8, pp. 1019–1038.

Parkins, RN & Singh, PM 1990, 'Stress corrosion crack coalescence', *Corrosion*, vol. 46, no. 6, pp. 485–499.

Parkins, RN, Blanchard JR., WK & Delanty, BS 1994, 'Transgranular stress corrosion cracking of high-pressure pipelines in contact with solutions of near neutral pH', *Corrosion Engineering*, May, pp. 394–408.

Roberge, PR 1999, *Handbook of Corrosion Engineering*, McGraw Hill Professional, Ontario. pp. 99-125 & 787-869.

Song, F 2008, 'Overall mechanisms of high pH and near-neutral pH SCC, models for forecasting SCC susceptible locations, and simple algorithms for predicting high ph SCC crack

growth rates', *Corrosion 2008 Conference & Expo,* 16-20 March 2008, NACE International, New Orleans, Paper 8129, pp 1-23.

Sutherby, R & Chen, W 2004, 'Deflected stress corrosion cracks in the pipeline steel', *International Pipeline Conference*, 4-8 October 2004, American Society of Mechanical Engineers, Calgary, pp. 1-9.

Venegas, V, Caleyo, F, Baudin, T, Hallen, JM & Penelle, R 2009, 'Role of microtexture in the interaction and coalescence of hydrogen-induced cracks', *Corrosion Science*, vol. 51, pp. 1140–1145.

Wang, YZ, Atkinson, JD, Akid, R & Parkins, RN 1996, 'Crack interaction, coalescence and mixed-mode fracture mechanics', *Fatigue Fracture Engineering Material Structures*, vol. 19, no. 4, pp. 427–439.

Wang, J & Atrens, A 2003, 'Analysis of service stress corrosion cracking in a natural gas transmission pipeline, active or dormant?', *Engineering Failure Analysis*, vol. 11, pp. 3–18.

Xie, J, Yang, L, Sen, M, Worthington, R & King, F 2009, 'Mechanistic investigation of deflected stress corrosion cracking in pipeline steels', *Corrosion 2009 Conference & Expo*, Paper 09121.

Zadow, L & Gamboa, E 2011, 'SCC sample selection criteria–tomography of inclined SCC', *Final Report for Energy Pipelines CRC*, The University of Adelaide, Adelaide.

Appendices:

Appendix A: Pipeline Layout and SCC colony locations

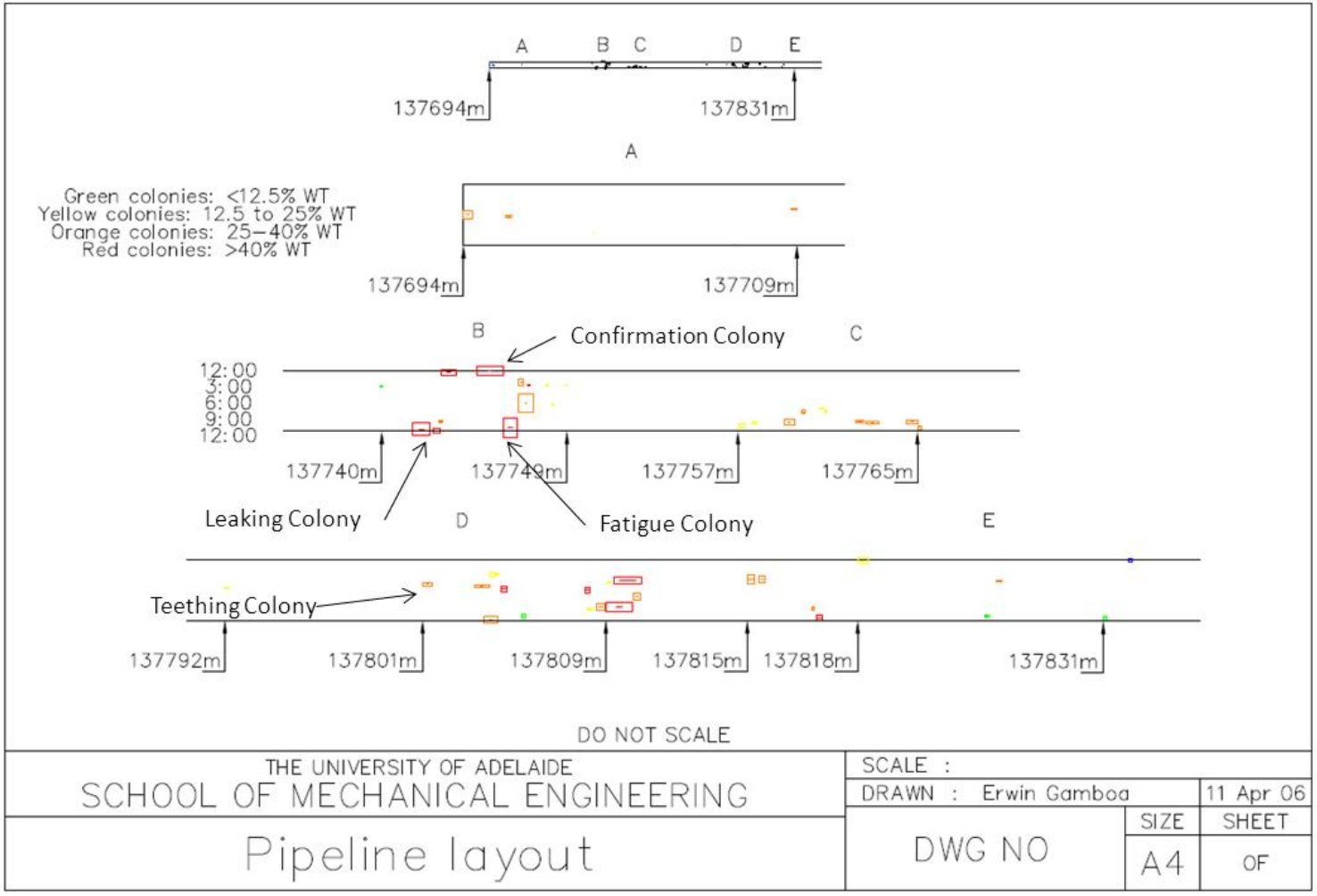

Appendix B: Raw Data Collation Sample (all data shown is entered as the raw data recorded)

Sample summary of morphological data describing the SCC investigated:

Crack Code	Crack Number	Colony Classification	Type	Surface Length (mm)	Max. Depth (mm)	Max Hoop Travel (mm)	Observed Interactions	Status
Alpha	1	Sparse	Inclined	11	2.330	1.132	Subsurface	Done
FC-I8-2	1	Dense	Straight	5.5	1.549	0.297	None	Done
FC-I8-2	2	Dense	Straight	4	1.117	0.184	None	Done
FC-I8-2	3	Dense	Straight	4	1.104	0.151	None	Done
CC-2-E2A	1	Sparse	Inclined	8	1.821	1.337	None	Done
FC-I8-3	1	Dense	Straight	4.5	1.392	0.305	Surface	Done
FC-I8-3	2	Dense	Straight	3	0.918	0.253	Surface	Done
FC-I8-3	3	Dense	Straight	4	1.019	0.168	None	Done
K (f)	1	Sparse	Inclined	6	1.745	1.188	None	Done
CC-1-C3-1	1	Sparse	Inclined	7.5	1.405	0.289	None	Done
CC-1-C3-1	2	Sparse	Inclined	6	1.246	0.371	None	Done
CC-1-C3-1	3	Sparse	Inclined	10	1.526	0.371	Surface + Subsurface	Done
CC-1-C3-1	4	Sparse	Inclined	7	1.000	0.450	Subsurface	Done
CC-1-C3-1	5	Sparse	Inclined	7	1.477	0.371	Subsurface	Done
CC-1-C3-2	1	Sparse	Inclined	9	1.972	0.767	None	Done
CC-1-C3-2	2	Sparse	Inclined	11	1.980	0.978	None	Done
CC-1-C3-2	3	Sparse	Inclined	8.5	1.795	0.743	None	Done
CC-1-C3-3	1	Sparse	Inclined	12	1.570	0.811	Subsurface	Done
CC-1-C3-3	2	Sparse	Inclined	7.5	1.515	0.558	None	Done
CC-1-C3-3	3	Sparse	Inclined	11	1.697	0.822	None	Done
CC-1-C3-3	4	Sparse	Inclined	8	1.755	0.602	Subsurface	Done
CC-1-C3-4	1	Sparse	Inclined	13	1.980	0.751	Subsurface	Done

Interactions:

Crack Code	Crack Number	Colony Classification	Type	Surface Length (mm)	Observed Interactions	Circumferential Spacing	Axial Spacing	Circumferential Spacing (Calc)	Axial Spacing (Calc)	Circumferential Interaction (Calc)	Axial Interaction (Calc)	Count for Interaction	Interacting? (Calc)
Alpha	1	Sparse	Inclined	11	Subsurface					No	No	0	No
I8-2	1	Dense	Straight	5.5	None					No	No	0	No
I8-2	2	Dense	Straight	4	None					No	No	0	No
I8-2	3	Dense	Straight	4	None					No	No	0	No
CC-2-E2A	1	Sparse	Inclined	8	None					No	No	0	No
I8-3	1	Dense	Straight	4.5	Surface	0.2	0.1	0.525	0.938	Yes	Yes	2	Yes
I8-3	2	Dense	Straight	3	Surface	0.2	0.1	0.525	0.938	Yes	Yes	2	Yes
I8-3	3	Dense	Straight	4	None					No	No	0	No
K (f)	1	Sparse	Inclined	6	None					No	No	0	No
CC-1-C3-1	1	Sparse	Inclined	7.5	None					No	No	0	No
CC-1-C3-1	2	Sparse	Inclined	6	None					No	No	0	No
CC-1-C3-1	3	Sparse	Inclined	10	Surface + Subsurface	0.1	0.1	1.225	1.75	Yes	Yes	2	Yes
CC-1-C3-1	4	Sparse	Inclined	7	Subsurface	0.7	0.1	0.98	1.75	Yes	Yes	2	Yes
CC-1-C3-1	5	Sparse	Inclined	7	Subsurface	0.7	0.1	0.98	1.75	Yes	Yes	2	Yes

Summary of Angles:

Crack Code	Crack Number	Colony Classification	Type	AVG Angle Seg (deg)	AVG Final Angle (deg)	Final Angle Direction	Final Angle Direction	Surface Length (mm)	Max. Depth (mm)
Alpha	1	Sparse	Inclined	34.2	44.9	8		11	2.330
FC-I8-2	1	Dense	Straight	30.6	38.3	4		5.5	1.549
FC-I8-2	2	Dense	Straight	34.7	30.8	8		4	1.117
FC-I8-2	3	Dense	Straight					4	1.104
CC-2-E2A-1	1	Sparse	Inclined	39.1	43.5	8		8	1.821
FC-I8-3	1	Dense	Straight	32.6	42.1	4		4.5	1.392
FC-I8-3	2	Dense	Straight					3	0.918
FC-I8-3	3	Dense	Straight					4	1.019
K (f)	1	Sparse	Inclined	35.1	41.2	8		6	1.745
CC-1-C3-1	1	Sparse	Inclined	23.2	30.8	4		7.5	1.405
CC-1-C3-1	2	Sparse	Inclined	32.7	34.7	4		6	1.246
CC-1-C3-1	3	Sparse	Inclined	34.3	32.9	8		10	1.526
CC-1-C3-1	4	Sparse	Inclined		33.1	8		7	1.000
CC-1-C3-1	5	Sparse	Inclined	31.8	34.9	8		7	1.477
CC-1-C3-2	1	Sparse	Inclined	32.3	37.6	4		9	1.972
CC-1-C3-2	2	Sparse	Inclined		28.8	8	4	11	1.980
CC-1-C3-2	3	Sparse	Inclined		34.2	8		8.5	1.795

Straight Section:

	CC		FC		LC		TC		CMI
	Straight Section Depth (µm)		Straight Section Depth (µm)		Straight Section Depth (µm)		Straight Section Depth (µm)		Straight Section Depth (µm)
CC-J2	201	FC-I8-2	1043	LC-Z1-1	556			CMI-1	567
	875		696		0				253
	435		1153		173				468
	743		1383		762				344
	629		1015		525				679
	487		377		600				429
	545		484		855				429
	583		1051		578				267
	501		1117		382				349
	704		762		454				465
	385	FC-I8-3	412	LZ-Z1-2	259				492
	481		400		734				313
	575				0				366
CC-A2-1	248				495				413
	335				765				0
	355			LC-Z4-1	633				0
	478				517			CMI-2	283
	1166				842				272
	454				248				319
	541				432				490

Inclination Direction:

Confirmation Colony*									
Crack Code	**Crack Number**	**Colony Classification**	**Type**	**AVG Angle Seg (deg)**	**AVG Final Angle (deg)**	**Final Angle Direction**	**Final Angle Direction**	**Surface Length (mm)**	**Max. Depth (mm)**
Alpha	1	Sparse	Inclined	34.2	44.9	8		11	2.330
CC-2-E2A-1	1	Sparse	Inclined	39.1	43.5	8		8	1.821
CC-1-C3-1	1	Sparse	Inclined	23.2	30.8	4		7.5	1.405
CC-1-C3-1	2	Sparse	Inclined	32.7	34.7	4		6	1.246
CC-1-C3-1	3	Sparse	Inclined	34.3	32.9	8		10	1.526
CC-1-C3-1	4	Sparse	Inclined		33.1	8		7	1.000
CC-1-C3-1	5	Sparse	Inclined	31.8	34.9	8		7	1.477
CC-1-C3-2	1	Sparse	Inclined	32.3	37.6	4		9	1.972
CC-1-C3-2	2	Sparse	Inclined		28.8	8	4	11	1.980

*This analysis was completed for each colony

All raw data and processed graphs completed and shown in file “Crack_Raw_Data.xls”.

All data and images for each crack investigated stored in “Metallography” folder in attached files.